TR-6417-1

LDV WAKE VORTEX DETECTION SYSTEM ASSESSMENT

28 February 1992

TASC
THE ANALYTIC SCIENCES CORPORATION

TASC
THE ANALYTIC SCIENCES CORPORATION

TR-6417-1

LDV WAKE VORTEX DETECTION SYSTEM ASSESSMENT

28 February 1992

Prepared under:

Contract No. DTRS-57-89-C-00040
Functional Area: ISE
TTD No. IA0020, Work Order No. 5

for:

VOLPE NATIONAL TRANSPORTATION SYSTEMS CENTER
U.S. Department of Transportation
Cambridge, Massachusetts 02142

Prepared by:

Joseph A. D'Appolito
David A. Whitney

Approved by:

E. Michael Geyer

TASC
55 Walkers Brook Drive
Reading, Massachusetts 01867

TABLE OF CONTENTS

LIST OF FIGURES

LIST OF FIGURES (Continued)

LIST OF TABLES

1. INTRODUCTION

1.1 OBJECTIVE

This report summarizes the methodology and findings of an engineering evaluation of the Laser Doppler Velocimeter (LDV). The LDV is owned and operated by the Department of Transportation, and is used as a research tool in the aircraft Wake Vortex program. *The purpose of this effort is to perform an independent technical review of the capability of the LDV to provide quantitative data concerning the location, velocity, size, and strength of aircraft wake vortices.* The LDV was evaluated from two perspectives:

- Basic hardware/signal processing capabilities and limitations
- Post-test data processing procedures.

To understand the basic hardware/signal processing characteristics of the system, an analytic LDV simulation was developed and exercised. This simulation captures the major sensor characteristics and its operation, and provides an understanding of what the LDV data collection limitations are.

Frequent discussions and meetings were held with VNTSC staff as part of the review and evaluation of post-test data processing procedures currently applied to the LDV data. LDV, tower* anemometer, and other meteorological data were analyzed by TASC in order to compare LDV and tower measurement capabilities, to identify and explain discrepancies, and to make recommendations for modifications to the LDV post-test data processing procedures. Several modifications that have the potential to improve the quality of information extracted from the LDV were identified.

*LDV data is often collected near a tower instrumented with meteorological and additional vortex velocity sensors.

1.2 REPORT OVERVIEW

Chapter 2 of this report describes the LDV analytic simulation and its application to performance prediction. The effects captured in the simulation are discussed (LDV geometry, optical focal volume, etc.), and simulated results of operating the LDV under a variety of conditions are presented.

Chapter 3 presents the results of evaluating LDV data processing procedures. The data analysis results support the validity of the simulation described in Chapter 2. Insights gained from the LDV analytic simulation are used to help identify fundamental limitations to information extraction and to suggest alternative processing schemes. LDV and tower anemometer data from selected Idaho Falls tests are processed and compared to each other, and to model-based predictions of LDV performance. *Chapter 4* summarizes the results of the work and makes recommendations for LDV improvements.

2. LDV SIMULATION

The simulation employed in this work was developed to provide a basic analytic model for evaluation of the LDV sensor and measurement process, and to compare model predictions with recorded LDV data. An extensive review of the LDV design literature, together with a limited examination of typical LDV wake vortex velocity measurement data provided by VNTSC, was performed by TASC. This lead to the preliminary conclusion that the following key elements dominate the performance and accuracy of the LDV wake vortex measurement system and should therefore be included in any LDV performance assessment simulation:

- LDV/Vortex geometry
- LDV response function (i.e., optics)
- LDV velocity estimation limits
- LDV velocity quantization
- LDV spectrum averaging
- LDV elevation scan rate
- Wind.

Hardware specific elements are covered briefly in Section 2.1. The remaining elements are discussed in more detail in the later sections. The simulation does not include a detailed representation of the laser or laser optics and its associated electronics, which are assumed to be working as designed. Nor does the simulation include measurement noise. Although noise levels directly affect LDV performance and noise level estimates can be made using the technique of Ref. 1, the levels computed often bear little resemblance to experimental data. As later sections of this chapter will show, the key elements listed above alone lead to simulation results which are fully consistent with observed LDV performance, allow one to directly determine those elements of LDV performance that limit wake vortex parameter recovery, and lead directly to recommendations for system improvement.

2.1 LDV OPERATION

The Laser Doppler Velocimeter (LDV) uses a continuous wave CO_2 laser operating in the far infrared region at a wavelength of 10.6 microns. The LDV operates in the backscatter mode, using naturally occurring aerosols as scattering targets. Doppler shifts in the return signals measure the component of particle velocity along the laser line-of-sight (LOS).

A block diagram of the LDV system is shown in Fig. 2.1-1. The LDV is comprised of a very stable single-frequency CO_2 laser, a Mach-Zender interferometer, transmit-receive optics (the telescope), range-angle scanner, spectrum analyzer and data processor with associated displays and recorders. The telescope can focus the laser beam at any point in space from 32 to 600 m. The telescope also receives the backscatter radiation which is mixed with part of the transmitted signal at the detector to produce a doppler difference frequency signal in the range of 0 to 8 MHz which is proportional to velocity magnitude. The mixing operation does not yield velocity direction, i.e., whether particles are moving toward or away from the laser source. The doppler signal is fed to a Surface Acoustic Wave (SAW) filter acting as a spectrum analyzer. The SAW filter has a frequency resolution of 100 KHz and an effective bandwidth of 6 MHz. These specifications translate into a

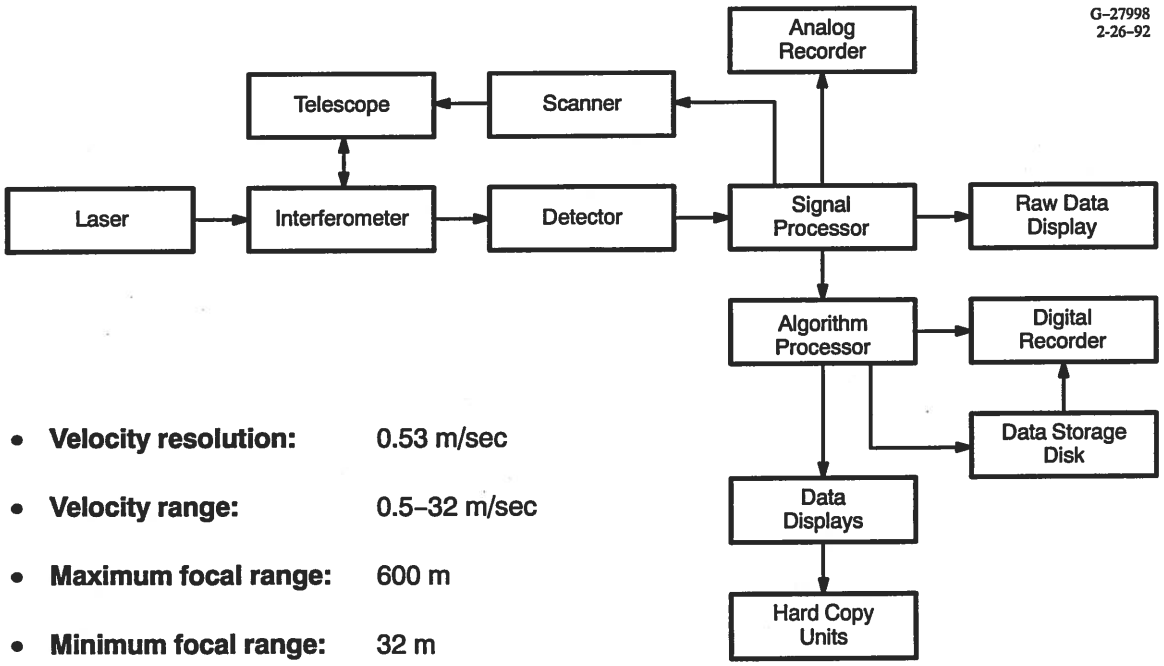

Figure 2.1-1 LDV Functional Block Diagram with LDV Specifications

velocity resolution of 0.53 m/sec with an upper velocity limit of 31.8 m/sec. System noise and null offset uncertainty make the first 3 velocity levels or bins unreliable. These levels are zeroed out in the final processing. Output from the SAW filter is averaged in the signal processor for 4 msec to produce a smoothed velocity spectrum as further discussed in Section 2.2.3.

2.2 LDV SIMULATION DESCRIPTION

2.2.1 The Vortex Model

The wake vortex is modelled as a two-dimensional line vortex. There are at least three simple potential candidate models for the 2D line vortex. They are the Rankine model, the Lamb model and the Hoffman-Joubert model (Ref. 2). In all of these 2D models, lines of constant velocity form concentric circles. The Rankine model is the simplest and perhaps best known. However, it contains singularities in higher derivatives which complicate its use in simulations and gives a greatly over simplified velocity distribution near the core radius. The Hoffman-Joubert model also contains singularities and leads to physically impossible results at zero and large radii. Of the three models, the Lamb model, which is an exact solution to the Navier-Stokes equations for the 2D line vortex in laminar flow, is the only model which is analytic in the mathematical sense; i.e., all derivatives exist. The Lamb model is used in the simulation. The Lamb and Rankine model velocity distributions are compared in Fig. 2.2-1 for a core strength, Γ, of 600 m^2/sec and a radius of 2 m. Notice that the Rankine model has an abrupt change in slope at the core radius while the Lamb model transitions smoothly through this region. Well away from the core radius in either direction the two models agree. The equations for the Lamb vortex model are:

$$V(r) = (\Gamma/2\pi R)\,(1 - \exp\,[-(R/R_c)^2]) \qquad (2.2\text{-}1)$$

where:
Γ = vortex strength
R_c = vortex core radius
R = distance from vortex center.

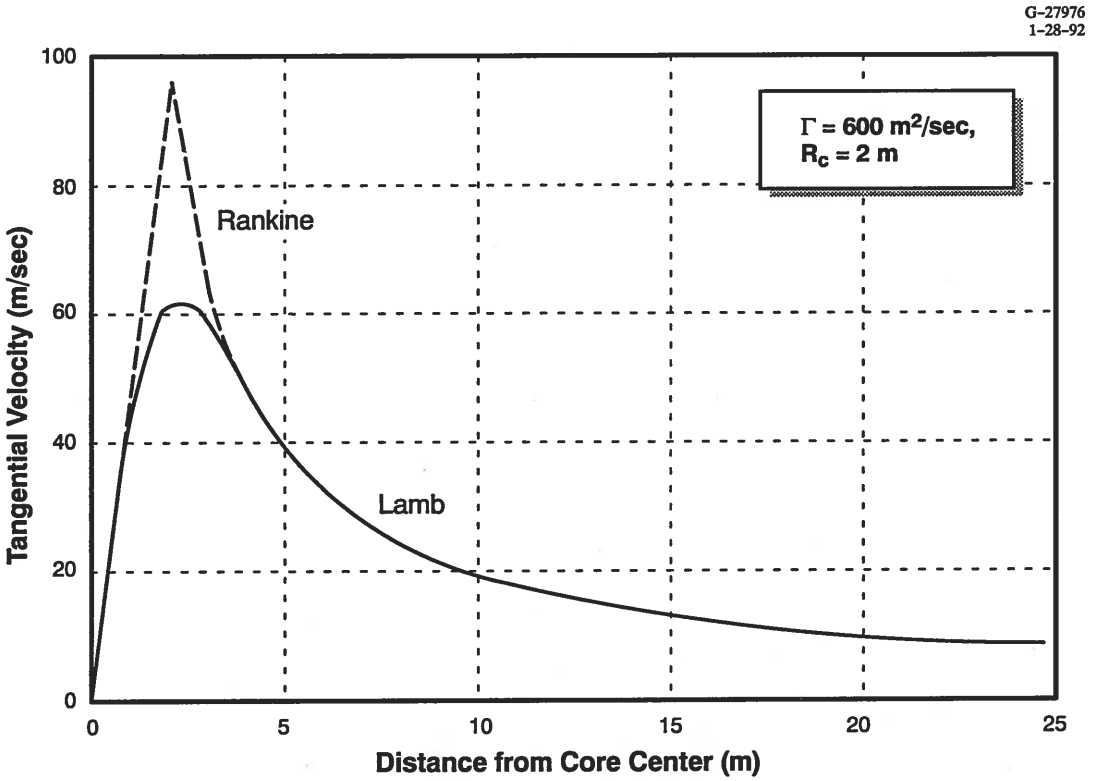

Figure 2.2-1 Lamb vs. Rankine Vortex Models

2.2.2 LDV/Vortex Geometry

The LDV/Vortex simulation geometry is shown in Fig. 2.2-2. A single vortex is modeled in the simulation. The LDV scans continuously in elevation and in discrete steps in range. The vortex may be viewed as a set of concentric cylinders of constant velocity extending into the paper in Fig. 2.2-2. In general, the plane swept out by the elevation scan of the LDV radial does not cut the vortex axis at right angles. The cutting angle between this plane and the vortex axis, denoted as CA, is illustrated in Fig. 2.2-3. During any single scan the vortex is assumed to be stationary. Since a complete scan at 30 deg/sec typically takes less than 0.4 sec, this assumption is reasonable for wind speeds of 2 m/sec or less.

The sampling volume shown in Fig. 2.2-2 is characterized by an angle, $\theta\gamma$, and a distance R_s. The angle is determined by the LDV signal processor averaging time, fixed at 4 msec, and the LDV angular scan rate, an input to the simulation. The length, R_s, is a function of the system telescope optical response. The LDV optics respond to backscattered energy over a broad distance centered about the focal point, R_f. Response on either side of the focal point falls off according to the following equation (Ref. 3):

$$I_i = \frac{I_o}{1 + \left(\frac{R_i - R_f}{dR}\right)^2} \qquad (2.2\text{-}2)$$

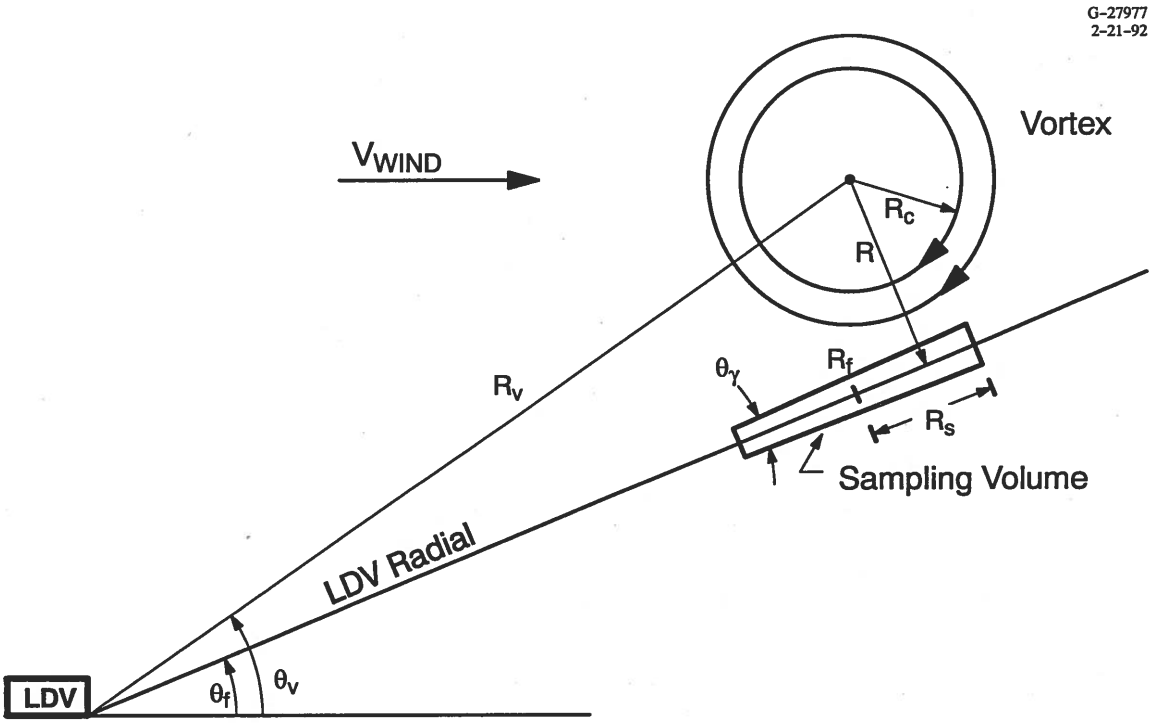

Figure 2.2-2 LDV/Vortex Simulation Geometry

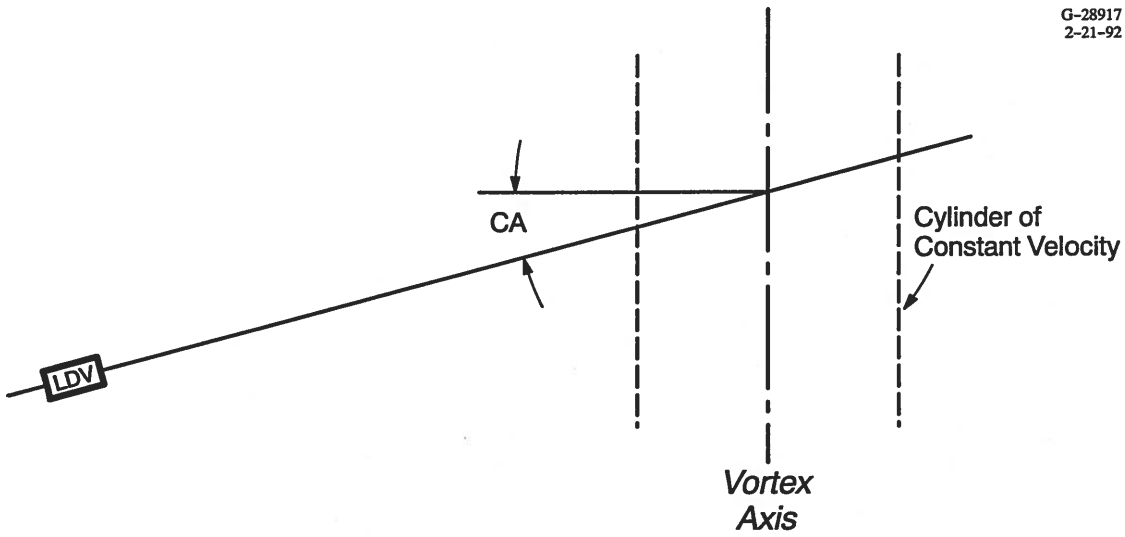

Figure 2.2-3 Definition of the LDV/Vortex Cutting Angle, CA

where

I_i = return intensity at R_i
I_o = return intensity at R_f
R_i = range of interest along LDV radial
dR = half-power distance from R_f
= $R_f^2/2032$ m

Eq. 2.2-2 is illustrated in Fig. 2.2-4. The focal volume is defined as the distance between the two points either side of the focal point where the intensity response is down by one-half relative to the response at the focal point. In (Eq. 2.2-2), dR is the distance from the focal point to the half-power point. dR varies directly as the square of the focal range, R_f. For simulation purposes the sampling volume, R_s, is taken as the distance where intensity response, I_R, is down by a factor of 20 relative to the focal point, but limited to a maximum of 50 m, i.e.,

$$R_s = \begin{cases} 4.36\ dR & \text{if } R_s < 50\ m \\ 50 & \text{otherwise} \end{cases} \qquad (2.2\text{-}3)$$

The upper limit of $R_s = 50$ m, which is reached when $R_f \geq 153$ m, constitutes the maximum useful coherence length of the laser beam at the extremes of doppler frequency shift.

2.2.3 Quantization and Spectrum Averaging

An expanded view of the sampling volume, showing how it is treated in the simulation, is shown in Fig. 2.2-5. The sampling volume is broken up into many small cells. The cells in the sampling volume are first scanned in range at a fixed elevation, then the elevation angle is incremented and the radial scan repeated. The vortex tangential velocity at the center of each cell is computed and resolved along the LDV radial. The resolved velocity component is then quantized into one of 60 velocity bins (see Section 2.1), weighted by the response function and added to the tally of "hits" in the same bin to produce a measured spectrum. At the end of each radial scan a histogram is obtained containing the weighted total number of hits in each velocity bin. Assuming uniform aerosol density within the sampling volume, this histogram is directly proportional to the signal power spectrum coming out of the SAW filter. The elevation angle is then incremented by a small step within the sampling volume and the radial scanning process is repeated. When the entire sampling volume has been scanned the several spectra are combined to yield an average spectrum over the sampling volume — see Fig. 2.2-6.

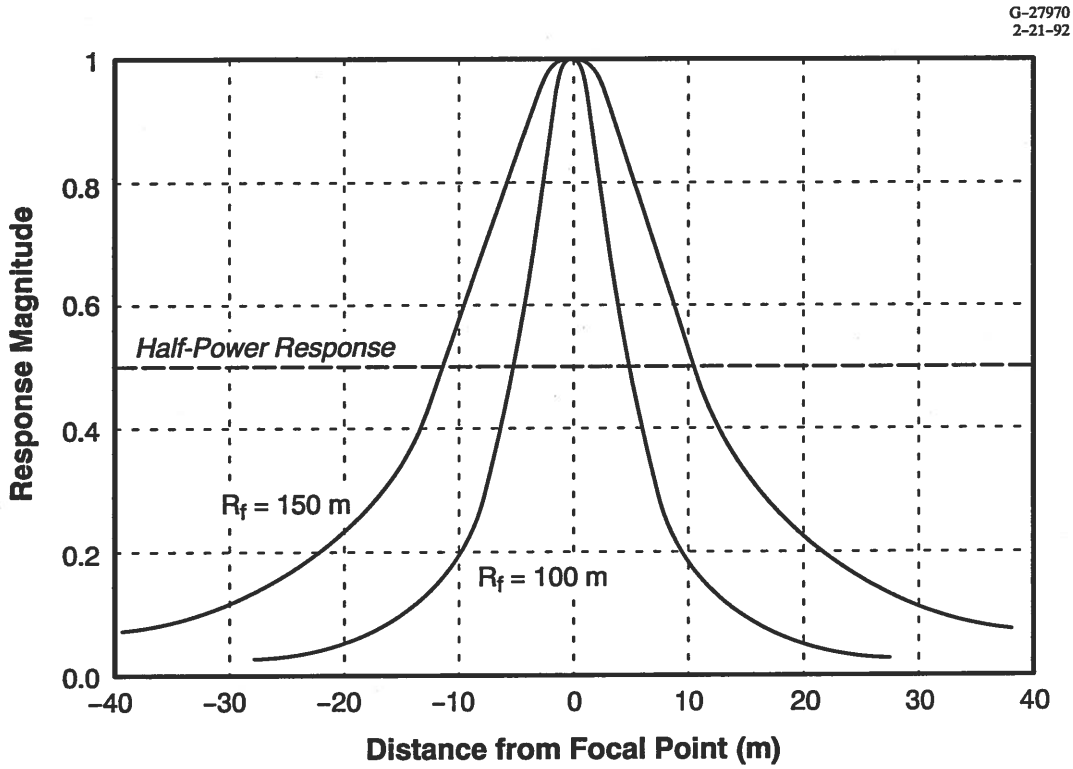

Figure 2.2-4 LDV Response Function (LDV Optics)

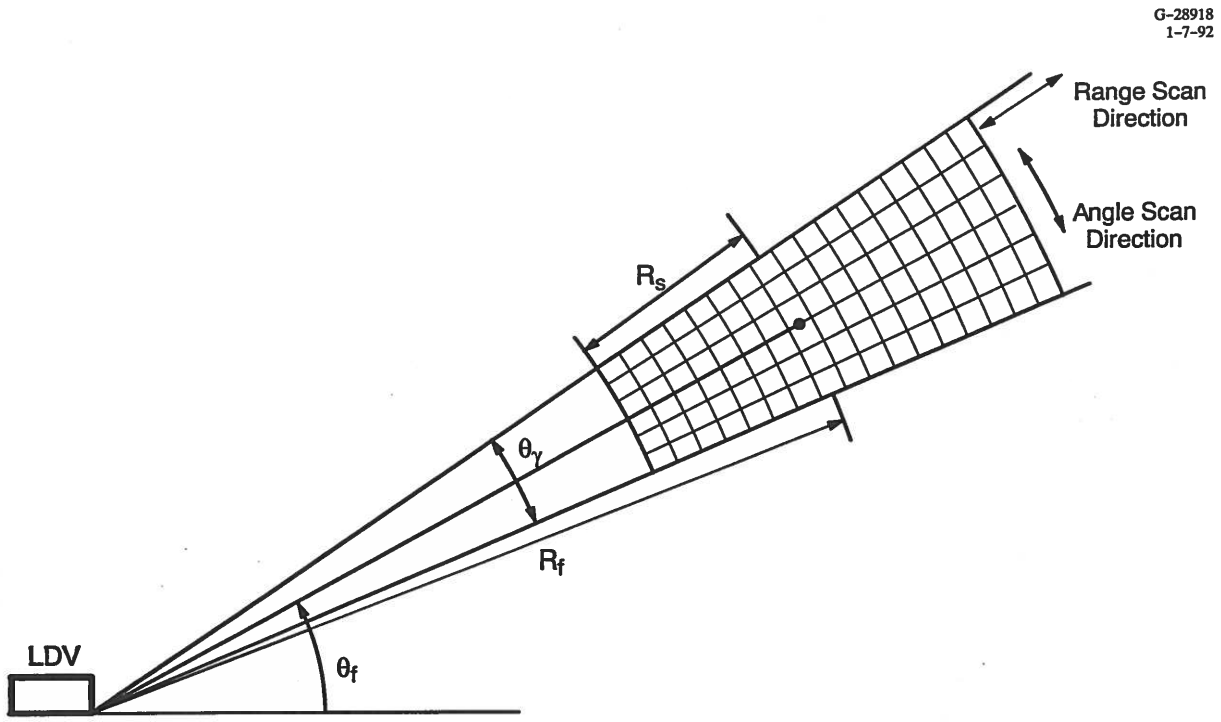

Figure 2.2-5 Expanded View of Sampling Volume

Referring to Fig. 2.2-2, it can be seen that the highest velocity within the sampling volume occurs at the point where the LDV radial is tangent to a constant velocity contour. In the simulation, the estimate for this velocity is formed by searching from the highest bin down until the first peak in the velocity spectrum is found. This value is called V_{max} and is illustrated in Fig. 2.2-6. The simulation procedure for estimating the highest velocity is the same as that employed by VNTSC during post-mission data processing.

2.2.4 User Inputs

The following inputs are available to the user to describe vortex and sensor characteristics when conducting an LDV system performance analysis:

- Vortex strength, core radius and location
- LDV focal range and sample volume size
- LDV scan angle limits and scan angle rate
- LDV/vortex axis cutting angle
- LDV spectrum averaging time
- Horizontal wind speed.

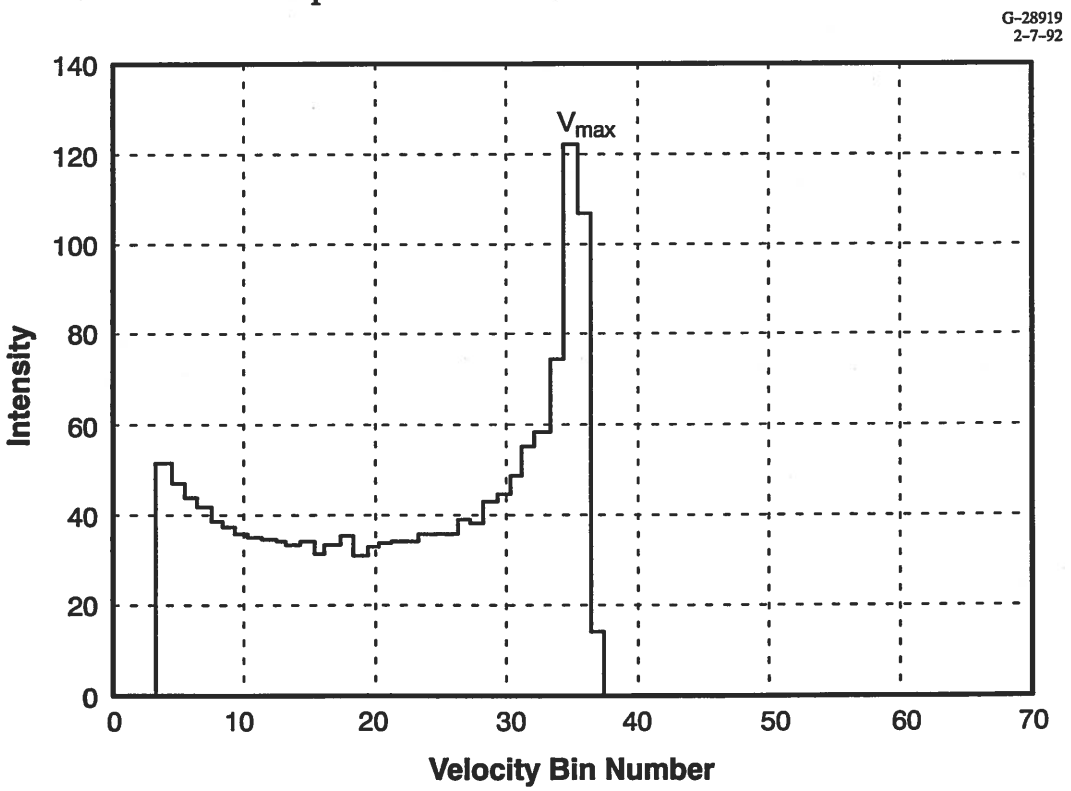

Figure 2.2-6 Typical SAW Filter Output Spectrum

2.3 SIMULATION RESULTS

2.3.1 Scope of Simulation Studies

In general two types of simulation analyses are conducted. The first involves a detailed examination of the LDV measurement process within a single sampling volume. Here we examine the effect of LDV/vortex geometry, wind, off-focus conditions, non-zero cutting angle, and SAW filter quantization and limiting on LDV SAW filter spectra (in particular the return signal power). These studies are referred to as *LDV radial scan studies* in the sequel. The second type of analysis simulates the complete elevation scan across a vortex and quantifies the effect of LDV quantization, averaging and velocity limiting, wind, off-focus conditions and non-perpendicular scanning on the estimation of critical vortex parameters such as vortex strength, core radius and peak velocities. These studies are referred to as the *LDV angular scan studies* in the sequel.

2.3.2 LDV Radial Scan Studies

In this group of simulations the effects of off-focus scanning, wind and non-perpendicular scanning, and SAW filter limiting on LDV spectra and return signal power are examined. First a reference run is made to establish a baseline which can then be compared to the off-nominal conditions.

The Reference Radial Scan — The reference run parameters are listed in Table 2.3-1. The simulation results are shown in Fig. 2.3-1 and Table 2.3-2. In the reference run the vortex is placed 30 deg above the horizontal at a range of 100 m. The vortex parameters are those of Fig. 2.2-2. Individual runs were made with the sampling volume centered at distances of 0, 1.25, 2.5, 5 and 10 m from the core center (denoted by R in Fig. 2.2-2) with the LDV telescope also focused at 100 m.

Table 2.3-1 Radial Scan Reference Run Parameters

CONDITIONS FOR REFERENCE RADIAL SCAN		
Γ	=	600 m^2/sec
R_c	=	2 m
R_f	=	R_v = 100 m
θ_v	=	30 deg
R_s	=	20 m
$\theta\gamma$	=	0.2 mrad

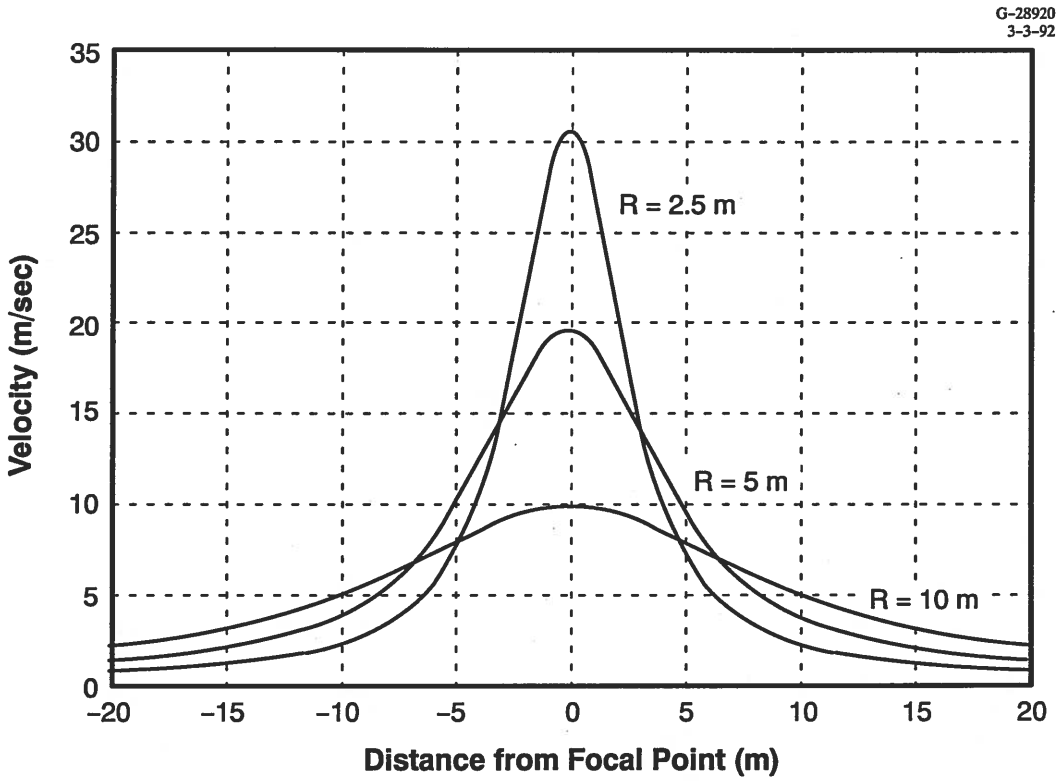

a.) Average Velocity Along LDV Radial

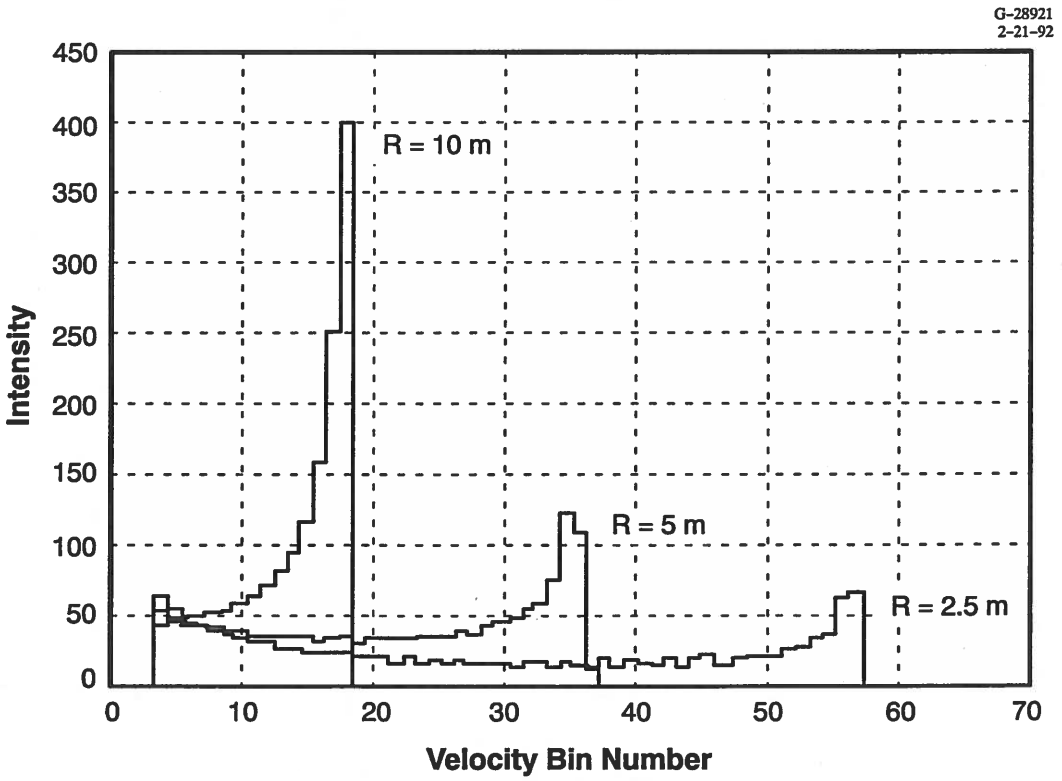

b.) SAW Spectra

Figure 2.3-1 Results of Reference Radial Scan

Table 2.3-2 Reference Radial Scan Results

R (m)	V_t (m/sec)	V_{max} (m/sec)	TOTAL RETURNS	V_{max} RETURNS	V_{max} dB
10	9.56	9.54	1570	400	0
5	19.07	18.55	1486	116	-10.8
2.5	30.20	30.21	1360	65	-15.8
1.25	24.79	23.32	1200	43	-19.4
0	0	2.12	113	100	-12

Figure 2.3-1a shows the averaged across angle at each range Line-of-sight (LOS) velocity along the LDV radial within the sampling volume for three of the five runs. The corresponding spectra are shown in Fig. 2.3-1b. Since the total number of cells in each sampling volume is the same, the maximum possible total return power at each elevation angle is the same (The number of usable returns will vary as a result of thresholding tests applied to the data). At 10 m from the core (θ_f = 24.27 deg), the LOS velocity varies over roughly a 5-to-1 range. The resulting power spectrum covers only 14 velocity bins and the number of "hits" in the bin encompassing the peak tangential velocity is high. This fact is reflected in the corresponding spectrum (Fig. 2.3-1b), which shows that this V_{max} has the largest signal power of the spectra shown.

As the scan volume moves in closer to the vortex core, the range over which the LOS velocity varies increases. At R = 5 m, the LOS velocity varies over a range of 17-to-1. The resulting spectrum spreads out over 34 bins and the number of "hits" in the velocity bin containing the peak tangential velocity drops substantially. As shown in the table, signal power has dropped by 10.8 dB relative to the 10 m value.

The LOS velocity varies over a range of 50-to-1 at R = 2.5 m. The resulting spectrum now spans 53 bins and the signal power in the peak velocity bin at an intensity level of 65 is down by 15.8 dB relative to the 10 m value. For the scanning volume spanning the core center most of the hits are below the LDV velocity threshold and total return signal power has dropped by 23 dB relative to the 10m level.

Table 2.3-2 summarizes the results of the reference run. Column 2 lists the true tangential velocity, V_t, at each distance from the core. Column 3 lists the measured tangential velocity, V_{max}. Notice that the first three measured velocities are all within one quantum level of the true value, while the velocity error at R = 1.25 m and at the core center are 1.47

and 2.12 m/sec respectively. Referring to Fig. 2.2-2, the velocity error far from the core is on the order of a quantum level because the tangential velocity variation over the sampling volume is small relative to a quantum. The velocity error at the core center is large, however, because the LDV sampling volume spans a region where V_t varies from 0 to 4.77 m/sec. Thus, in the noise free case considered herein, when tangential velocity variation over the sampling volume is small, velocity error is dominated by quantization granularity. When the tangential velocity variation over the sampling volume is large relative to a quantum, velocity averaging dominates.

Column 4 of Table 2.3-2 presents the count of usable returns from each sampling volume, while column 5 gives the number of returns in the V_{max} bin, the "signal" bin. Column 6 lists the signal level in the V_{max} bin in dB relative to the level at 10 m. What is clear is that the signal level drops continuously as the scan moves toward the vortex longitudinal axis. To first order, signal power is in proportional to distance form the core center. Thus when noise is present the signal-to-noise ratio (SNR) will also drop as one moves in toward the core center.

Off-Focus Effects on Radial Scan — Figure 2.3-2a shows the velocity profiles along the LDV radial as a function of focal distance. The corresponding velocity spectra are given in Fig. 2.3-2b. As in the reference run, the vortex core center is 30 deg above the horizontal at a range of 100 m. The sampling volume mean elevation angle is 27.14 deg, corresponding to R = 5 m in the reference case. Velocity profiles are shown for focal distances of 90, 100 and 110 m. Also shown dotted is the LDV focal response function for R_f equal to 100 m. This response function is approximately correct for 90 and 110 m also. The peak velocity for all three profiles is the same. However, the signal strength for each of the two off-focus peaks is down roughly by a factor of four due to the fall-off of the response function.

Table 2.3-3 summarizes the off-focus response at focal ranges of 90, 95, 100, 105 and 110 m. Although the correct velocity (to within one quantum) is measured in all cases, the signal power drops off rapidly with increasing focal distance mismatch. Because of its shorter focal volume, the response at 90 m suffers more attenuation than that at 110 m. Thus SNR will fall with increasing off-focus conditions when noise is present.

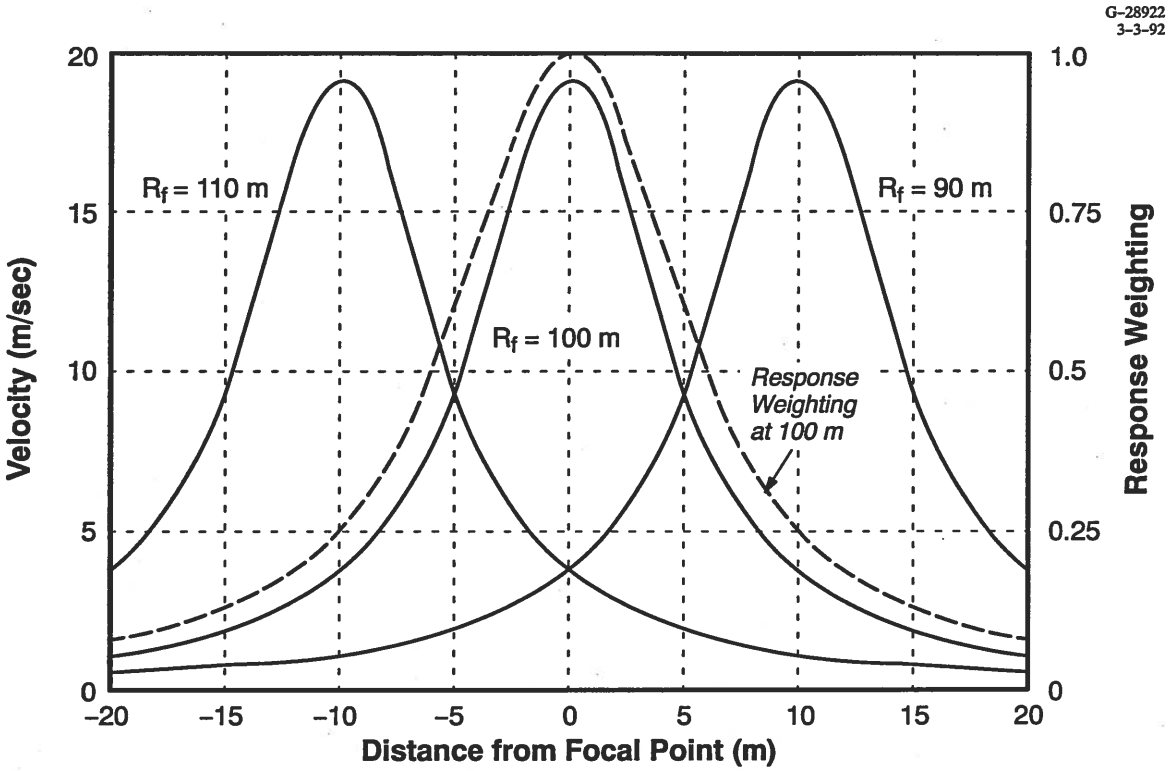

a.) Average Velocity Along LDV Radial

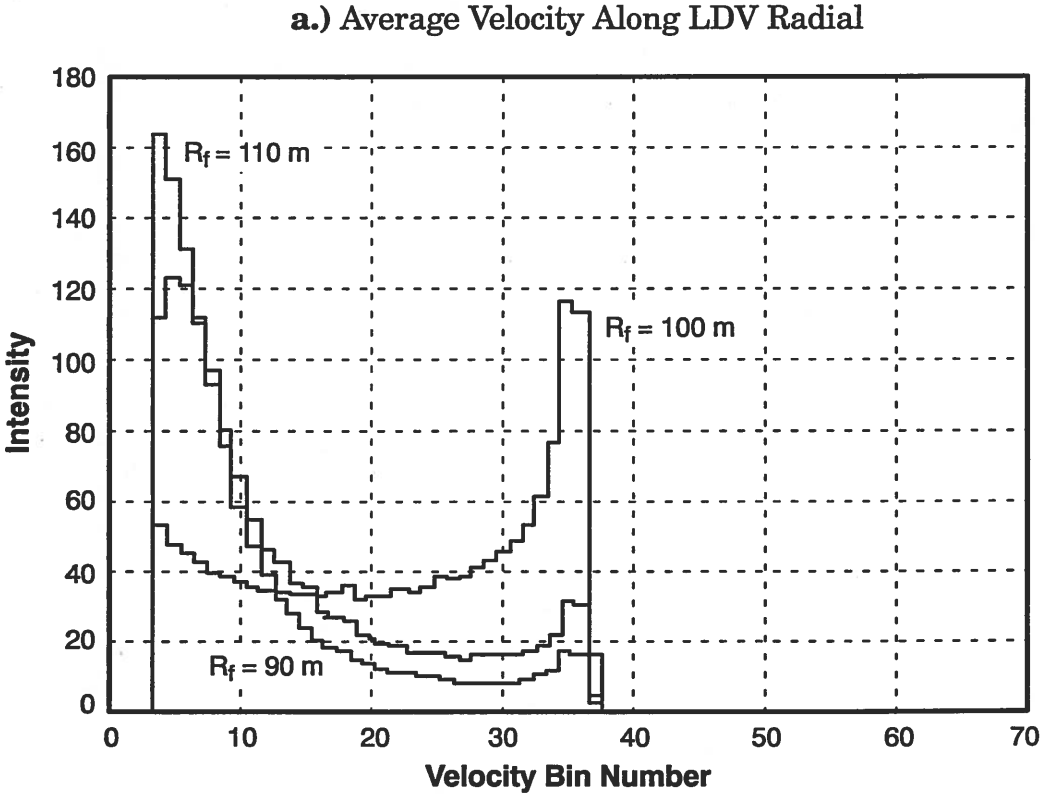

b.) SAW Spectra

Figure 2.3-2 The Effect of Misfocusing on Radial Scan

Table 2.3-3 Off-Focus Radial Scan Results
R_v = 100 m, R = 5 m (θ_f = 27.14 deg)

R_f (m)	V_t (m/sec)	V_{max} (m/sec)	TOTAL RETURNS	V_{max} RETURNS	V_{max} dB
90	19.07	18.55	1102	17	-16.7
95	19.07	18.55	1342	55	-6.5
100*	19.07	18.55	1486	116	0
105	19.07	18.55	1552	63	-5.3
110	19.07	18.55	1422	31	-11.5

*Reference Run results

Non-perpendicular Radial Scan Effects — Figure 2.3-3a contrasts the velocity profiles along the LDV radial for cutting angles of 0 and 30 deg. The corresponding power spectra are shown in Fig. 2.3-3b. The CA=0 condition corresponds to R = 5 m in the reference runs. It is clear that the peak sensed velocity at 30 deg is less than that at 0 deg. Table 2.3-4 summarizes results for cutting angles of 0, 15 and 30 deg. To first order the measured velocity is just the true tangential velocity, V_t, times the cosine of the cutting angle. There is a slight rise in return signal power at larger cutting angles due to the reduction in velocity change over the sampling volume.

Effect of Wind on Radial Scans — In this section the effect on the sensed velocity of a constant wind is examined. The geometry is that of Fig. 2.2-2, with θ_v = 30 deg and R_f = R_v = 100 m. A wind speed of 2 m/sec is assumed; results are shown in Fig. 2.3-4 for LDV elevation angles of 27 deg and 33 deg. The "with wind" results are contrasted with the cases where V_{wind}=0 and θ_f = 27 deg or 33 deg (curves are identical). At the higher elevation angle the wind adds to the vortex velocity, while at the lower elevation angle the opposite is true. Velocity profiles along the LDV radial are shown in Fig. 2.3-4a. At the lower elevation angle the net velocity becomes negative at roughly $\pm$16 m from the focal point. Of course, the LDV measures only velocity magnitude, which explains why the 27 deg curve reverses direction at those points. Referring to Fig. 2.3-4b, the spectral peaks with wind are seen to shift above and below the no-wind spectrum as one would expect. Table 2.3-5 lists numerical results for the wind effect radial scan runs. Total return power is slightly less with wind at the lower elevation because more of the radial velocity profile falls below bin 3 and is not counted. The opposite is true at the higher elevation angle.

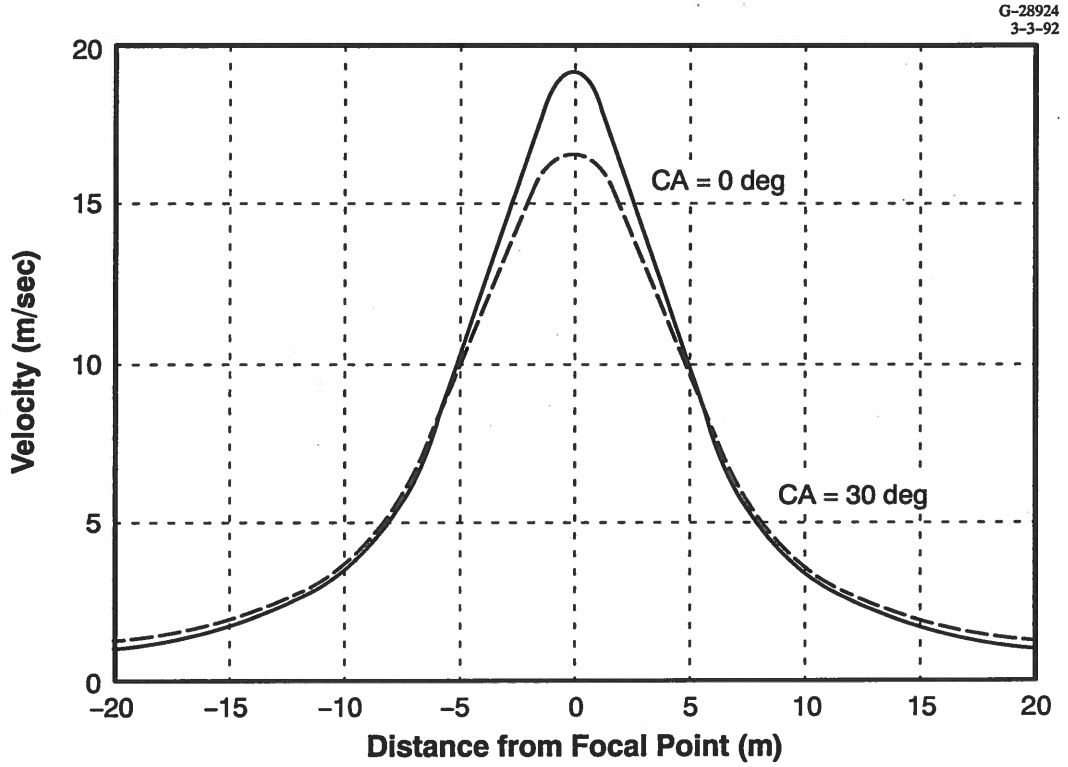

a.) Average Velocity Along LDV Radial

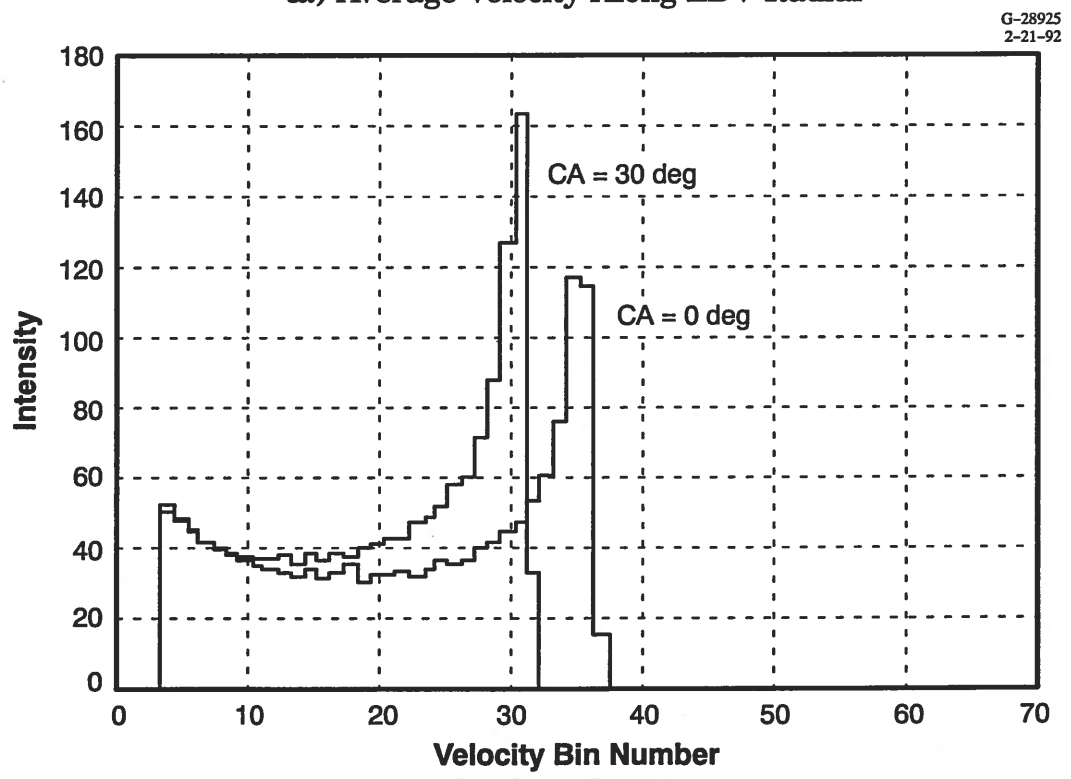

b.) SAW Spectra

Figure 2.3-3 Effect of Cutting Angle on Radial Scan

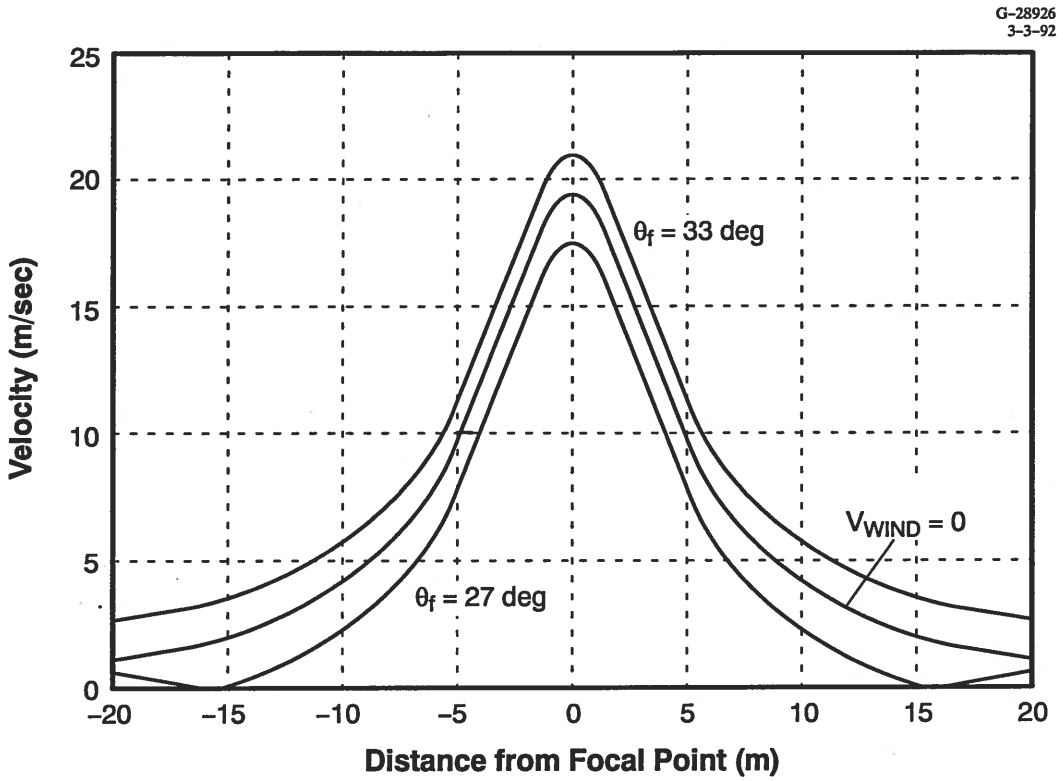

a.) Average Velocity Along LDV Radial

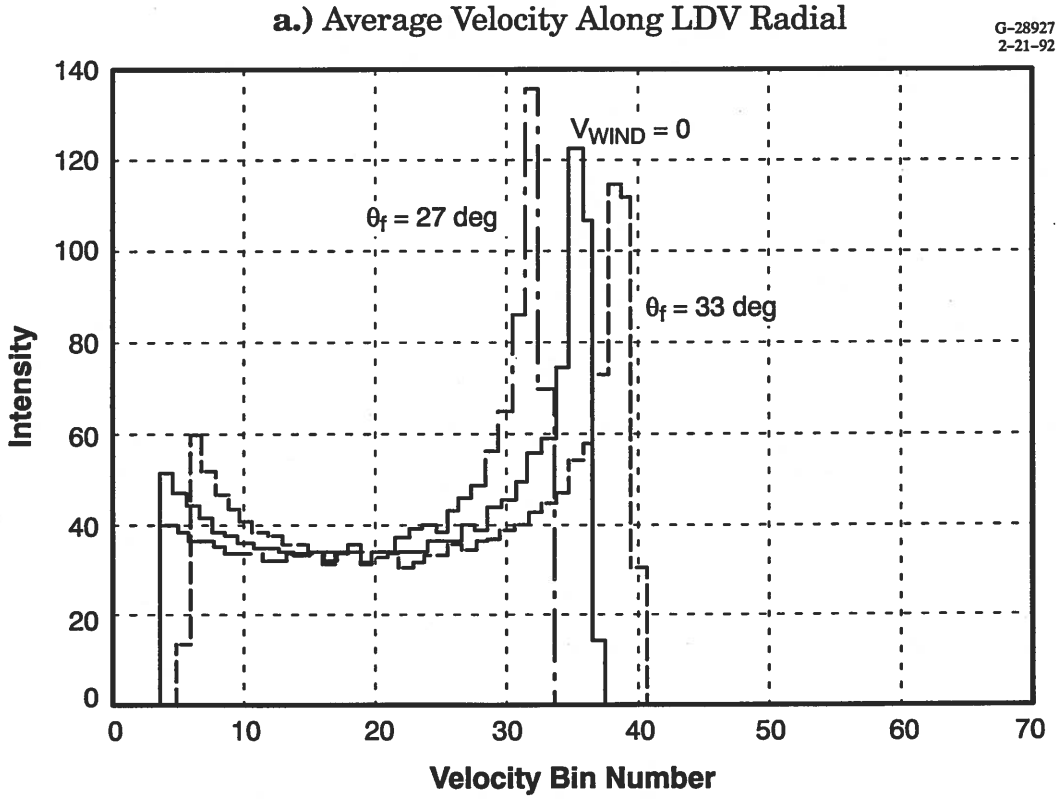

b.) SAW Spectra

Figure 2.3-4 The Effect of Wind on Radial Scan Results

2.3.2.1 Effect of LDV SAW Filter Limiting — The SAW Filter signal processor cannot detect velocity levels in excess of its 60 bin range, which corresponds to a maximum velocity of 31.8 m/sec. SAW filter limits are not exceeded at any point in the reference run. In order to attain velocities in excess of 31.8 m/sec, runs were made with core radii reduced to 1.5 and 1 m and compared with the 2 m reference run. Results are shown in Fig. 2.3-5 and Table 2.3-6 for R = 2.5 m (θ_f = 28.6 deg). Referring to the table first, notice that the SAW filter velocity estimate of 31.27 m/sec for the smaller radii falls in bin 59. With realistic noise levels the velocity error will generally be much larger. Examination of Figs. 2.3-1b and 2.3-5b makes clear what is happening. With a core radius of 2 m, the SAW filter spectrum peaks sharply at bin 57, just inside the filter bandwidth limit (Fig. 2.3-1b). For R_c = 1 m, the spectral peak would be at bin 72, well beyond the filter response limit. The region between 40 and 60 bins is very flat and of low signal power. The dashed line in Fig. 2.3-5b represents a typical real world noise level. Notice that with this noise level the max velocity estimate would be placed at bin 36 or 19.08 m/sec, grossly underestimating the true velocity.

Table 2.3-4 Non-respendicular Radial Scan Results
$R_v = R_f$ = 100 m, R = 5 m (θ_f = 27.14 deg)

CA (deg)	V_t (m/sec)	V_{max} (m/sec)	TOTAL RETURNS	V_{max} RETURNS	V_{max} dB
0*	19.07	18.55	1486	116	0
15	19.07	18.02	1491	135	+1.3
30	19.07	16.43	1507	162	+2.9

*Reference Run results

Table 2.3-5 Effect of Wind on Radial Scans
$R_v = R_f$ = 100 m

θ_f (deg)	V_{wind} (m/sec)	V_t (m/sec)	V_{max} m/sec	TOTAL RETURNS	V_{max} RETURNS	V_{max} (dB)
33	2	-18.27	19.61	1570	147	0
33	0	-18.27	18.02	1493	146	0
27	0	18.27	18.02	1493	147	0
27	2	18.27	15.90	1337	126	-1.3

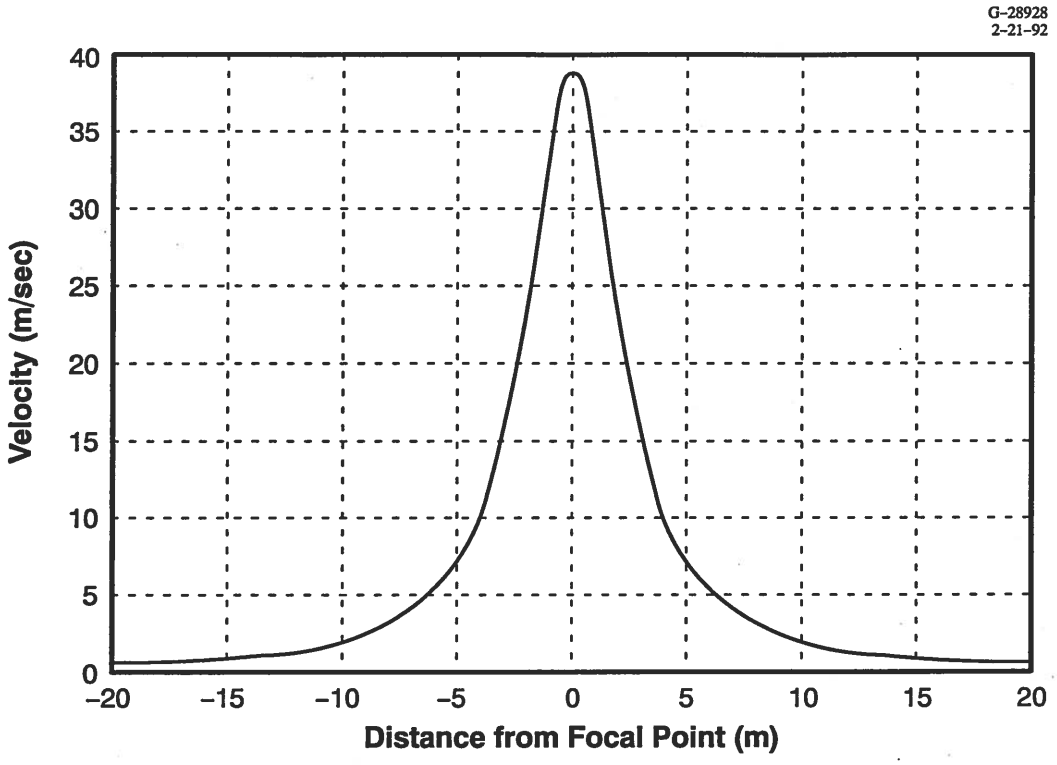

a.) Average Velocity Along LDV Radial

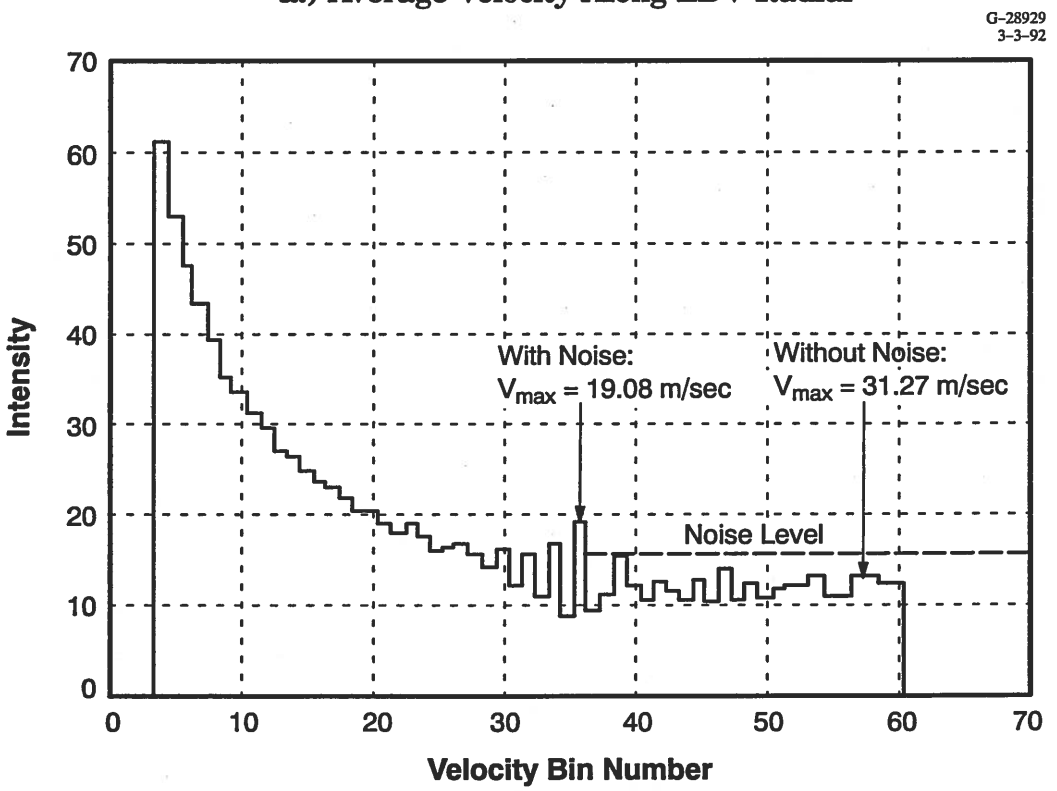

b.) SAW Spectra

Figure 2.3-5 The Effect of SAW Filter Limiting on Radial Scan Results (R_c = 1 m)

Table 2.3-6 Effect of Velocity Limiting on Radial Scan
$R_v = R_f = 100$ m, R = 2.5 m ($\theta_f = 28.6$ deg)

R_c (m)	V_t (m/sec)	V_{max} (m/sec)	TOTAL RETURNS	V_{max} RETURNS	V_{max} dB
2.0*	30.20	30.21	1360	65	0
1.5	35.86	31.27	1137	16.3	-12
1.0	38.19	31.27	1103	13.2	-13.8

*Reference Run results

2.3.3 LDV Angle Scan Studies

In this group of simulations the effects of off-focus scanning, wind, non-perpendicular scanning and LDV SAW filter limiting on the estimation and recovery of vortex and wind parameters is examined. As with the radial scan studies of Section 2.3.2, a reference run is made first to establish a baseline against which off-nominal conditions may be compared.

The Reference Angle Scan — Conditions for the angle scan reference run are listed in Table 2.3-7. In all cases to follow the vortex is placed 30 deg above the horizontal at a range of 100 m and the LDV is scanned from 24 deg to 36 deg above horizontal. For the reference run the LDV is focused at 100 m with V_{wind} and the cutting angle, CA, set to zero.

Table 2.3-7 Angle Scan Reference Run Conditions

R_f	=	$R_v = 100$ m
R_c	=	2 m
V_{peak}	=	30.18 m/sec
Γ	=	600 m^2/sec
θ_v	=	30 deg
θ_f	=	24 deg – 36 deg

Angle scan reference run results are summarized in Fig. 2.3-6. Figure 2.3-6a compares the true vortex radial velocity with the LDV velocity measurement. The velocity error is shown in Figure 2.3-6b. Notice that that the error is on the order of one quantum level or less for distances of 3 m or more from the core center. Inside 3 m the error is generally much larger. This is consistent with the radial scan results of the previous section, and again confirms the observation that in the noise-free case averaging error dominates

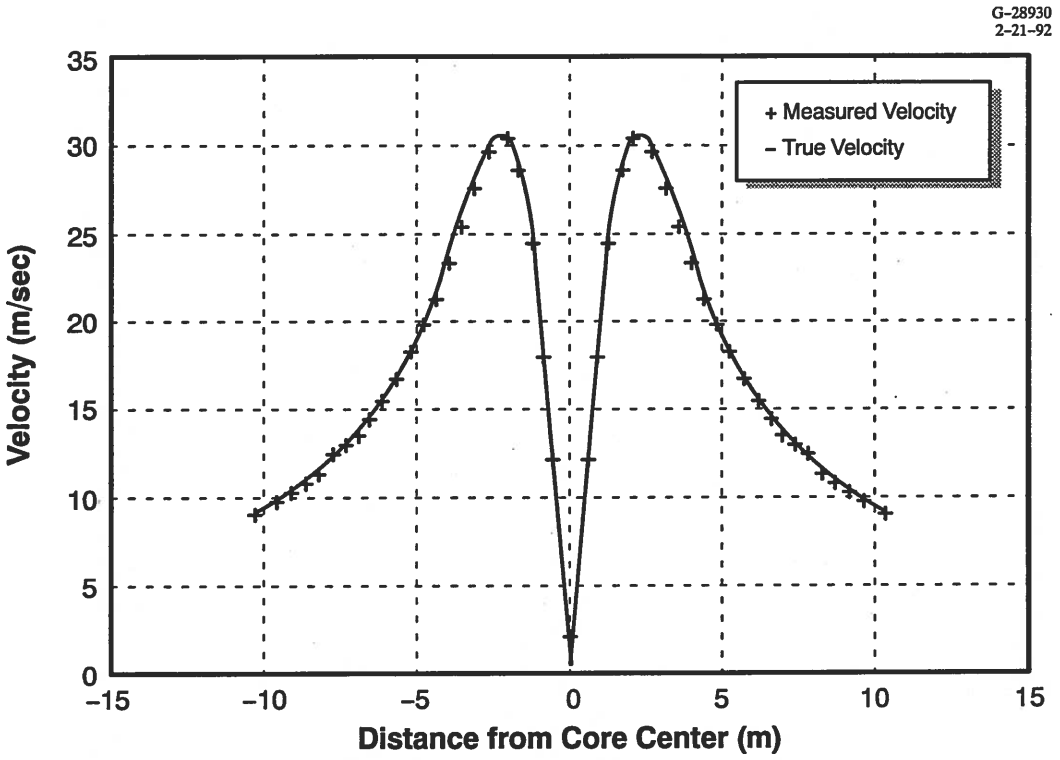

a.) True vs. Measured Radial Velocity

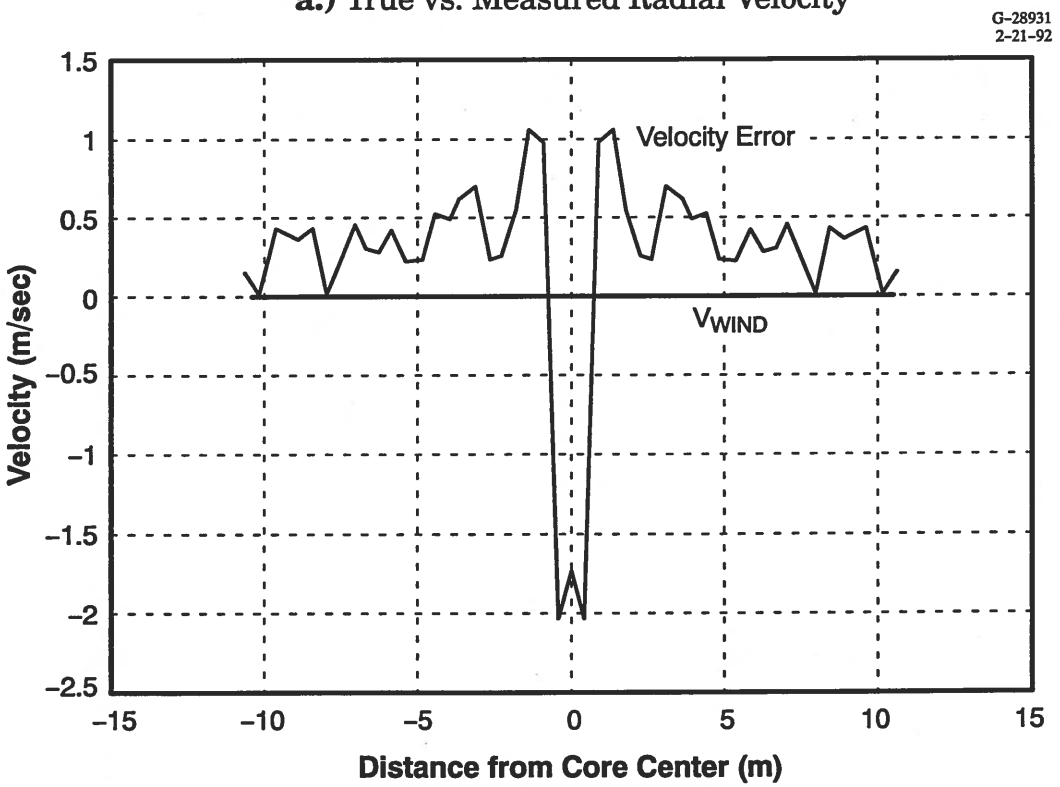

b.) Radial Velocity Error and Wind Velocity

Figure 2.3-6 Angle Scan Reference Run

quantization error in the regions where velocity is changing rapidly relative to the averaging time. The values for Γ, R_c, V_{peak} and V_{wind} estimated by the least squares algorithm formulated during this effort are given in Table 2.3-8. V_{peak} is simply the peak tangential velocity computed from the Lamb model (Eq. 2.2-1) using the estimated values for Γ and R_c. Estimator theory and performance will be discussed in more detail in Sections 2.4 and 3.3.

Wind Effect — Figure 2.3-7a compares LDV velocity estimates against the true radial velocity in the presence of a 2 m/sec constant wind. Notice that the LDV under estimates vortex velocities below the core and over estimates those at positions above the core. This is consistent with the earlier radial scan results. Figure 2.3-7b presents the tangential velocity error and also plots the wind velocity sense with reversed sign relative to vortex velocity. Notice how the raw velocity error tends to track the effect of the wind. Thus the wind effect is highly visible in the velocity error data and is easily estimated with a properly designed algorithm. Values for Γ, R_c, V_{peak} and V_{wind} are compared against the reference run in Table 2.3-8. Notice that the estimates of Γ and R_c are affected little by the wind when estimated with an algorithm that accounts for wind.

Table 2.3-8 Off-Focus Effects With and Without Wind (R_v = 100m)

FOCAL RANGE (m)	V_{wind} (m/sec)	$\hat{\Gamma}$ (m^2/sec)	$\hat{V}_{wind}$ (m/sec)	$\hat{R}_c$ (m)	$\hat{V}_{peak}$ (m/sec)
110	0	647	-0,04	2.2	29.49
110	2	649	1.85	2.2	29.50
*100	0	598	-0.04	2.0	29.90
100	2	592	1.84	2.0	29.68
90	0	532	-0.05	1.8	29.60
90	2	529	1.83	1.8	29.40

*Reference run results

Off-Focus Scanning Effect— Off-focus scan results are illustrated in Fig. 2.3-8 for the case where R_f = 90 m. All other conditions are as in the reference run. Recall from the radial scan studies that the LDV tends to measure the peak tangential velocity correctly even when off-focus (although with reduced signal power) because of the great extent of the sampling volume. Fig. 2.3-8b, however, shows a velocity error far in excess of the quantization error. The error arises because the correctly measured velocity is placed at the wrong location. Distance along the scan is determined by an arc length calculation using

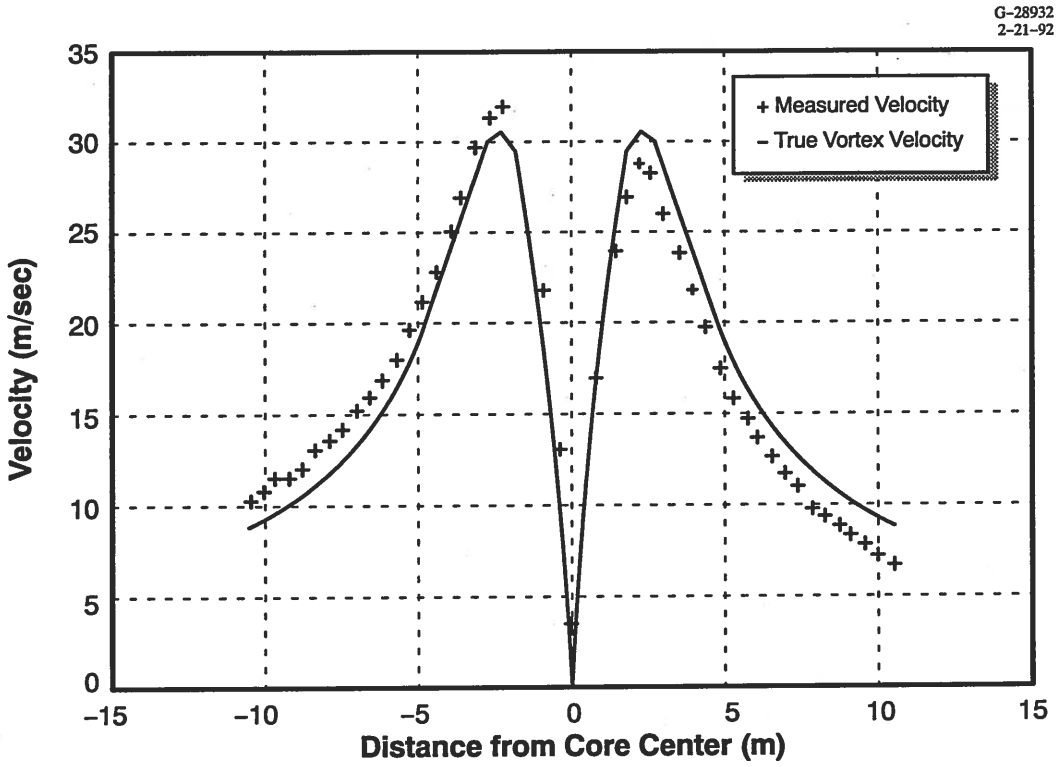

a.) True vs Measured Radial Velocity

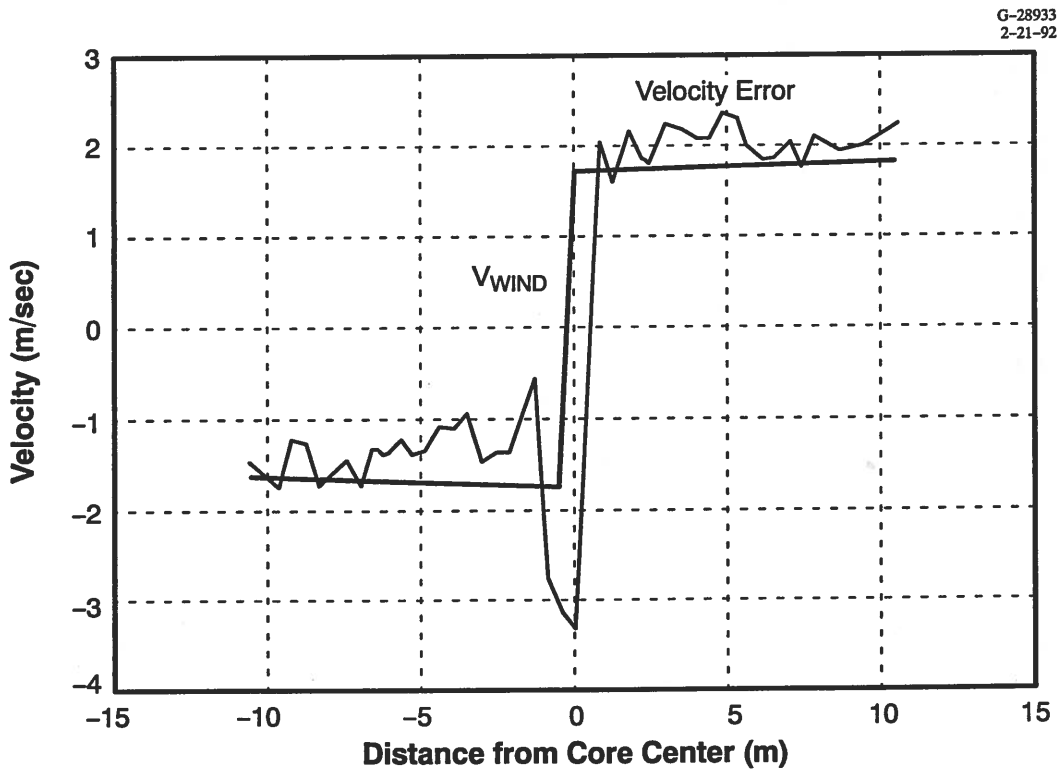

b.) Radial Velocity Error and Wind Velocity

Figure 2.3-7 Effect of Wind on Angle Scan Results

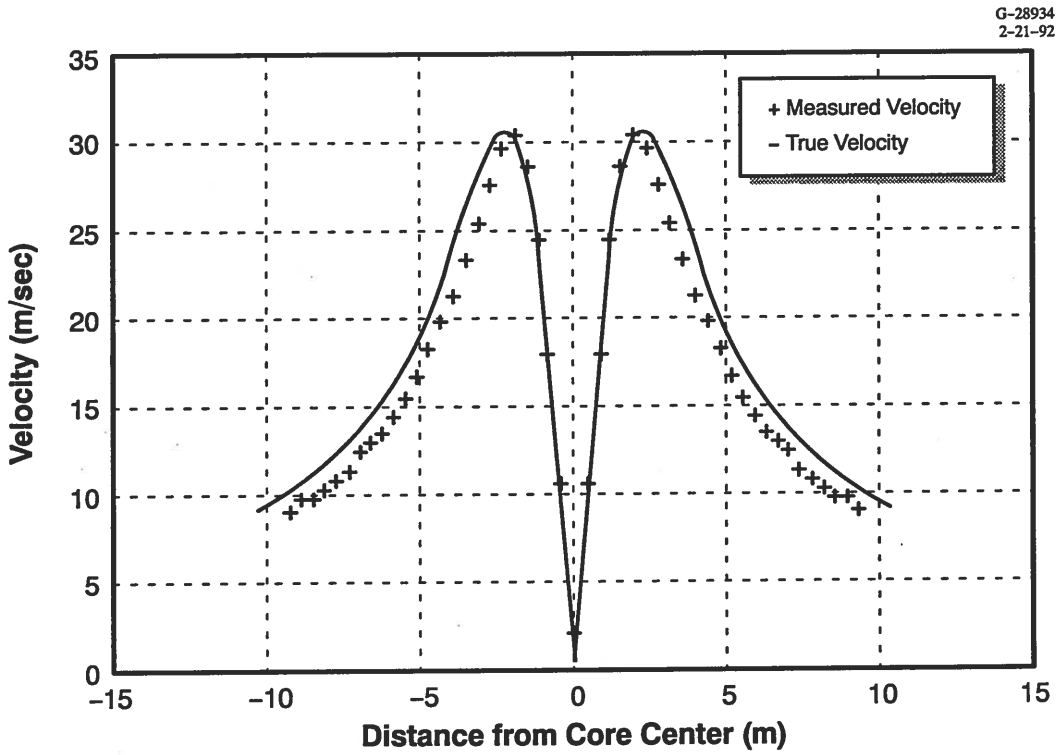

a.) True vs. Measured Radial Velocity

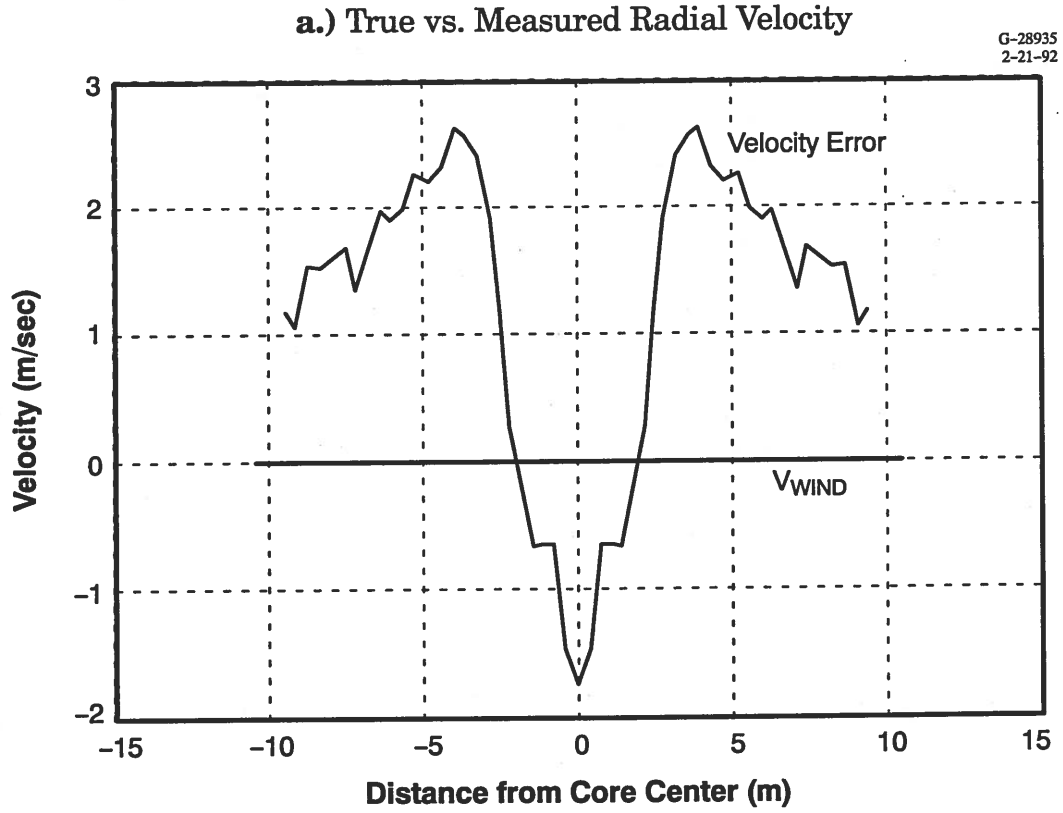

b.) Radial Velocity Error and Wind Velocity

Figure 2.3-8 The Effect of Off-Focus Scanning on Angle Scan Results (1 of 2)

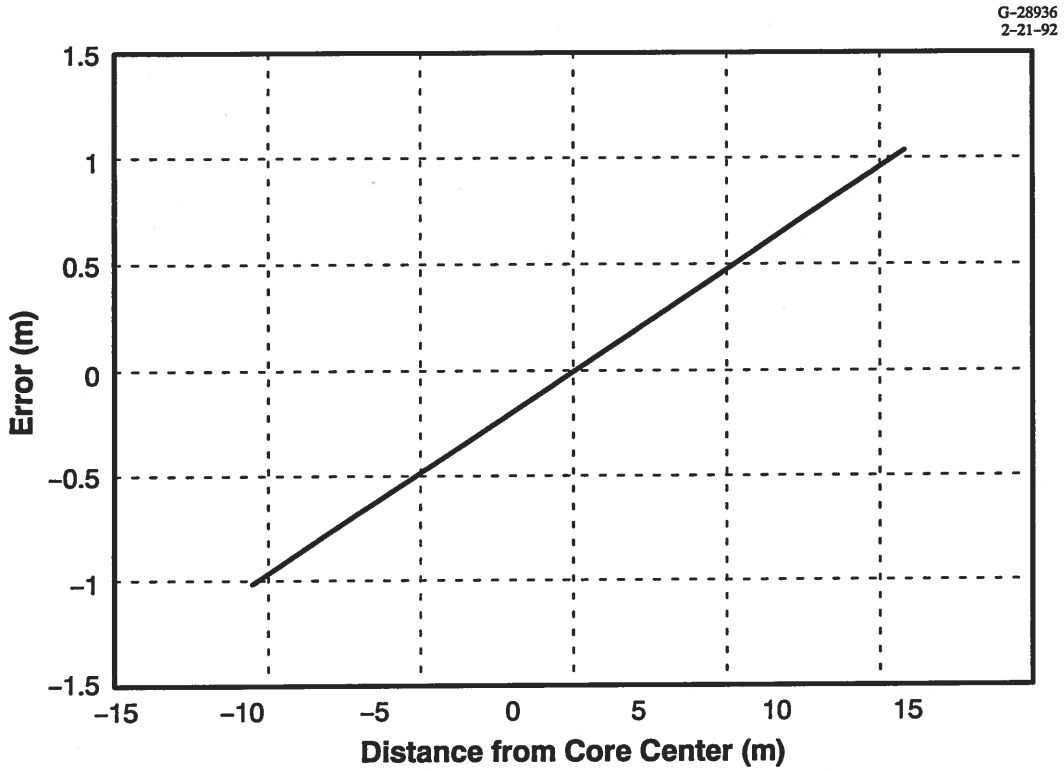

c.) Error in Location of Velocity Measurement

Figure 2.3-8 The Effect of Off-Focus Scanning on Angle Scan Results (2 of 2)

the angle traversed times the distance to the focal point. A 10% difference between R_v and R_f leads directly to a 10% error in linear position (although the angular position is correct). For example, at an elevation angle of 24.74 deg, the LDV correctly measures a velocity of 9.54 m/sec. This velocity corresponds to a location 10 m from the core center. However, because the LDV is focused at 90 m, it places this velocity point 9 m out from the core center. Radial location error for this run is shown in Fig. 2.3-8c.

Vortex parameter estimator performance for a sequence of off-focus runs with R_f ranging from 90 m to 110 m is summarized in Table 2.3-8. If the focal range is short of the true range the estimated vortex span is compressed. For this situation the vortex parameter estimation algorithm reduces the core strength and the core radius to make the Lamb model fit the data. If the focal range exceeds the true range the opposite occurs. For range errors on the order of 10% or less, the errors in Γ and R_c are of the same order. The effect of errors in Γ and R_c on the estimate for V_{peak} are of the opposite sense and thus almost cancel. Note that any scheme for estimating vortex parameters will suffer the same order of error due to off-focus conditions.

Nonperpendicular Scan Effects — Simulation results for cutting angles of 15 deg and 30 deg are shown on Fig. 2.3-9. Vortex parameter estimates for these runs are summarized in Table 2.3-9. Recall from the radial scan studies that the measured tangential velocity is to first order simply the true velocity times the cosine of the cutting angle, CA. From the figure it is clear that the measured velocity is everywhere less than the true velocity. For the 30 deg case the velocity error exceeds quantization error at every point. The estimates of core strength listed in Table 2.3-9 are also low and, to within the effects of quantization error, just the true vortex strength times the cosine of the cutting angle. Because core radius is correctly estimated, however, errors in estimated peak velocity are also low by a factor of cosine CA. For cutting angles of 15 deg and 30 deg, these factors are 3% and 13% , respectively.

Table 2.3-9 Cutting Angle Effect With and Without Wind

CUTTING ANGLE (deg)	V_{wind} (m/sec)	$\hat{\Gamma}$ (m^2/sec)	$\hat{V}_{wind}$ (m/sec)	$\hat{R}_c$ (m)	$\hat{V}_{peak}$ (m/sec)
0	0	598	-0.04	2.0	29.90
0	2	593	-0.04	2.0	29.60
15	0	572	-0.04	2.0	28.60
15	2	572	1.91	2.0	28.68
30	0	507	-0.05	2.0	25.40
30	2	511	1.85	2.0	25.60

Effect of LDV Velocity Limiting — In this group of two simulations the vortex core radius was reduced to obtain tangential velocities that exceed the upper limit of the SAW filter frequency response. All other parameters were as given for the reference run. Figures 2.3-10a and 2.3-10c show results for core radii 1.5 m and 1 m, respectively. In both cases the LDV response saturates at 31.8 m/sec in a region surrounding the core radius. Figures 2.3-10b and 2.3-10d show that velocity error rises substantially between 1 m and 3 m from the core center. Performance of the vortex parameter estimator for these runs is highlighted in Table 2.3-10. In both cases core strength is underestimated and core radius is overestimated. These results are consistent with the flattened shape of the measured velocity profile. In the worst case, core strength estimation error is no more than 8%. However, R_c is overestimated by 50% leading to an error in peak velocity of 38%. The models fitted to the data are shown in Fig. 2.3-11a and 2.3-11b. Fit in the tails of the data is excellent and accounts for the good estimate of Γ. Fit in the region around core radius is poor due

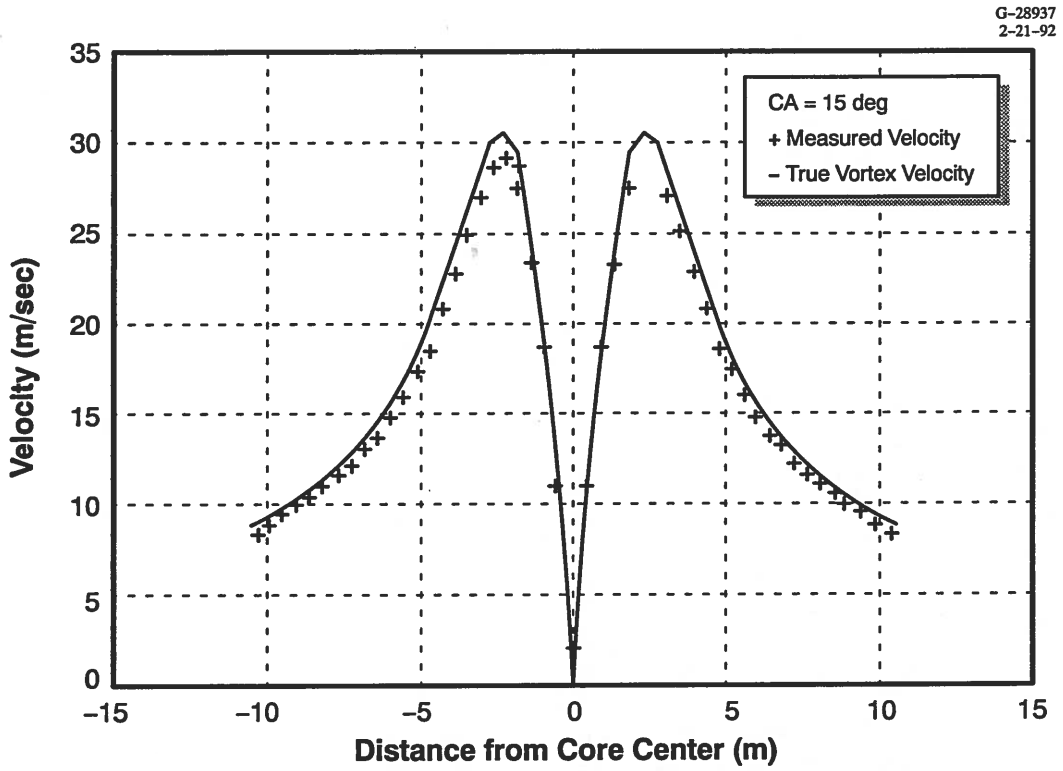

a.) True vs. Measured Radial Velocity

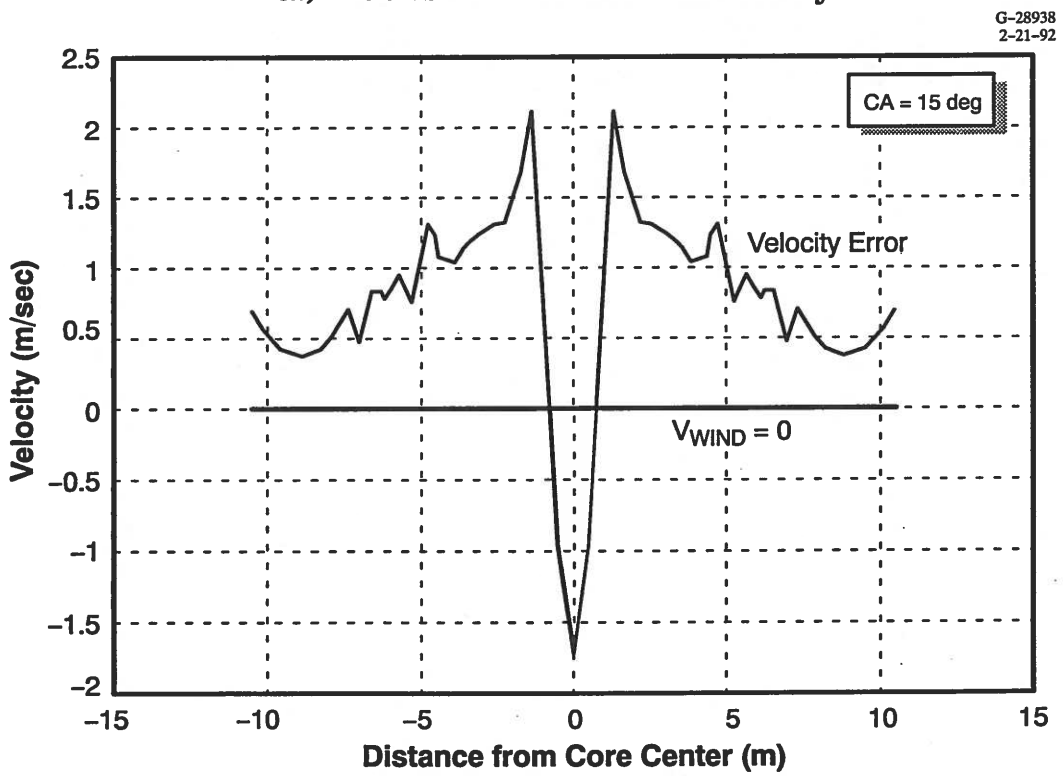

b.) Radial Velocity Error and Wind Velocity

Figure 2.3-9 Effect of Cutting Angle on Angle Scan Results (1 of 2)

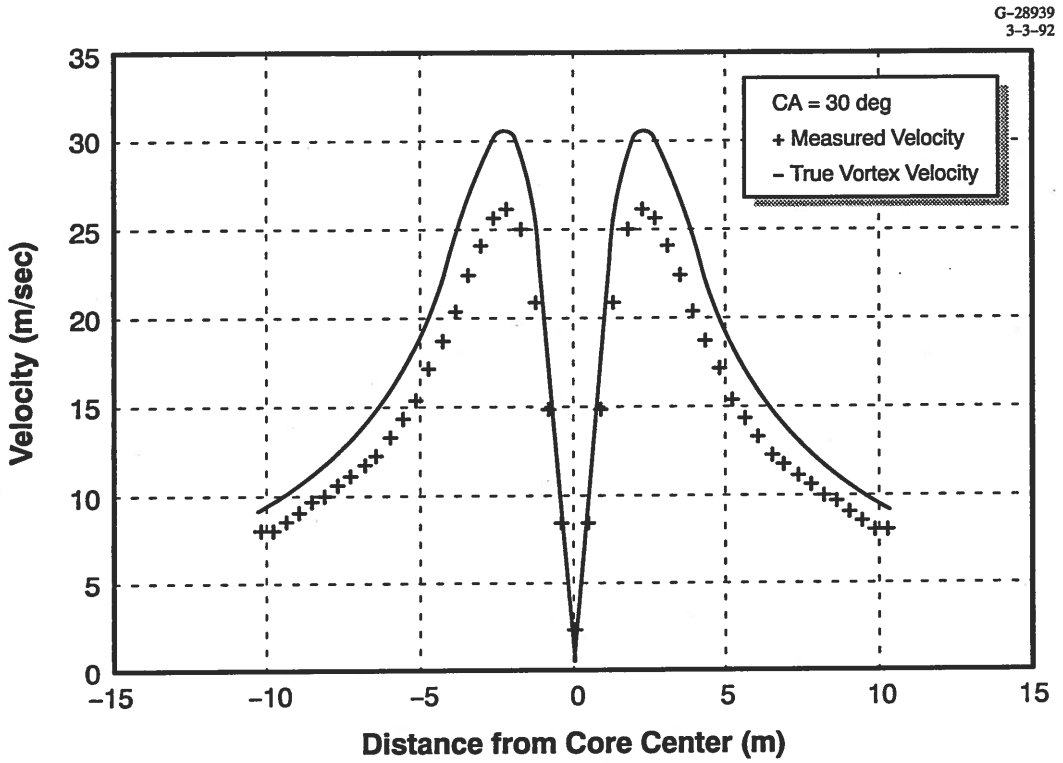

a.) True vs. Measured Radial Velocity

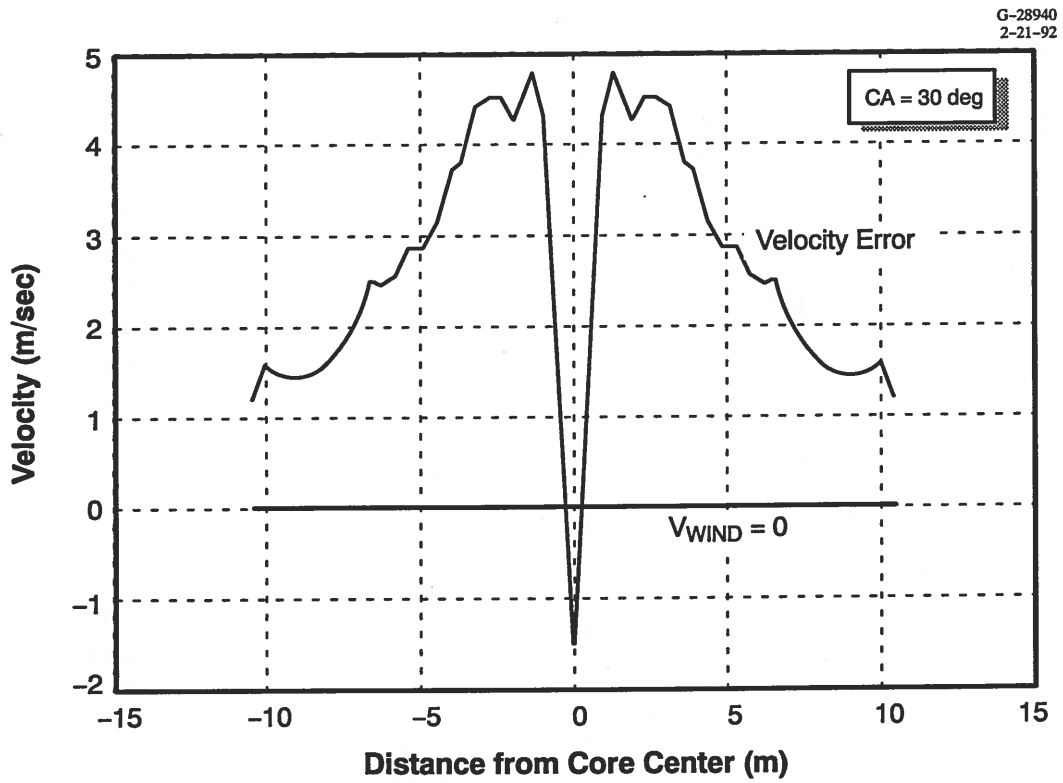

b.) Radial Velocity Error and Wind Velocity

Figure 2.3-9 Effect of Cutting Angle on Angle Scan Results (2 of 2)

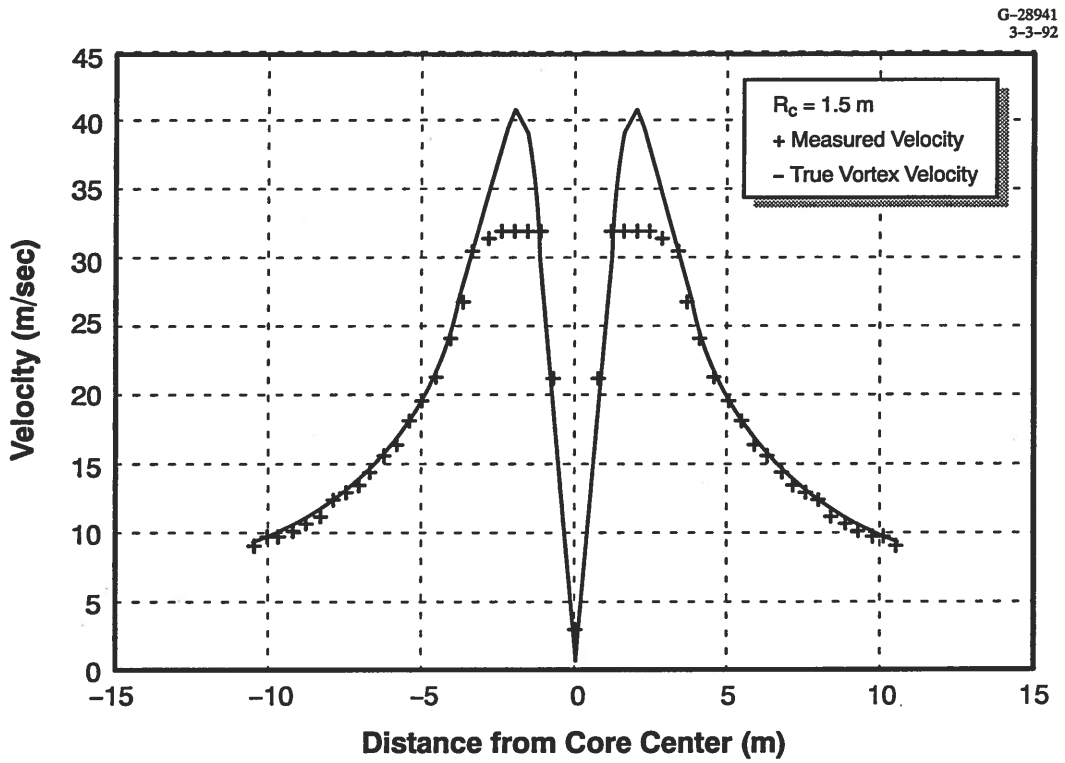

a.) True vs. Measured Radial Velocity

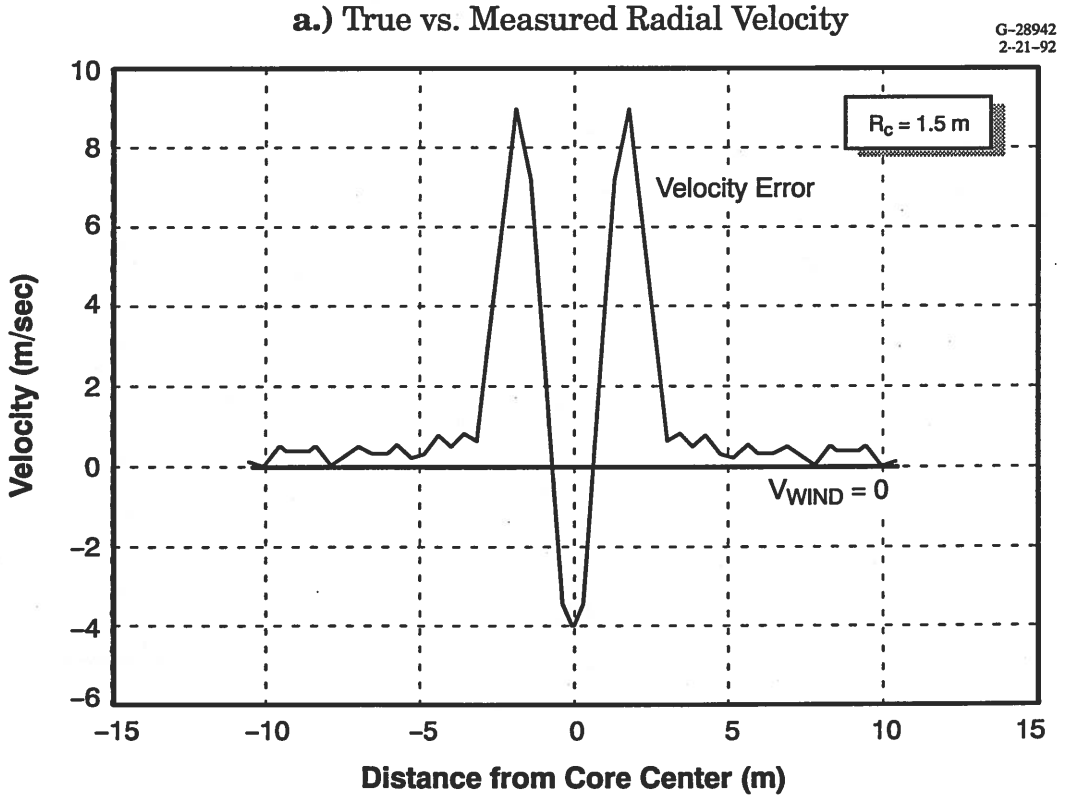

b.) Radial Velocity Error and Wind Velocity

Figure 2.3-10 The Effect of Velocity Limiting of Angle Scan Results (1 of 2)

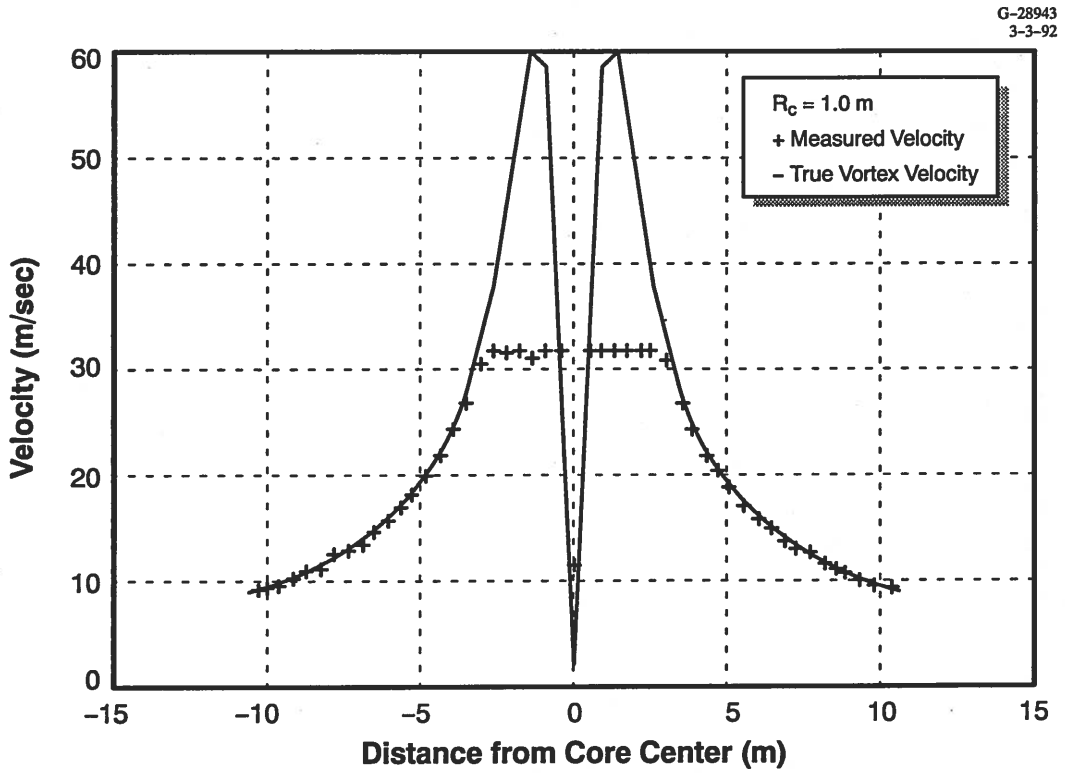

c.) True vs. Measured Radial Velocity

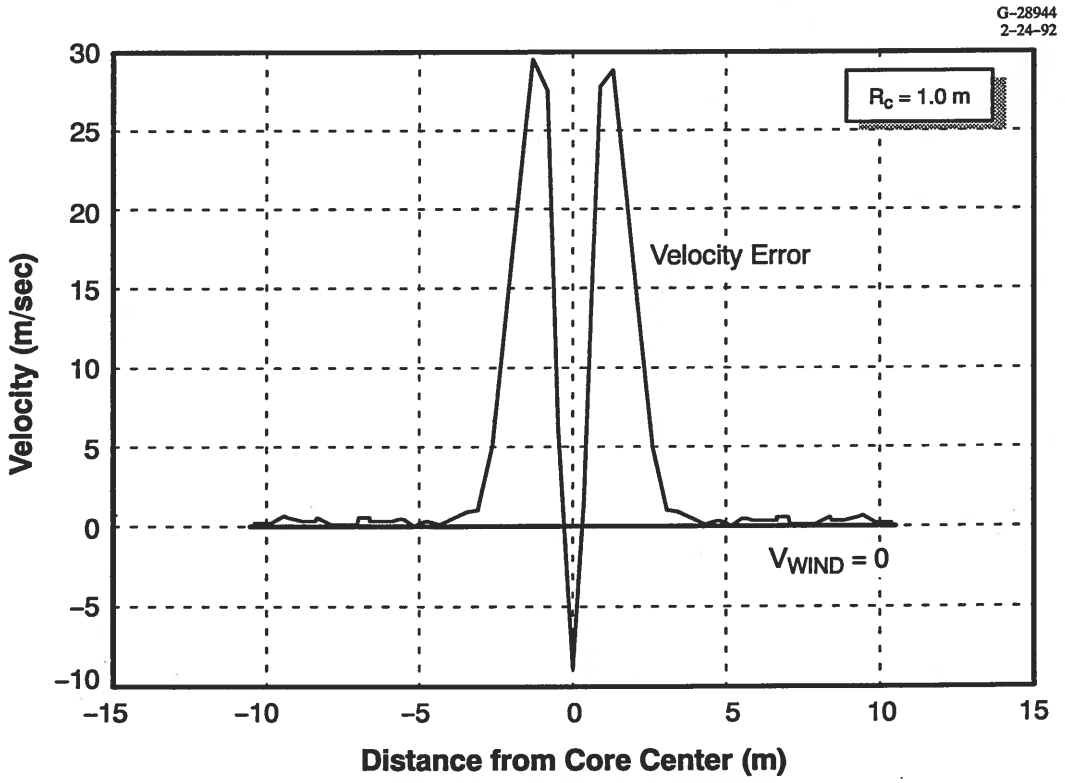

d.) Radial Velocity Error and Wind Velocity

Figure 2.3-10 The Effect of Velocity Limiting of Angle Scan Results (2 of 2)

to data limiting. Model based estimates of R_c and therefore peak vortex velocity are greatly influenced by the quality of the data near the core radius. At distances of more than $2R_c$ from the core vortex velocity is independent of R_c. As further discussed in Section 2.4, estimates of Γ are improved by removing bad data points in the core region from the estimation process.

Table 2.3-10 SAW Filter Limiting Effect With and Without Wind

R_c (m)	V_{peak} (m/sec)	V_{wind} (m/sec)	$\hat{\Gamma}$ (m^2/sec)	$\hat{V}_{wind}$ (m^2/sec)	$\hat{R}_c$ (m)	$\hat{V}_{peak}$
2*	30.18	0	598	-0.04	2.0	29.98
2	30.18	2	593	1.84	2.0	29.73
1.5	40.24	0	571	-0.11	1.6	35.78
1.5	40.24	2	569	1.39	1.6	35.67
1.0	60.36	0	555	-0.28	1.5	37.10
1.0	60.36	2	557	1.2	1.5	37.23

*Reference run results

Combined Effects — In the following paragraphs, LDV and vortex parameter estimator response to pairwise off-nominal conditions are examined. Pairs considered are:

- Off-focus plus wind,
- Non-perpendicular scanning plus wind,
- SAW filter limiting plus wind
- Off-focus with non-perpendicular scanning plus wind.

The purpose of these runs is to show that the wind signature, whose effect on measured velocity changes abruptly and uniquely as the LDV scan passes through core center, is easily separable form other contaminations in measured velocity.

Off-Focus Plus Wind — The results of a simulation run with R_f = 90 m and a wind speed of 2 m/sec are shown in Fig. 2.3-12. In the case of wind only (viz, without mis-focusing, Fig. 2.3-7), measured velocity points fall below true velocity to the right of core center and are above true velocity to the left. When focused at 90 m with no wind (Fig. 2.3-8), all measured velocity points fell below the true velocity curve. As shown in Fig. 2.3-12a, the combined effects of both off nominal conditions are canceled to the left of center and added to the right of core center. Figure 2.3-12b clearly shows the abrupt change in the velocity error profile around core center, characteristic of the presence of wind.

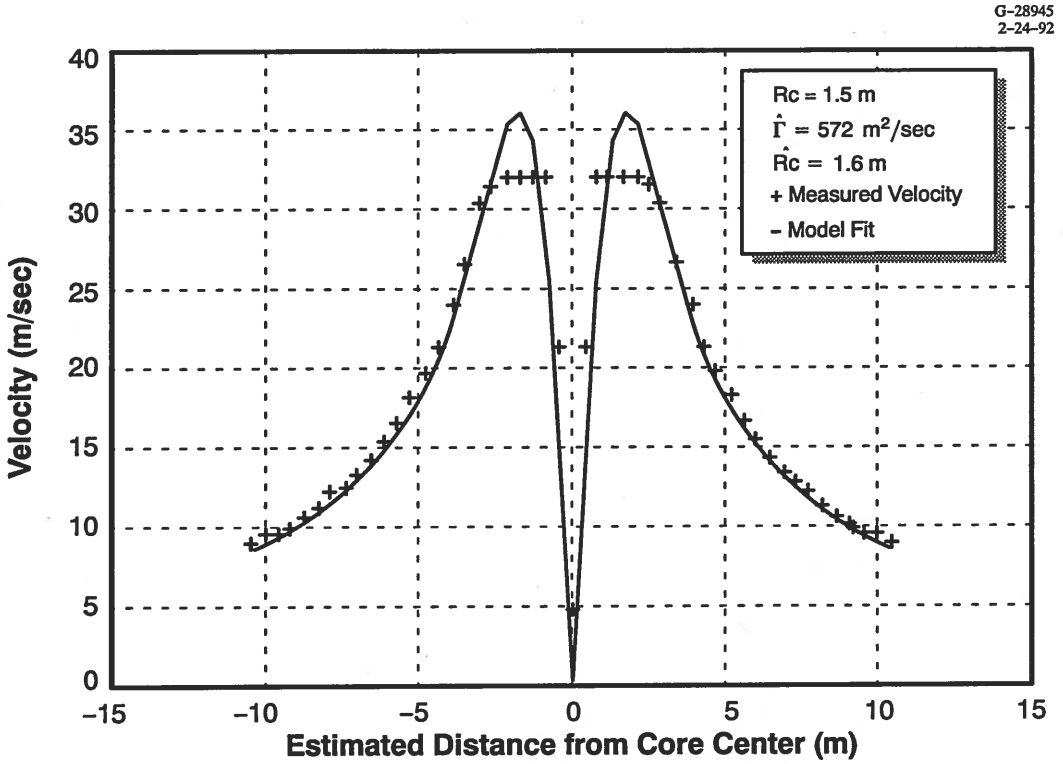

a.) Model Fit to Data Points

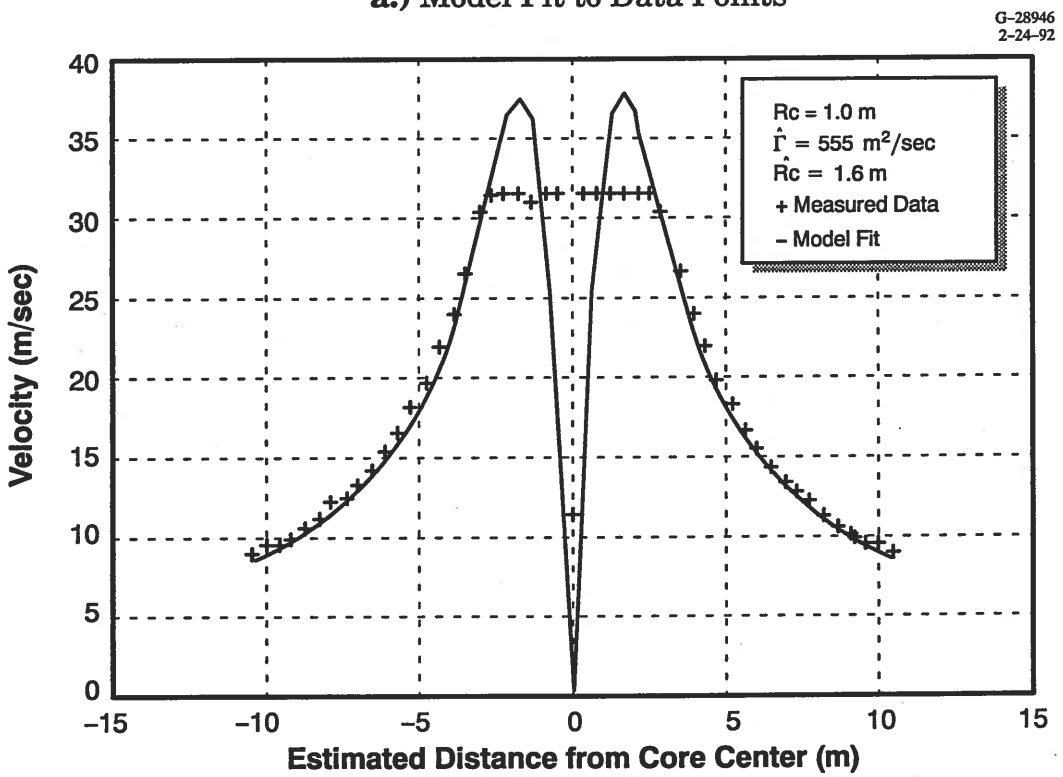

b.) Model Fit to Data Points

Figure 2.3-11 Model Fits to Velocity Limiting Runs of Figure 2.3-10

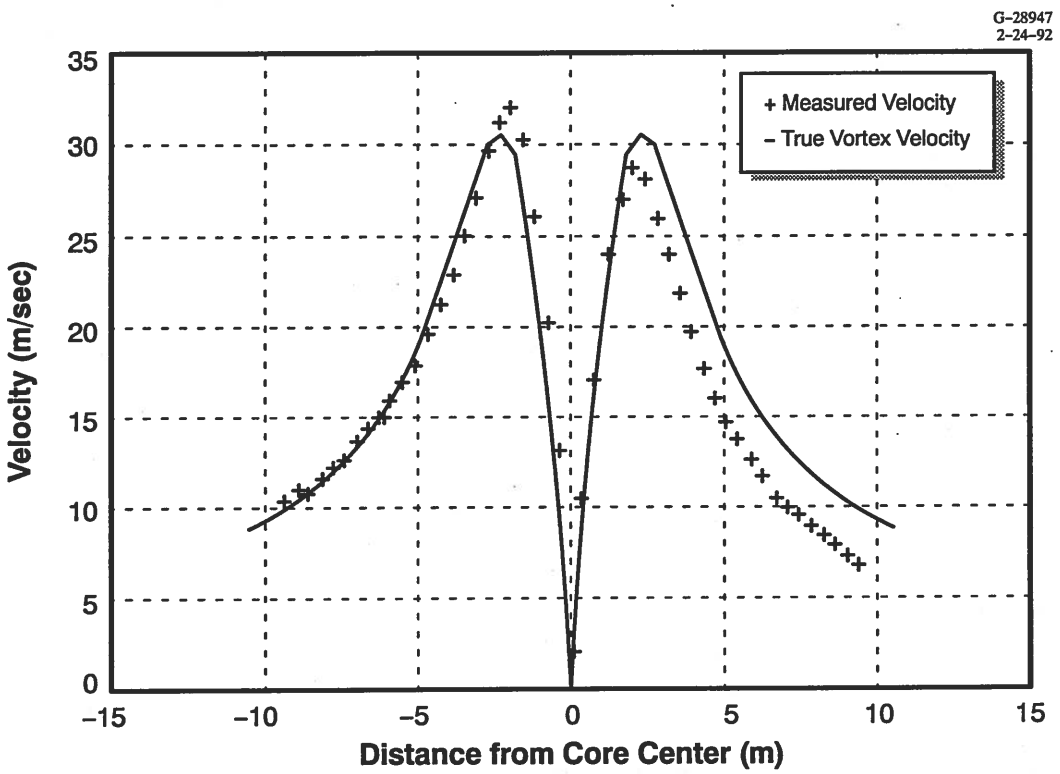

a.) True vs. Measured Radial Velocity

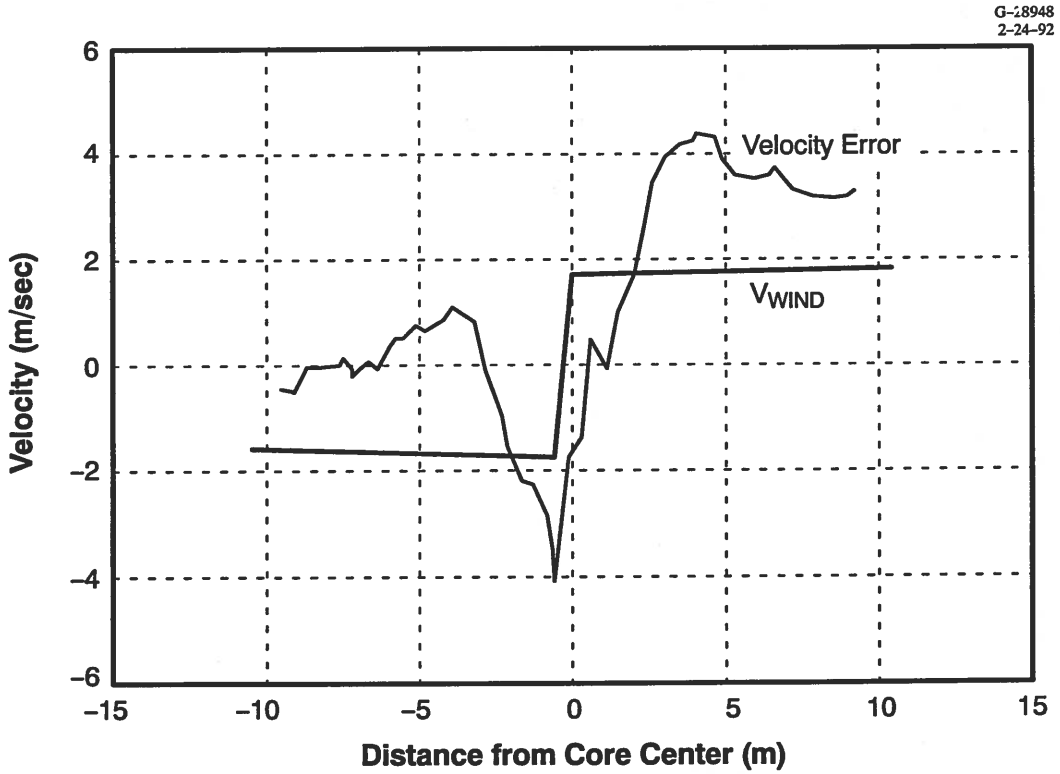

b.) Radial Velocity Error and Wind Velocity

Figure 2.3-12 Effects of Off-focus Plus Wind on Angle Scan Results

Vortex parameter estimator results are summarized in Table 2.3-8. Notice two things: Estimates of Γ, V_{peak} and R_c are essentially the same whether wind is present or not; and when present, wind speed along the LDV radial is recovered with good accuracy.

Nonperpendicular Scanning plus Wind — A typical result for these runs is shown in Fig. 2.3-13, where CA = 30 deg and V_{wind} = 2 m/sec. The effect of non-perpendicular scanning is very much like that of miss-focusing short of true range, and the resulting plots are similar to those of Fig. 2.3-12. In particular, the large jump in velocity error around core center should be noted. Table 2.3-9 summarizes vortex parameter estimator performance for these runs. Again it is seen that the estimates of Γ, V_{peak} and R_c are little changed by the presence of wind.

SAW Filter Limiting plus Wind — Figure 2.3-14 presents a typical results for this case where R_c = 1 m and V_{wind} = 2 m/sec. Notice the very rapid rise in velocity error starting about 3 m from the core center. At this point velocity has exceeded the upper limit of the SAW filter response and the velocity measurement saturates. Peak errors of 30 m/sec are experienced. Table 2.3-10 summarizes the results for these runs and compares them with the zero-wind case. Notice, as in all the other runs with two off-nominal conditions, that the estimates for Γ, and R_c are unaffected by the presence of the wind. Unlike the other cases, however, the velocity limiting does result in underestimating Γ and overestimating R_c. This in turn causes V_{peak} to be underestimated.

Non-perpendicular Scanning, Off-Focus Plus Wind — As a final example we consider two off-nominal conditions, off-focusing and non-perpendicular scanning with and without wind. Results for these runs are listed in Table 2.3-11. Results are also plotted for CA = 15 deg, V_{wind} = 2 m/sec and values of 95 and 105 m respectively in Figs. 2.3-15 and 2.3-16. Errors produced by short focusing at 95 m combined with a cutting angle of 15 deg, add to produce a 10% low error in estimating Γ. However the short focus produces a 5% low error in estimating R_c, partially offsetting the error in V_{peak}, which is also 5%. The estimated values for Γ, V_{wind}, and R_c are used to compute an estimated velocity profile. This profile is compared with the LDV measured velocity points in Figs. 2.3-15c and 2.3-16c. The fit is seen to be excellent.

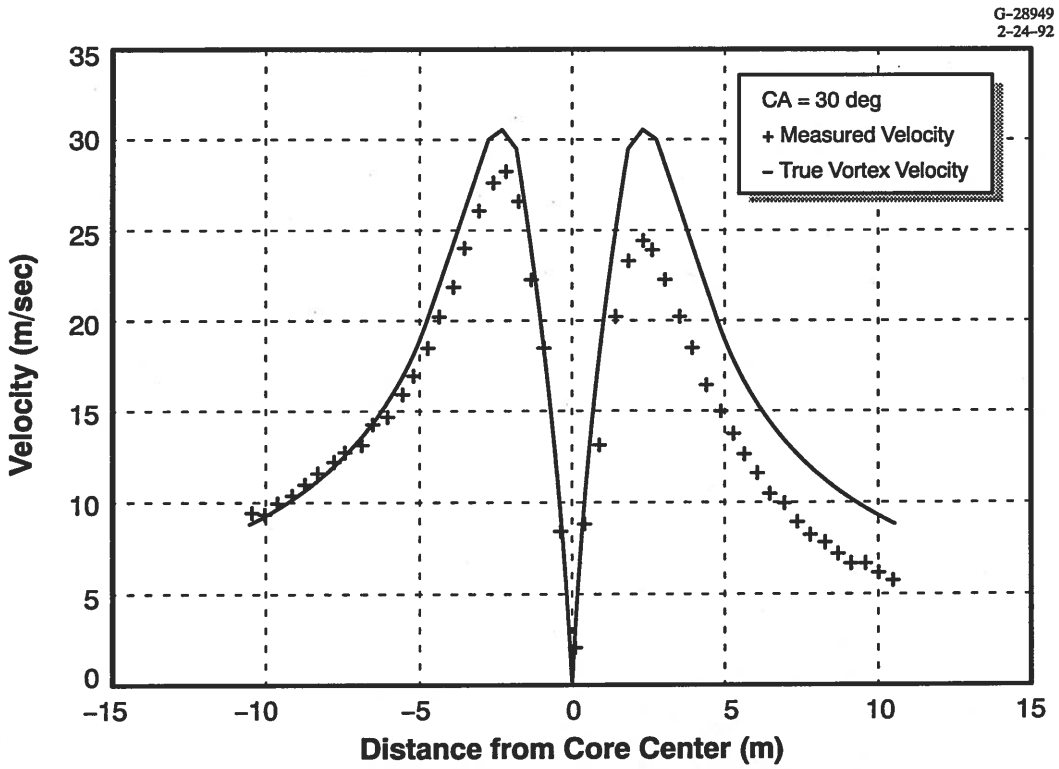

a.) True vs. Measured Radial Velocity

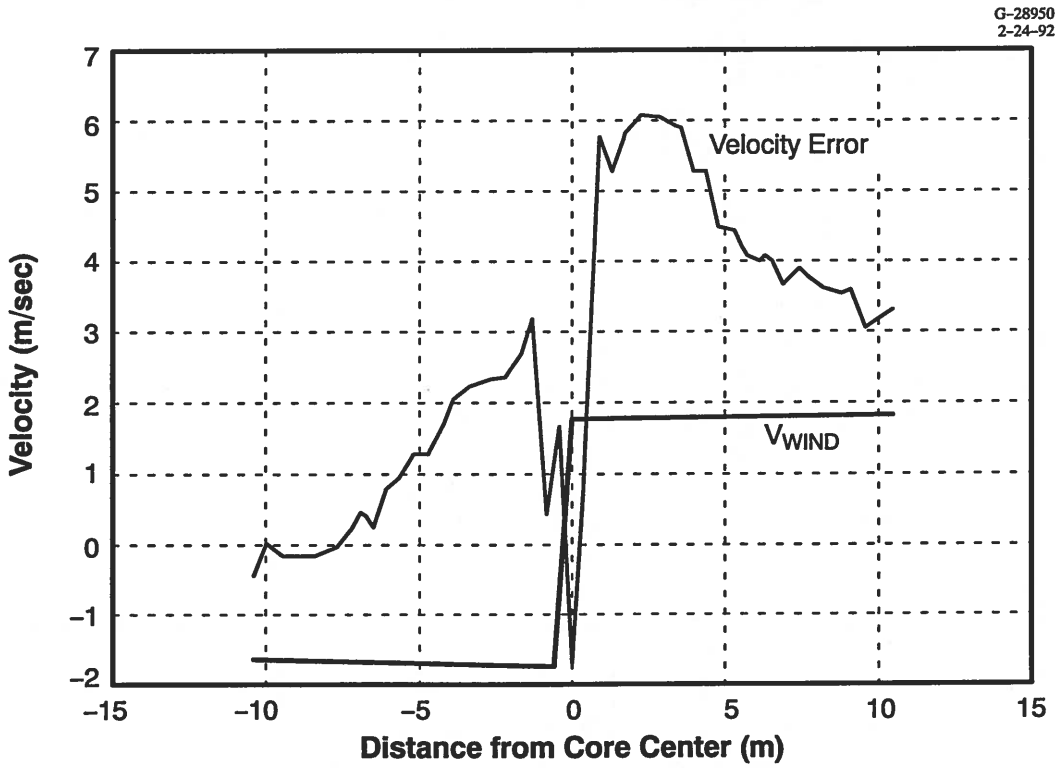

b.) Radial Velocity Error and Wind Velocity

Figure 2.3-13 The Effect of Non-perpendicular Scanning Plus Wind on Angle Scans

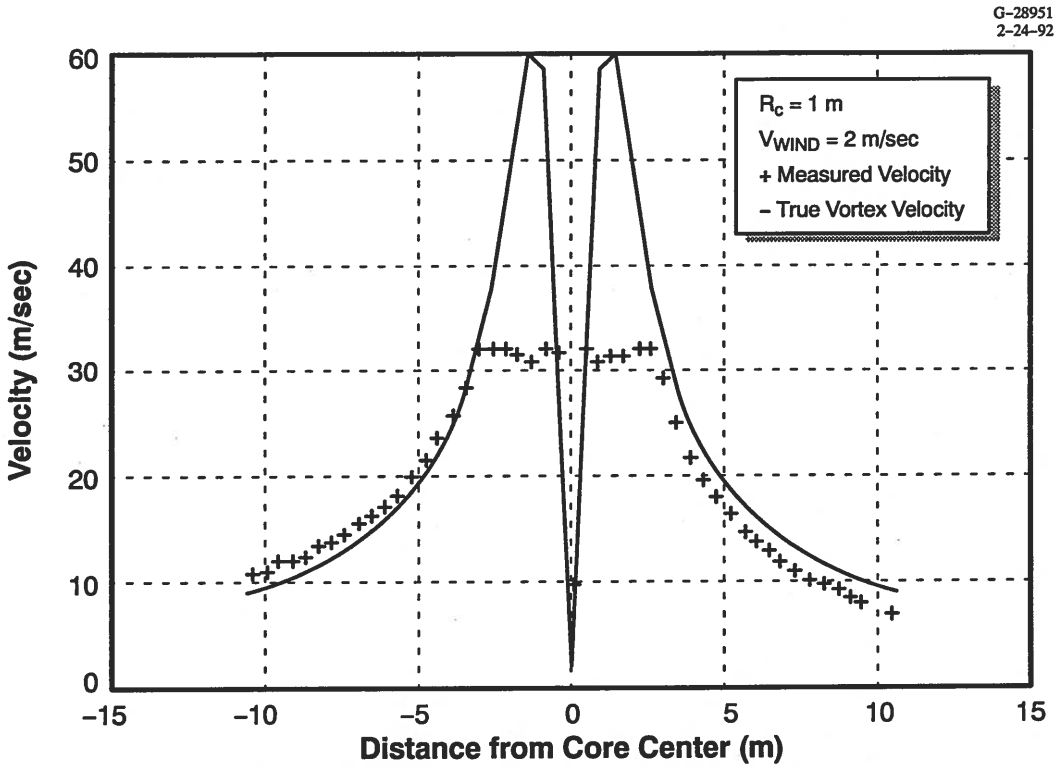

a.) True vs. Measured Radial Velocity

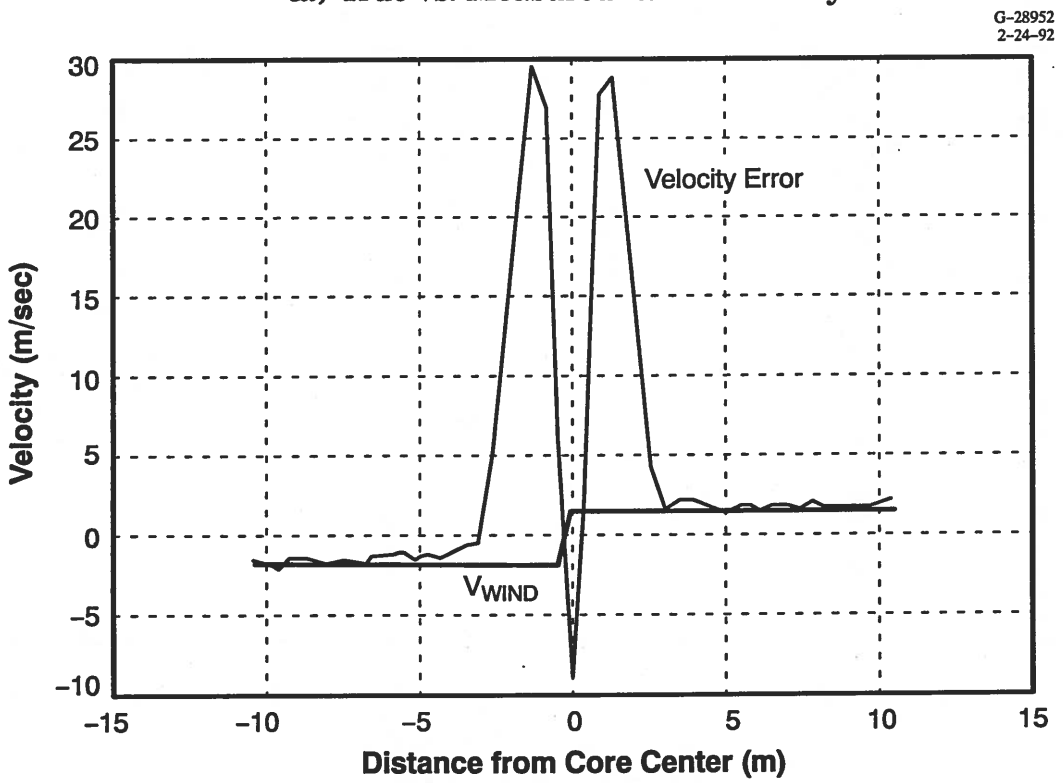

b.) Radial Velocity Error and Wind Velocity

Figure 2.3-14 The Effect of SAW Filter Limiting plus Wind on Angle Scans

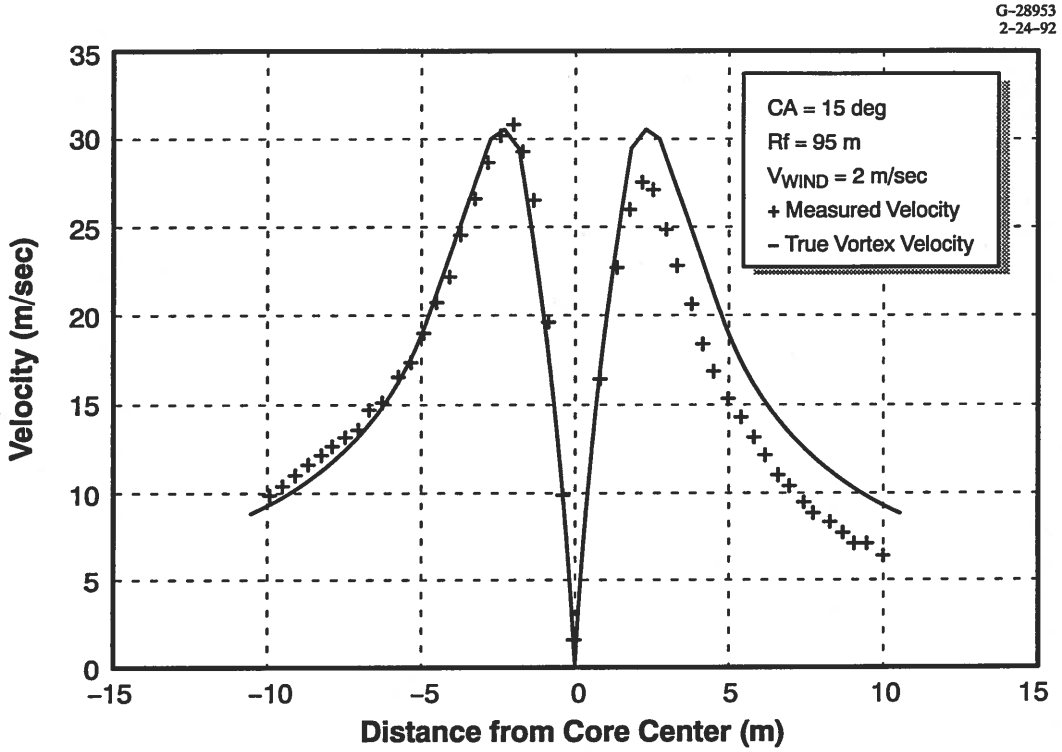

a.) True vs. Measured Radial Velocity

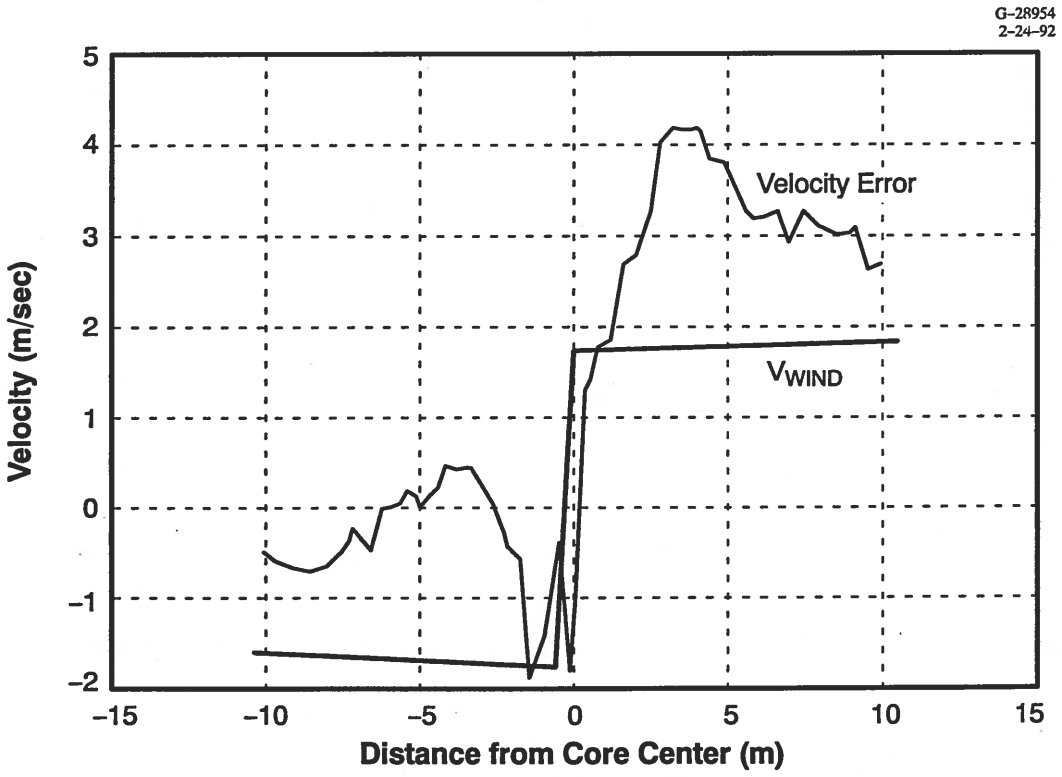

b.) Radial Velocity Error and Wind Velocity

Figure 2.3-15 The Effect of Non-perpendicular Scanning, Off-Focus Scanning and Wind on Angle Scans (1 of 2)

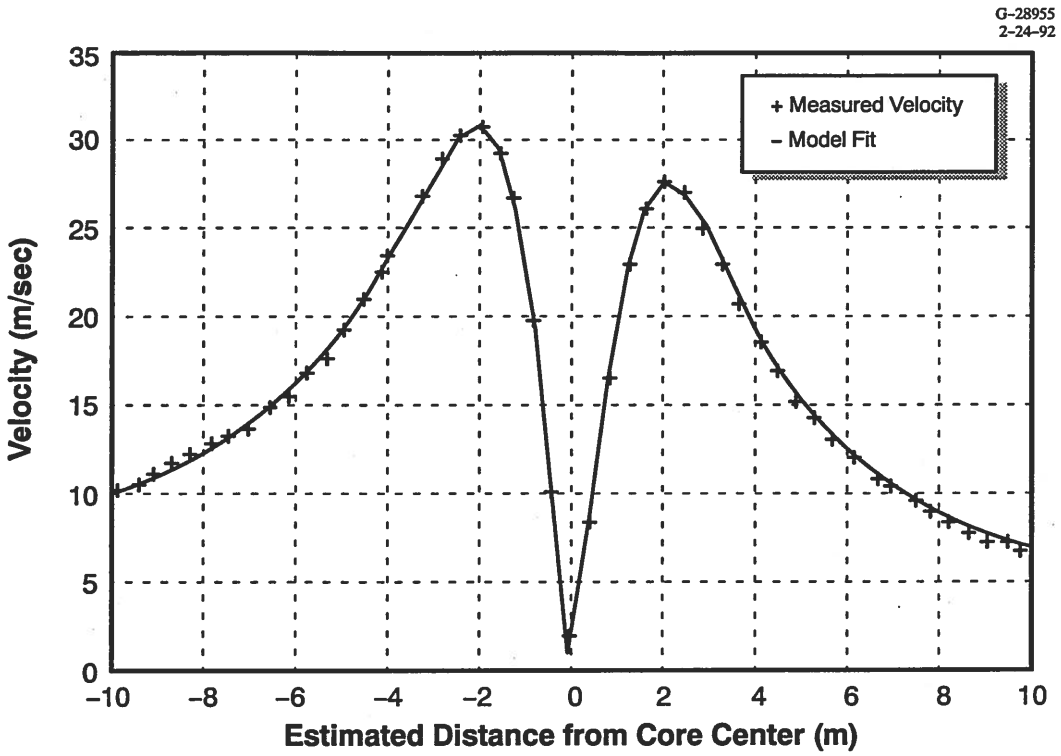

c.) Model Fit to Data Points

Figure 2.3-15 The Effect of Non-perpendicular Scanning, Off-Focus Scanning and Wind on Angle Scans (2 of 2)

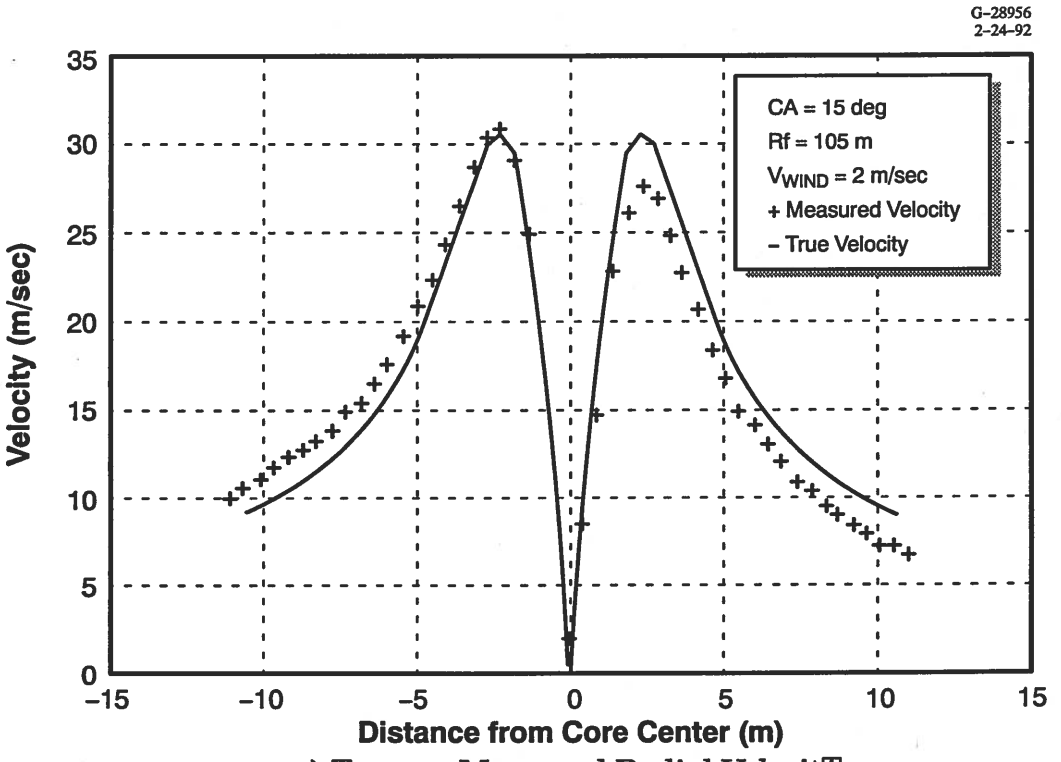

a.) True vs. Measured Radial Velocity

Figure 2.3-16 The Effect of Non-perpendicular Scanning, Off-Focus Scanning and Wind on Angle Scans (R_f = 105 m) (1 of 2)

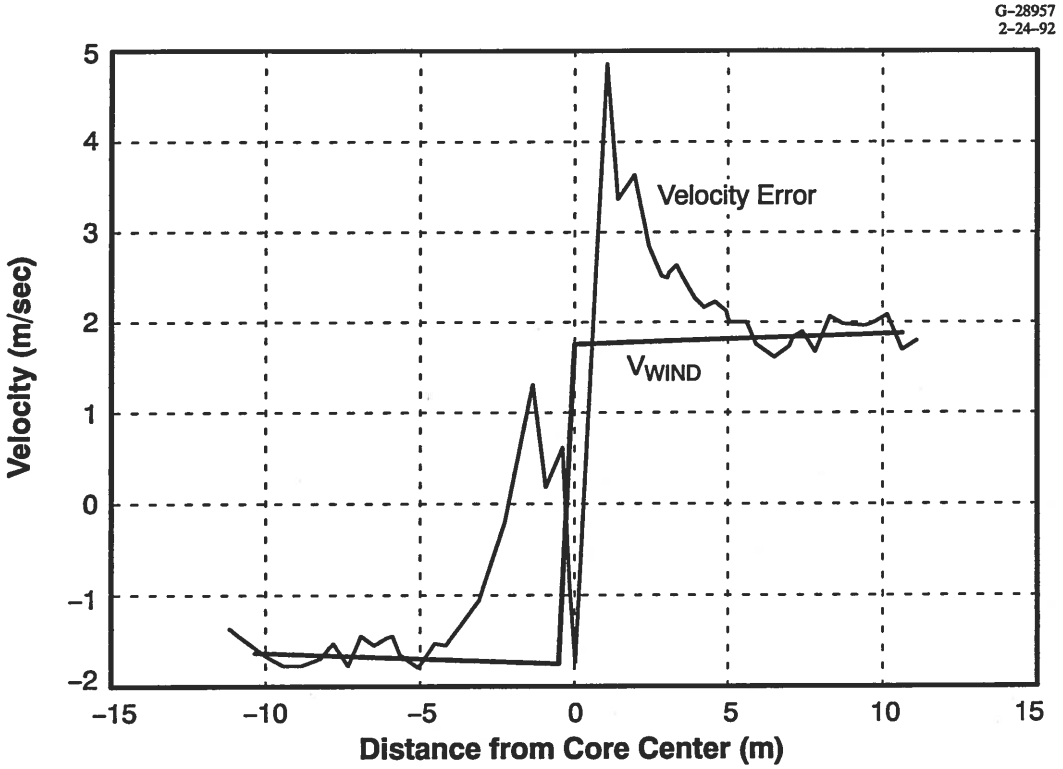

b.) Radial Velocity Error and Wind Velocity

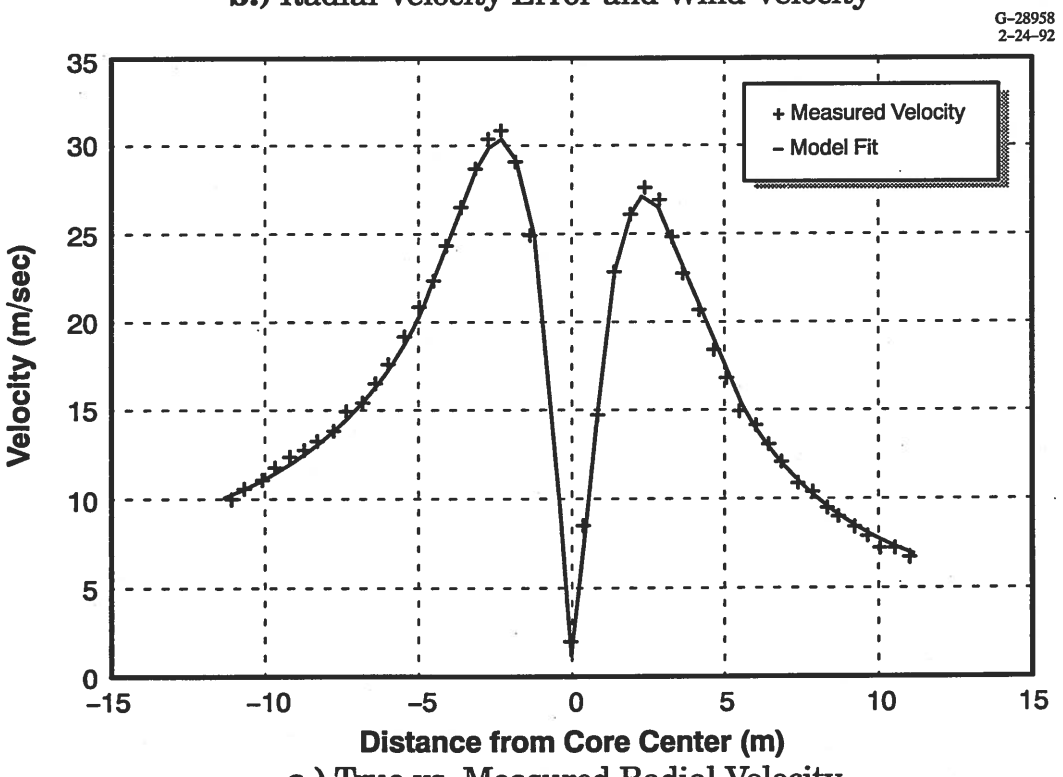

c.) True vs. Measured Radial Velocity

Figure 2.3-16 The Effect of Non-perpendicular Scanning, Off-Focus Scanning and Wind on Angle Scans (R_f = 105 m) (2 of 2)

Table 2.3-11 Two Off-Nominal Conditions With and Without Wind (CA=15 deg)

V_{wind} (m/sec)	R_f (m)	$\hat{\Gamma}$ (m^2/sec)	$\hat{V}_{wind}$ (m^2/sec)	$\hat{R}_c$ (m)	$\hat{V}_{peak}$ (m/sec)
0	105	605	-0.16	2.15	28.2
2	105	597	1.89	2.10	28.5
0	95	541	-0.16	1.90	28.6
2	95	542	1.89	1.90	28.6

2.4 VORTEX/WIND PARAMETER ESTIMATION

Vortex strength is currently estimated by direct integration of the measured velocity data. Wind effects are removed by averaging integration results from each sides of the vortex. A different approach is taken here which is more tolerant of measurement errors: an analytic model for the vortex velocity profile is fit to the data using least squares. The model and the fitting process are described in this section.

2.4.1 The Measurement Model

Each LDV velocity measurement is assumed to be comprised of three components: a component due to vortex velocity, one due to horizontal wind resolved along the LDV radial, and an error term due to LDV quantization. The measurement thus takes the form

$$z_i(r_i) = V_t(r_i) + V_{wind} \cos[\theta_f(r_i)] + n_i \qquad (2.4\text{-}1)$$

where:

r_i = Distance from core center for ith measurement

$V_t(r_i)$ = vortex tangential velocity at r_i given by Eq. 2.2-1

n_i = quantization error of ith measurement

$\cos[\theta_f(r_i)]$ = horizontal wind resolution factor

The unknown terms in this measurement model are: the vortex strength, Γ; the core radius, R_c; wind speed, V_{wind}; and the distance from the core, r_i. In the real world there would be additional terms caused by measurement noise, which would add to quantization noise and vortex descent rate. These terms could easily be added to the model.

A sequence of K measurements taken over an angle scan can be formed into a vector-matrix expression as follows:

$$Z(\underline{r}) = HX + N \tag{2.4-2}$$

where: $\underline{r} = [r_1 \ldots\ldots r_k]^T$ is a K x 1 vector

H = is a K x 2 matrix

$H(i,1) = (1-\exp(-(r_i/R_c)^2))/(2\pi r_i)$

$H(i,2) = \cos(\theta_f(r_i))$

$X = [\Gamma, V_{wind}]^T$ is a 2 x 1 vector

$N = (n_1 \ldots\ldots\ldots n_k)^T$ is a K x 1 vector

Notice that the measurement model is linear in Γ and V_{wind}. If the other parameters are known, a least-squares estimate for Γ and V_{wind} can be computed as follows:

$$\hat{X} = [\hat{\Gamma}, \hat{V}_{wind}]^T = (H^TH)^{-1}H^TZ \tag{2.4-3}$$

An alternative least squares wind estimation procedure that does not explicitly require knowledge of θ_f is described and shown to work well on LDV field test data in Section 3.3.

The estimated parameters $\hat{\Gamma}$ and $\hat{V}_{wind}$ may now be substituted in Eq. 2.4-4 and used to compute the Sum of Squared Residuals (SSR) of the model fit to the data as shown below:

$$SSR = (Z - H\hat{X})^T (Z - H\hat{X}) \tag{2.4-4}$$

The H matrix is a function of r_i and R_c. From Eqs. 2.4-1 and 2.4-2 it is seen that these parameters enter into the H matrix nonlinearly. Unlike the linear parameters for which a closed form analytic solution exists, estimation of these parameters via least squares methods involves a numerical search over the expected range of the parameters. Reasonably accurate estimates of core center location and therefore the values for the r_i can be obtained from a plot of the raw data. Due to the effects of averaging, velocity limiting and poor signal-to-noise ratio near the core center, however, visual estimates of R_c are very unreliable. Least squares estimation of R_c along with Γ and V_{wind} is illustrated below by example.

Figure 2.4-1 shows the results from a simulation with three off-nominal conditions: off-focus and non-perpendicular scanning in the presence of wind. Additionally, core radius has been reduced to 1.5 m to cause velocity limiting of the SAW filter. The effect of velocity limiting is clearly present in Fig. 2.4-1a. Wind causes velocity measurements to be high above the core and low below the core. In this example, however, the effect of wind is offset by the shortened focal range and non-perpendicular scanning. Examining Fig. 2.4-1b velocity measurements are seen to be essentially correct above the core, while the error below the core is roughly double that due to wind alone.

Figure 2.4-2a plots the Sum of Squared Residuals (SSR) obtained by solving Eq. 2.4-3 for several assumed values for R_c and using the resulting values for Γ and V_{wind} in Eq. 2.4-4 to obtain the SSR. Estimator results are listed in Table 2.4-1. Using all of the data points an SSR velocity error of 203 $(m/sec)^2$ attained at R_c=1. 48 m, very close to the true value. Γ is underestimated by 12% and V_{wind} by 25% due to the effects of short focus and non-perpendicular scanning. The model fit to the data is shown in Fig. 2.4-2b. The fit is quite good 3 m or more from the core, but poor in the region of SAW filter limiting.

Table 2.4-1 Least-Squares Parameter Estimate Example

ESTIMATED PARAMETER	TRUE VALUE	FULL DATA SET	EDITED DATA SET
$\Gamma(m^2/sec)$	600	553	591
$R_c(m)$	1.0	1.48	1.56
V_{wind} (m/sec)	2.0	1.21	1.97
V_{peak}(m/sec)	60.16	37.5	38
SSR($[m/sec]^2$)	—	203	3.6

The question naturally arises as to whether or not estimates are improved by eliminating the bad data points. If the first five data points either side of core center are eliminated the results shown in Fig. 2.4-3 are obtained. Figure 2.4-3a shows a shallow minimum at R_c=1.62 m. The resulting SSR of 3.6 $(m/sec)^2$ is almost two orders of magnitude less than before. The errors in Γ and V_{wind} are reduced to 10% and 4%, respectively. Model fit to the data points is shown in Fig. 2.4-3b. The great reduction in fit error is due to elimination of the bad data points. The fit beyond 3 m from core center differs little from that of Fig. 2.4-2b. The reason for this can be understood by referring back to Fig. 2.2-1.

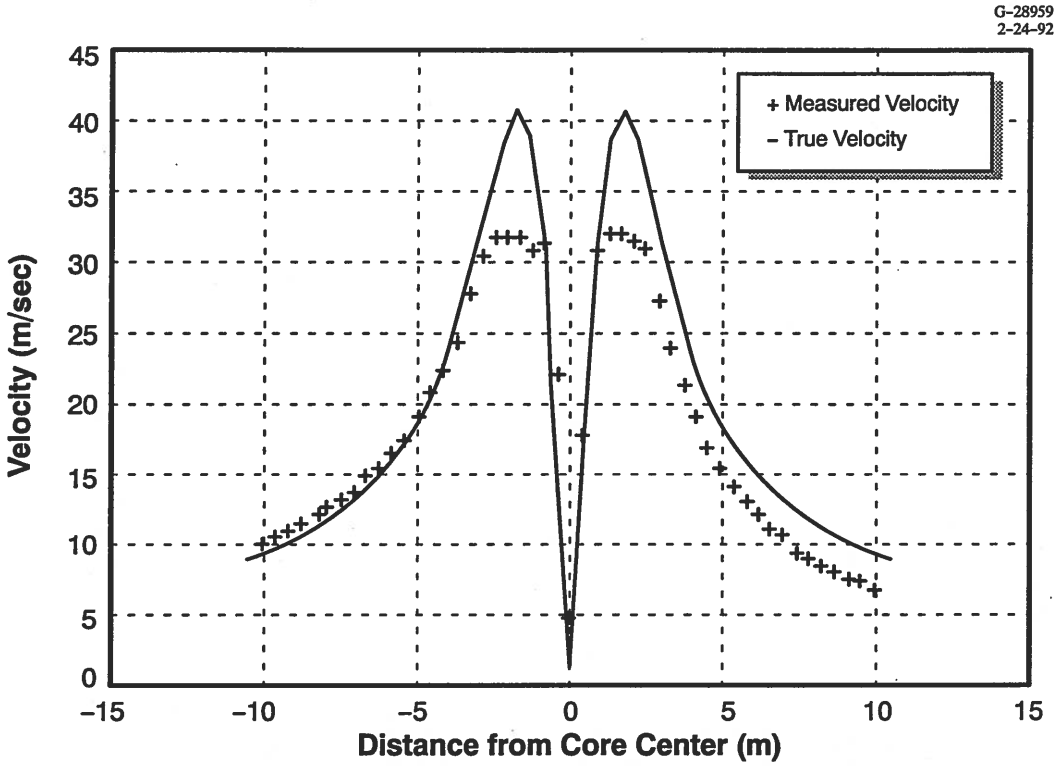

a.) True vs. Measured Radial Velocity

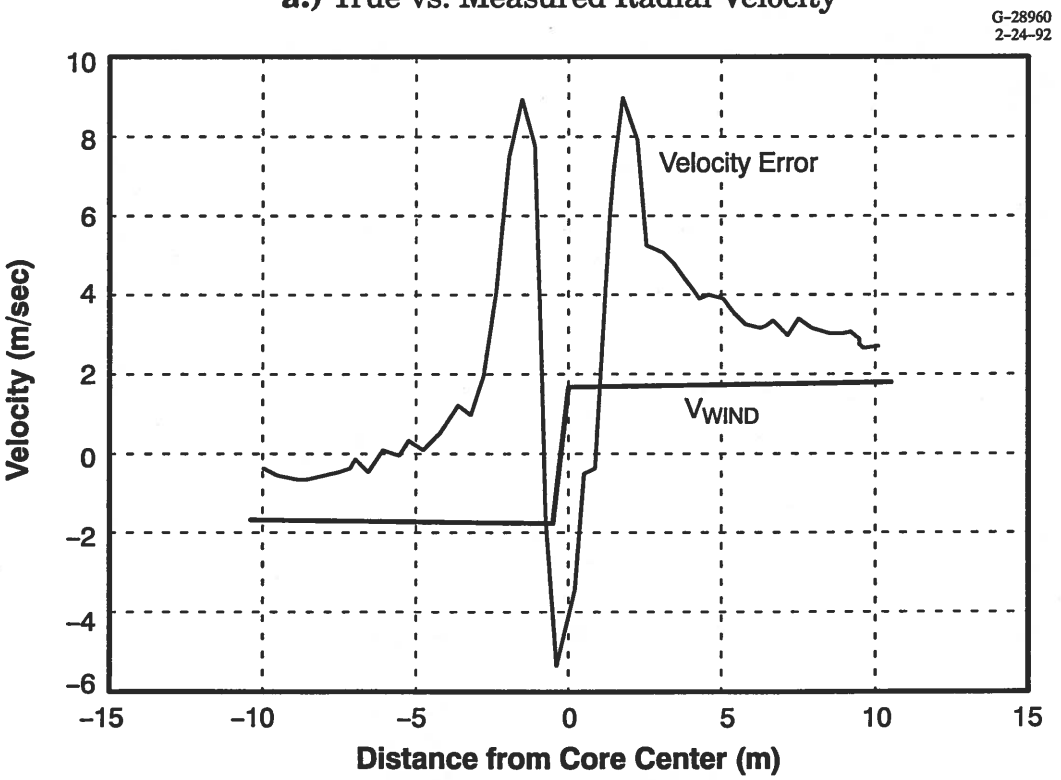

b.) Radial Velocity Error and Wind Velocity

Figure 2.4-1 Least-Squares Parameter Estimation Example

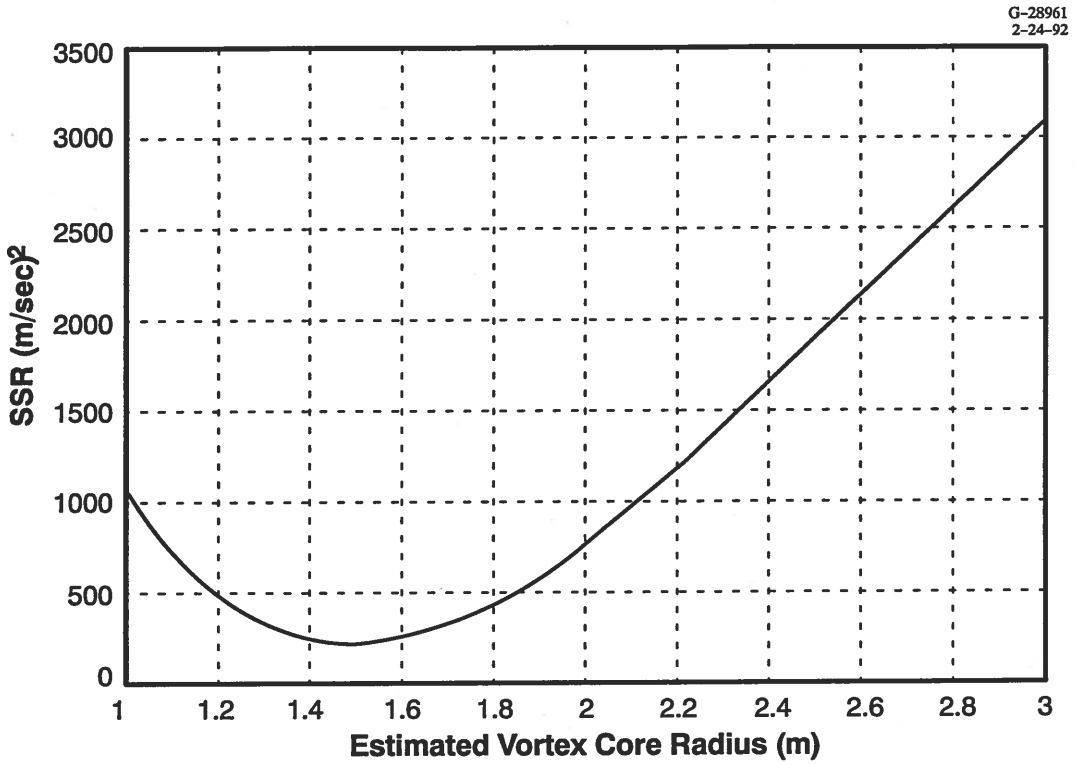

a.) Fit Error vs. Estimated Vortex Core Radius

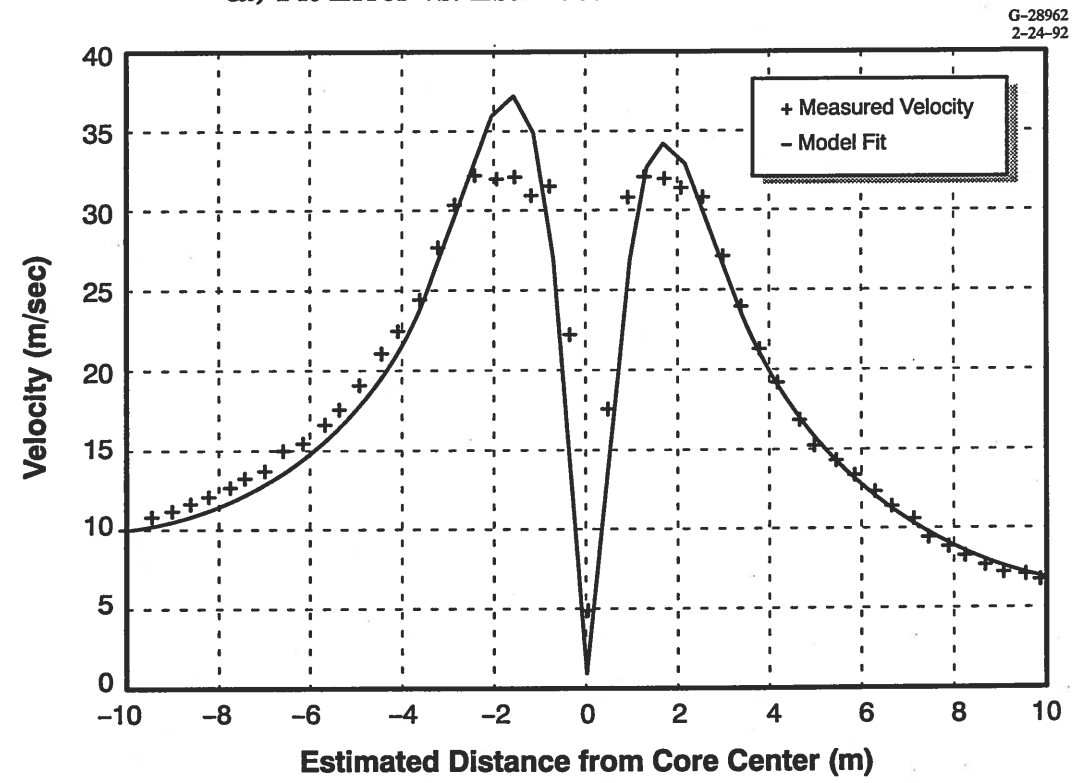

b.) Model Fit to Data Points

Figure 2.4-2 Least-Squares Parameter Estimation Example Using All Data Points

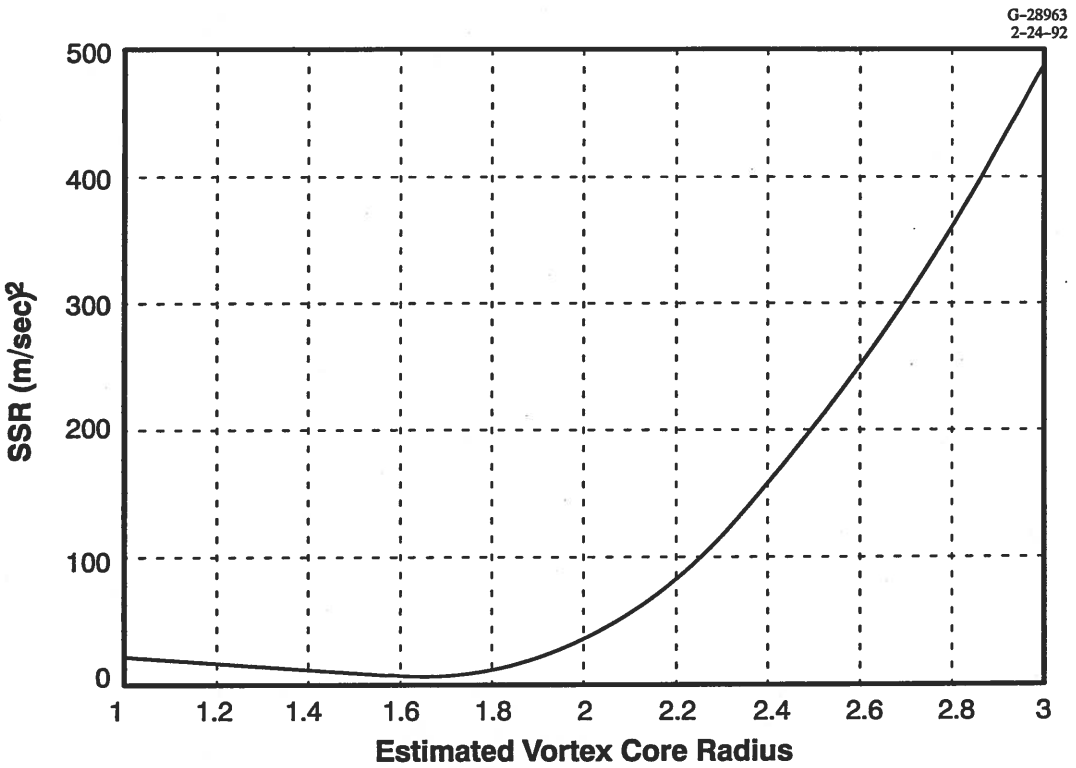

a.) Fit Error vs. Estimated Vortex Core Radius

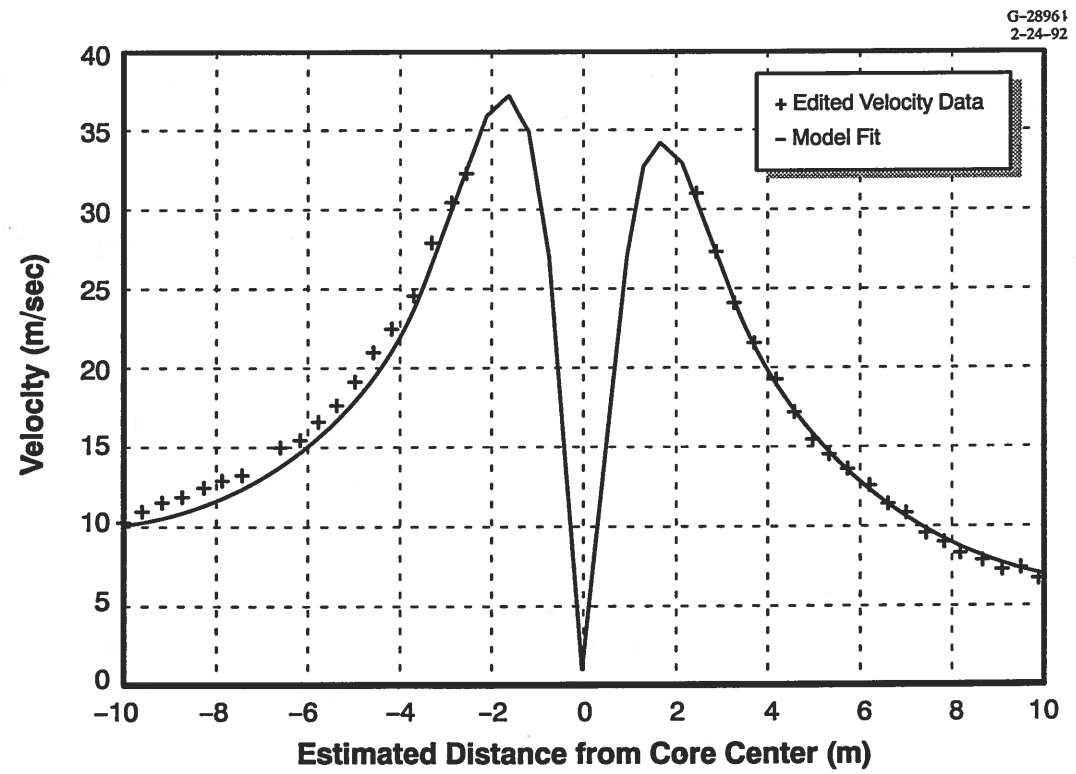

b.) Model Fit to Data Points

Figure 2.4-3 Least-Squares Parameter Estimation Example Using Edited Data Points

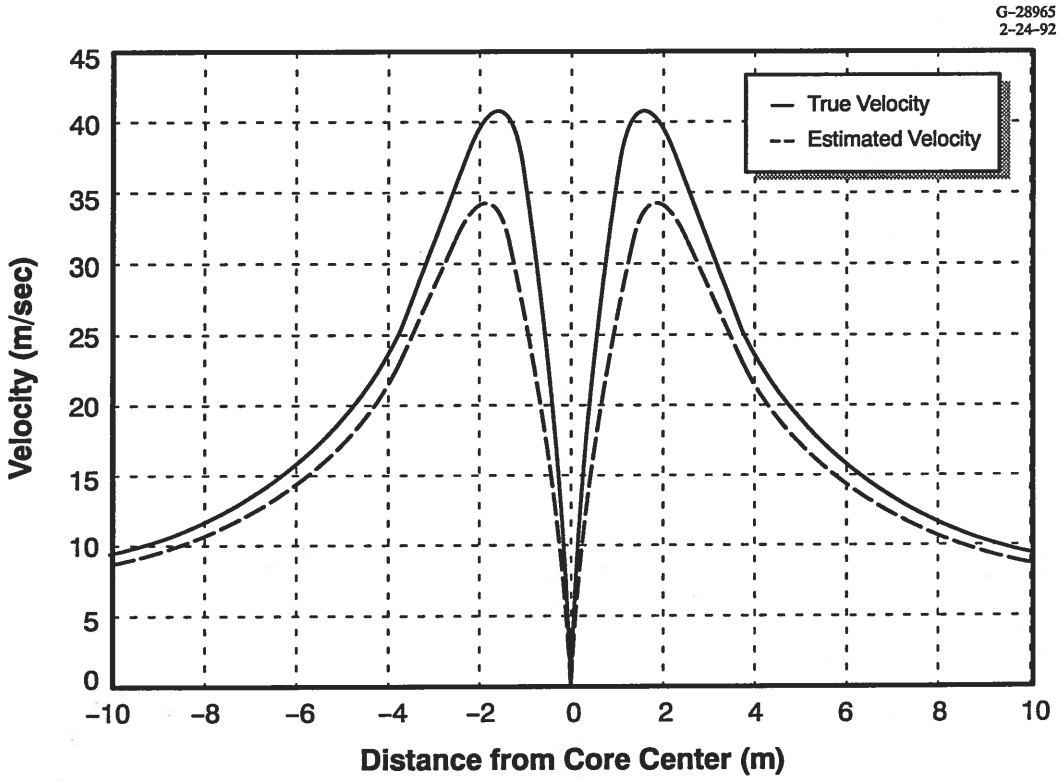

Figure 2.4-4 True and Estimated Vortex Velocity Profiles for Least-Squares Example

Beyond a distance of $2R_c$ from core center, tangential velocity is independent of the value of R_c. The accuracy of the data in the region around the core radius is critical to accurate recovery of R_c. Using only that data beyond the core radius gives good core strength and wind estimates, but poor estimates of core radius. Estimated and true vortex velocity profiles are compared in Fig. 2.4-4. Peak velocity is under-estimated by 15% for this example. Accurate estimates of core radius and vortex strength are needed for reliable estimates of peak vortex velocities from LDV data. Including the five points centered on the core axis would greatly improve the estimates of R_c and V_{peak}, but theses data points have very low signal power and would not be useable in the presence of realistic noise levels.

Cutting angle, CA, and misfocusing are not modelled in the measurement process because they are not strongly observable in single scans. In other words their presence yields measured velocity profiles which look just like valid profiles for slightly different vortex parameters. The effect of misfocusing and non-perpendicular scanning can only be sorted out by comparing scans at different focal ranges and azimuth angles. It is

interesting to note in the above example that misfocusing long at about 105 m would have largely canceled the effect of the 15 deg cutting angle.

2.5 SUMMARY OF SIMULATION RESULTS

The results derived from the simulation study are summarized below in two categories: LDV velocity measurement performance, and vortex parameter recovery algorithm performance.

LDV Velocity Measurement Performance:

- Quantization is not a major source of error in vortex velocity measurements.
- Spatial averaging error dominates when velocity variation over the averaging volume is large compared to a quantum level, i.e., near and inside the core radius.
- Return signal power is proportional to distance from the core center. It is maximum in the vortex tails and falls rapidly near the core radius and inside the core. It follows that SNR will be low in this region also.
- Return signal power decreases with increasing off-focus conditions.
- In general, the LDV cannot directly measure peak vortex velocities. This is a result of averaging, SAW filter limiting and/or poor SNR in the peak velocity regions.
- Velocity limiting in the presence of noise can lead to significant underestimation of velocity.

Vortex Parameter Recovery Algorithm Performance:

- With properly edited data, constant horizontal wind components are easily separated from vortex velocity.
- SAW filter velocity limiting can cause under estimation of core strength by as much as 15% and peak velocity by nearly 40%. These points should be edited out of measurement records to improve estimates of core strength. If greater accuracy in peak velocity is required, independent measurement of this quantity with alternative sensors is needed.
- To first order, errors in estimated vortex strength are directly proportional to off-focus error in percent and the cosine of cutting angle. Focusing long, however, can partially offset cutting angle error.

- Velocity limiting and poor SNR in the region around the core radius produce low or missed velocity data points. This in turn results in visually overestimating core radius and underestimating peak vortex velocity.
- Cutting angle and misfocusing errors are not observable from single angle scans. Their effect can only be sorted out by comparing scans at multiple focal ranges and azimuth angles.

Least-squares fitting of a model to vortex velocity measurements appears to be a consistent, robust approach to vortex parameter recovery. By adopting a range scan strategy in which range increments are proportional to focal volume, i.e., range squared, off-focus effects can be minimized. SAW filter limiting can be controlled by proper data editing. By employing these procedures, vortex strength should be recoverable with worst case errors of 10% and smaller average errors. Errors in peak velocity of 40% or less still appear to be possible, however. If better estimates of peak velocity are required, LDV data should be augmented with additional sensors such as tower anemometers.

3. LDV DATA ANALYSIS

The LDV simulation described in Chapter 2 is used to perform LDV analytic modeling to assess basic capabilities and limitations of the current LDV hardware implementation. This chapter describes the results of the *analysis of experimental wake vortex data collected in the field* by the LDV and other test instruments. These data are used in two ways to:

- Compare the analytic model predictions to experimental data
- Evaluate current LDV post-test data processing procedures.

3.1 DATA SOURCES

To perform the LDV Engineering Review, wake vortex data were obtained from VNTSC and analyzed. Several types of data were obtained from the Idaho Falls test series:

- LDV velocity profiles and selected SAW spectrum data
- Tower data from anemometers at 10 ft spacing
- Meteorological data (Ref. 4)
- Tower data from anemometers at 2 ft spacing (Ref. 5; available only in printed form for a small number of runs and vortex ages).

In addition, VNTSC provided TASC with the standard software programs used by VNTSC for reviewing SAW spectra and creating and identifying vortex velocity profiles. A set of representative Idaho Falls data for processing with this software was also provided.

In addition to the Idaho Falls data, a limited amount of SAW spectrum data for the Dallas-Fort Worth tests were also obtained. These data were processed by VNTSC using a different SAW spectrum thresholding technique than was used on the Idaho Falls data.

3.2 SAW SPECTRUM THRESHOLDING

For each angular sweep increment and for each scan, the maximum sensed line-of-sight velocity is obtained from the SAW spectrum. The spectra are noisy (due to the SAW hardware and environmental factors), quantized (to 1.8 fps or 0.53 m/sec resolution), and limited to sensing a maximum velocity of approximately 100 ft/sec. A typical SAW spectrum is shown in Fig. 3.2-1.

Two techniques have been applied for automatic thresholding of SAW spectrum:

- A constant (over velocity bins) threshold
- A threshold which varies for each velocity bin.

These thresholds are illustrated in Fig. 3.2-2. Idaho Falls data has been processed using the constant threshold, while the variable threshold has been used for Dallas-Fort Worth data processing. The variable threshold aims to more accurately account for frequency-dependent ambient noise variation, and is determined at the start of a run using a "vortex-free" vertical scan of the LDV. The constant threshold is determined by the LDV operator as he inspects SAW spectrum visually at the start of the test to determine an appropriate noise floor.

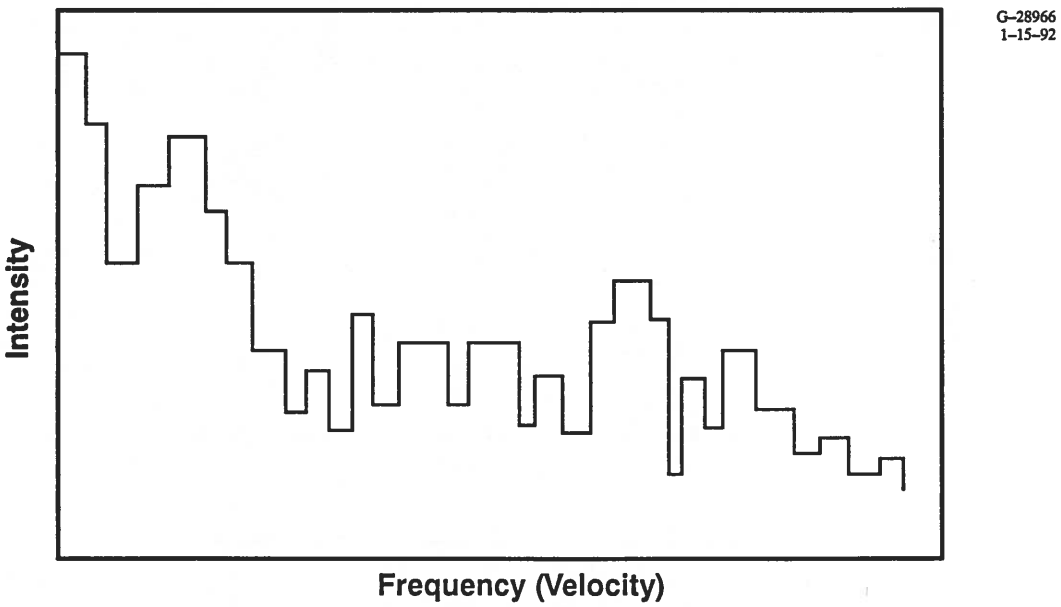

Figure 3.2-1 Representative SAW Spectrum

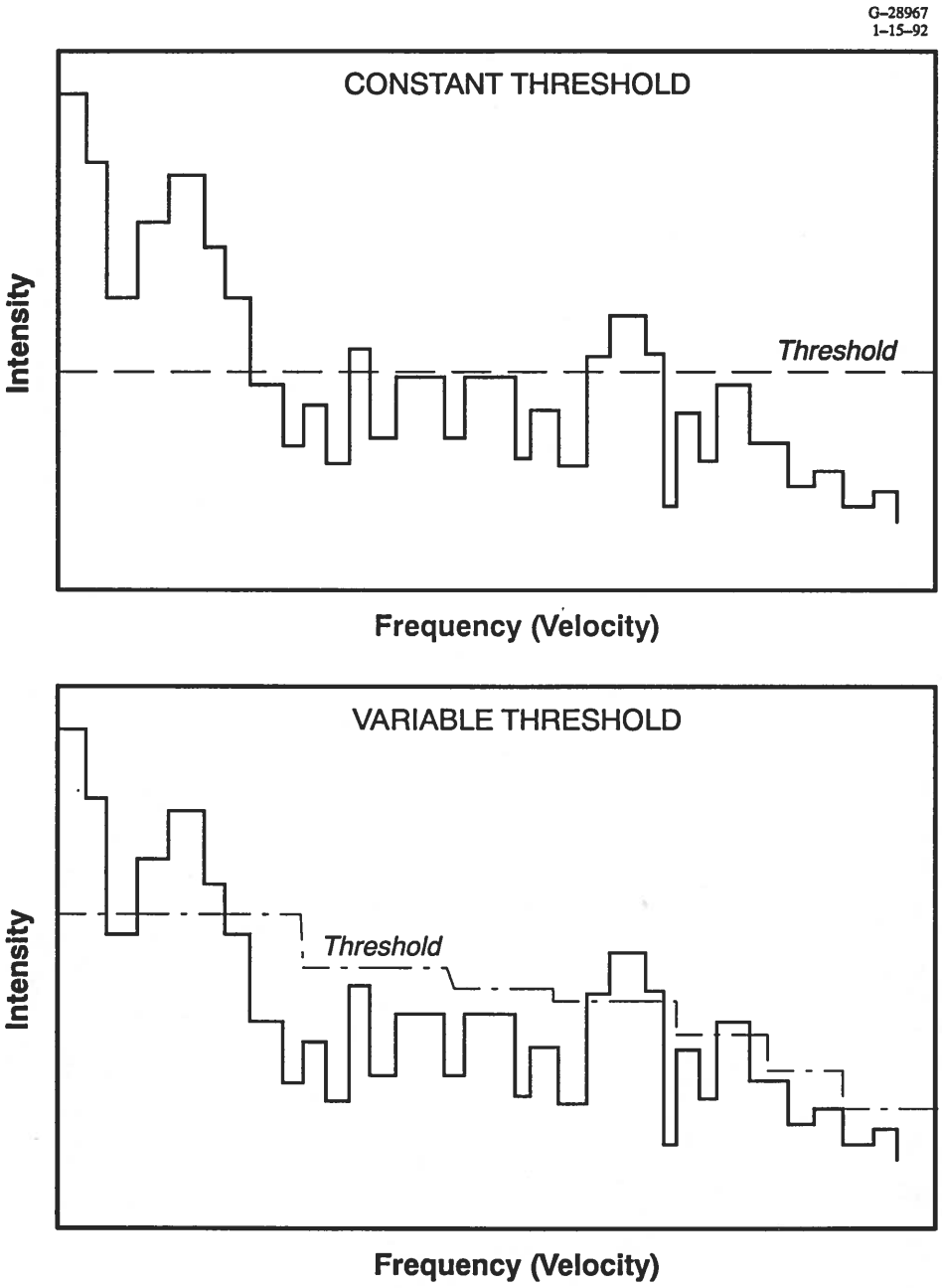

Figure 3.2-2 SAW Spectrum Thresholding Techniques

Both the techniques are suboptimal. The constant threshold technique can often be seen to set too high a threshold — vortex-induced velocity spectral peak structures can often be seen in the high velocity bins of the spectrum, at magnitudes less than the threshold. The variable threshold does allow lower threshold is in higher velocity bins where return energy from the background is less. However, inspection of the Dallas-Fort Worth data shows that while the overall shape of the SAW spectrum may persist over a run, its magnitude can change. This results in an effective bias in the variable threshold value, since this value is currently set once at the beginning of a run.

Review of the data by TASC and analysis conducted by VNTSC indicate that additional manual inspection of spectrum and the application of spectral matching techniques can improve the estimation of peak velocities (Ref. 6). Investigation of ways to formally automate these techniques (e.g., through morphological image processing techniques for automated feature identification) is a subject for additional work.

3.3 ESTIMATION OF WIND EFFECTS

Raw LDV velocity return data include energy from both the vortex and the ambient wind along the line-of-sight. Collaterial meteorological data is currently used in a preprocessing step to correct the LDV data by removing the effect of the ambient wind. Another approach to removal of the wind effects is to estimate wind directly from the data and subtract the wind estimate from the LDV return data. Both the LDV simulation and the analysis of LDV and meteorological data given below show that this can be done effectively.

Section 2.4 describes a batch least squares estimation procedure for removal of a constant horizontal wind component. An analogous technique using a least squares fit of a low-order (3) polynomial to the LDV velocity profile has been found to be effective in estimating constant wind effects from velocity profiles without any *a priori or* collateral information, such as LDV elevation angle as described in Section 2.4. Since the time and location of collected wind data seldom correspond to the spatio-temporal location of a particular vortex when it is illuminated by the LDV, a data-derived wind estimate eliminates the need for interpolation of meteorological data. On the other hand, the model of a constant horizontal wind used in the least-squares wind estimation is a simplification. However, even this elementary model produces wind estimates that are consistent with the independent meteorological data.

The wind estimation technique is illustrated in Figs. 3.3-1 through 3.3-3. Figure 3.3-1 shows an uncorrected LDV velocity profile for a Boeing 767 collected during Run 23 at Idaho Falls. This is a downwind vortex with an age of 19 sec. The left half of the vortex is marked by x's, the right half by asterisks. The vortex halves show a characteristic wind-induced asymmetry. Figure 3.3-2 shows the two halves of the vortex "folded over" about the radius origin on a single plot. The solid and dashed lines in Fig. 3.3-2 are least-squares fits of two low order polynomials, one to each half of the vortex. The fit is done on the tails of the vortex profile only, the region where LDV returns are most accurate, so as to get a better estimate of bias wind effects. The difference between the two polymonial fits to velocity at different radii are calculated, averaged, and divided by two to get an estimate of the constant wind. This correction is then added or subtracted to each half of the vortex. Figure 3.3-7 plots the corrected LDV velocity profile. The solid and dashed lines in the figure are an overlay of a symmetric Lamb vortex model fit to the data, which serves to illustrate the improved correspondence between data and model that results after this simple correction. This fitting and correction procedure has been fully automated in an algorithm that can reduce the need for analyst intervention in post-processing of LDV data.

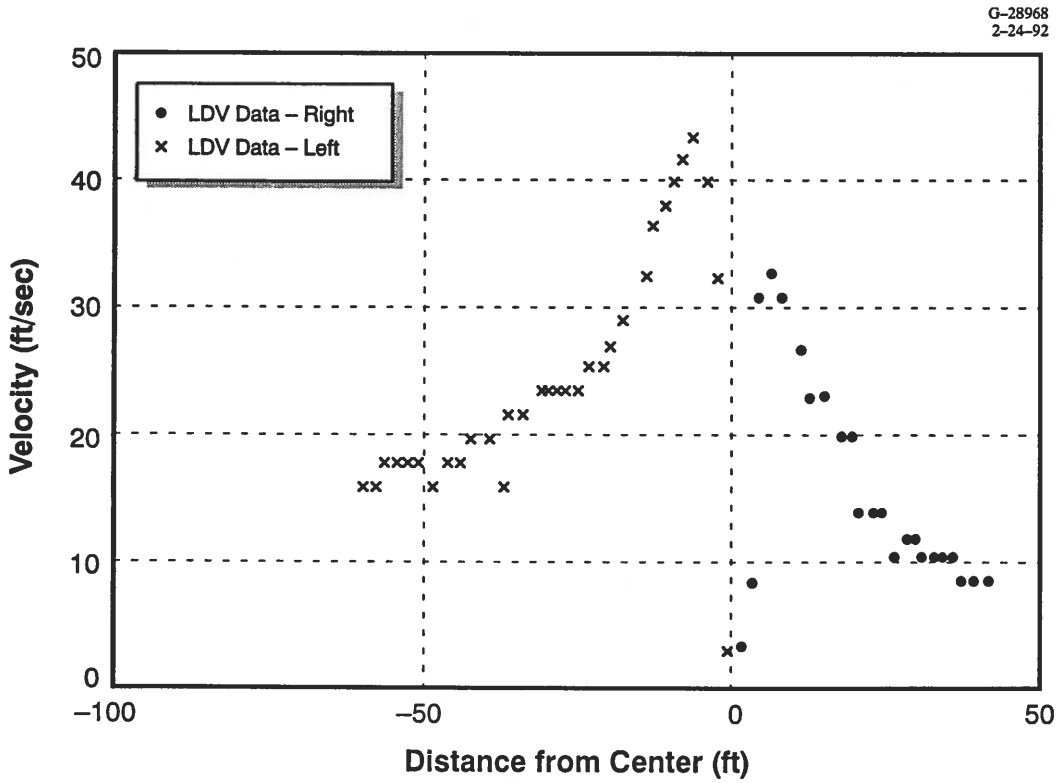

Figure 3.3-1 Uncorrected LDV Velocity Profile

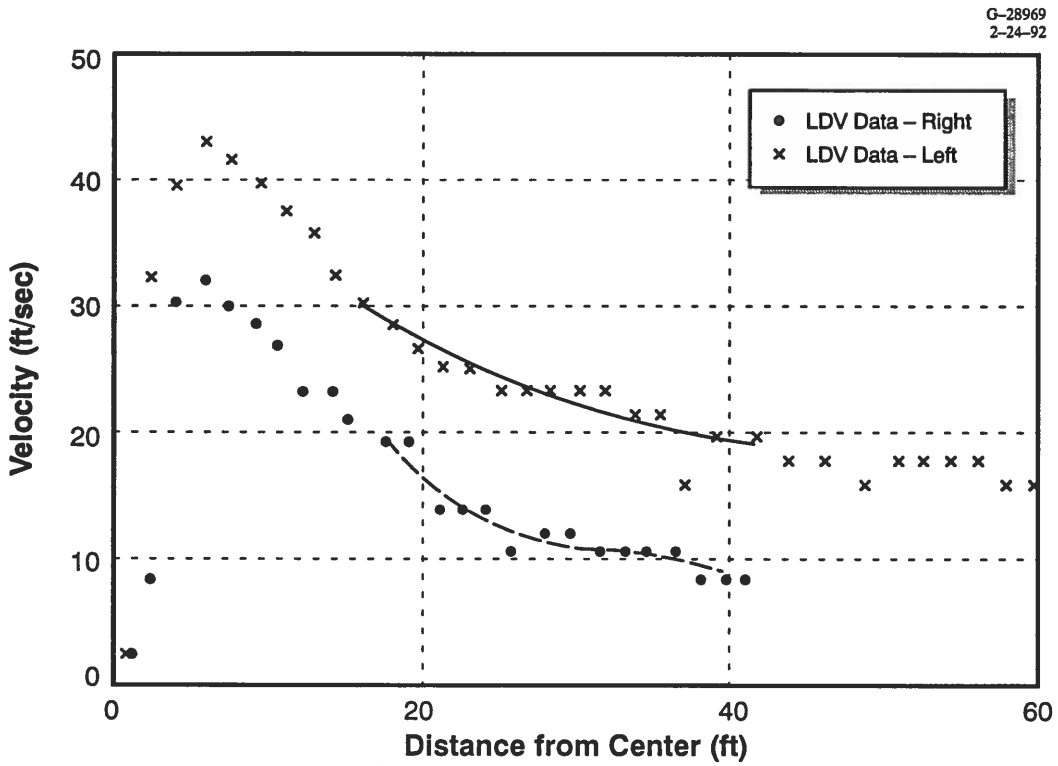

Figure 3.3-2 LDV Velocity Profile with Polynomial Fits for Wind Removal

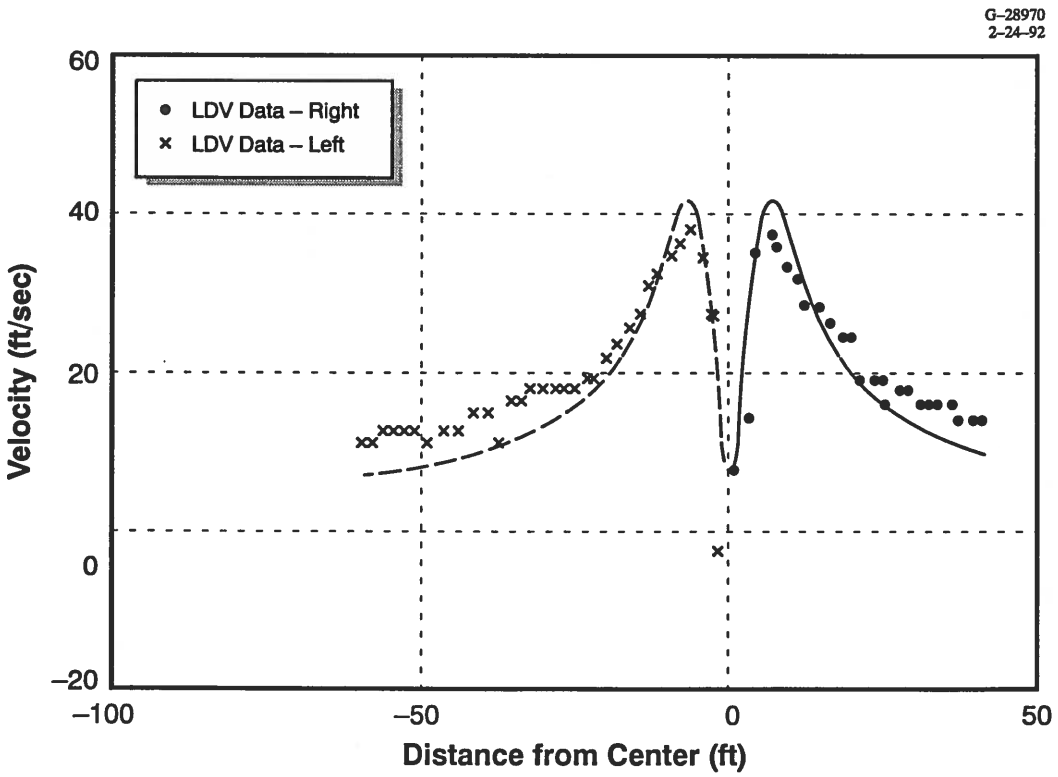

Figure 3.3-3 Corrected LDV Velocity Profile

3.4 COMPARING THE LDV SIMULATION WITH TEST DATA

In order to assess the fidelity of the LDV analytic simulation and to evaluate implications for data processing, comparisons between the simulation, LDV-measured data, and tower anemometer data at a 2-ft sensor spacing were made. LDV data from Idaho Falls Boeing 757 Run 10 are used here to illustrate this analysis.

3.4.1 Observed Velocity Profiles

Figure 3.4-1 shows the uncorrected velocity profiles for LDV and Tower data from Run 10. The LDV data is for a vortex with an age of 34 seconds, while the Tower data is for a profile with an age of 25 seconds, the best comparable data available in Ref. 5. The tower data plotted in the figure have been sub-sampled from the 2-ft spacing data while preserving the full-data profile shape.

Data-based wind removal as described in Section 3.2 was applied independently to the tower and LDV data. The estimated wind values for the tower and the LDV are in good agreement and are consistent with the meteorological data (which varies with altitude and time), as shown in Table 3.4-1. Figure 3.4-2 shows the LDV and Tower profiles in an overlay plot after the effect of wind has been removed.

The corrected LDV velocity profile has the twin peak structure predicted by theoretical vortex models. An overlay of the LDV data and a Lamb vortex model fit by least squares is shown in Fig. 3.4-3. Note that, under the assumption that the LDV scan focal range equals the vortex range, the vortex core radius is estimated to be 3.3 ft. However, since the LDV scan will not in general be focussed at the vortex range and because of the degredation in LDV estimation capability near the core as described in Chapter 2, this is a likely overestimate of the core radius. The tower data resolution is limited to the 2-ft spacing of the sensors, but the data indicates a core radius no larger than 2 ft. In fact, historical data indicates that a typical Boeing 757 vortex core radius ranges from 0.5 ft to 1.5 ft.

The Tower data shows a peak velocity of 290 ft/sec, while the LDV data shows a peak at 98 ft/sec, near the maximum velocity the SAW filter in the LDV can measure.

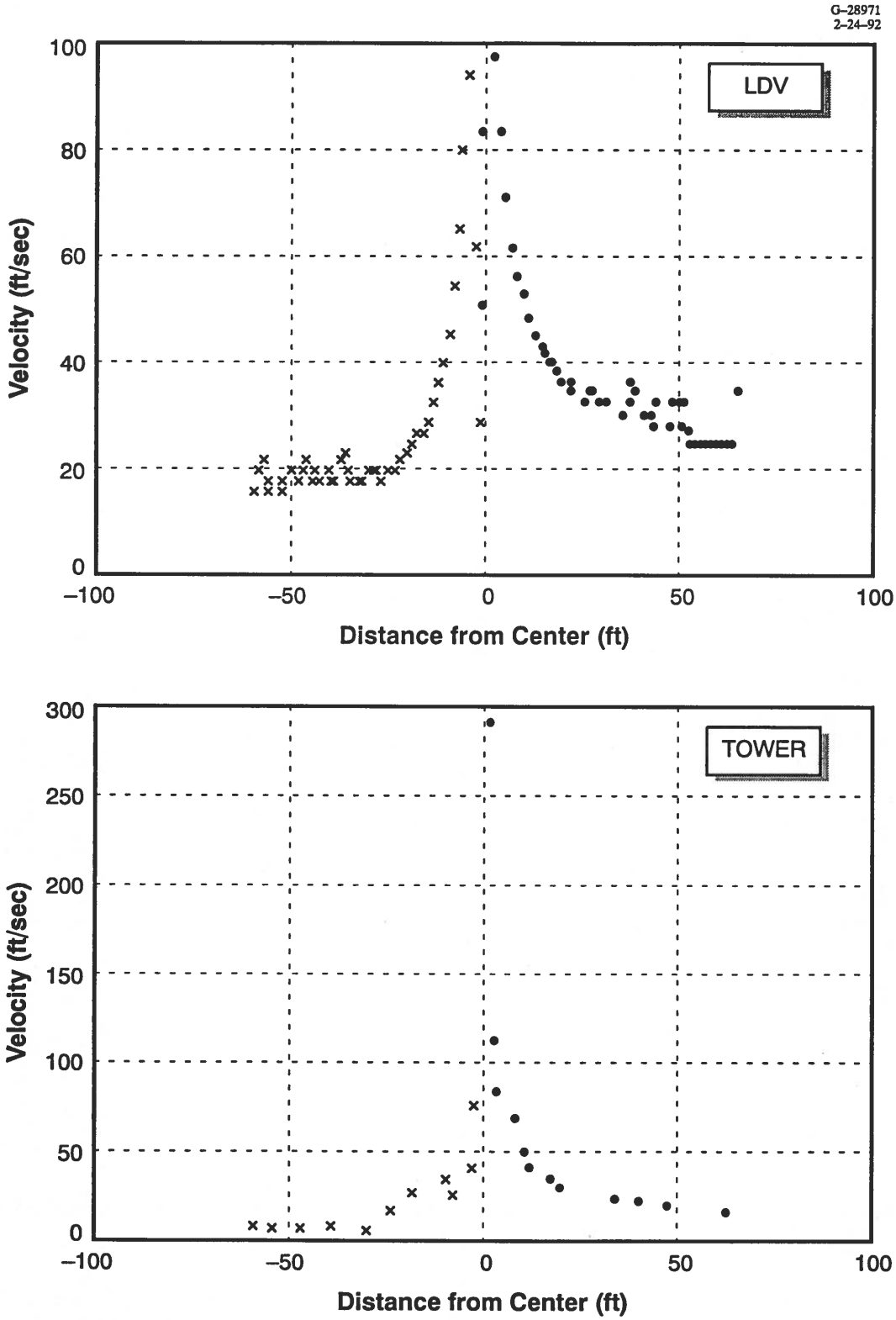

Figure 3.4-1 Uncorrected LDV and Tower Profiles for Run 10

The Lamb model (as well as alternative models such as Rankine, Hoffman-Jubere) predicts a velocity that is proportional to 1/(distance from core) as the distance grows large. The LDV data shows a slower fall-off in distance, which may be partially attributed to nonorthogonality of the LDV scan direction and the vortex axis (see Section 2.3.2). The tower data in Fig. 3.4-2, shows a dependence on velocity that more closely matches the predicted 1/(distance form core) dependence.

Table 3.4-1 Estimated Horizontal Wind

SENSOR	WIND ESTIMATE (ft/sec)
LDV	6.2
Tower	7.0
Met Data	5.0 — 9.0

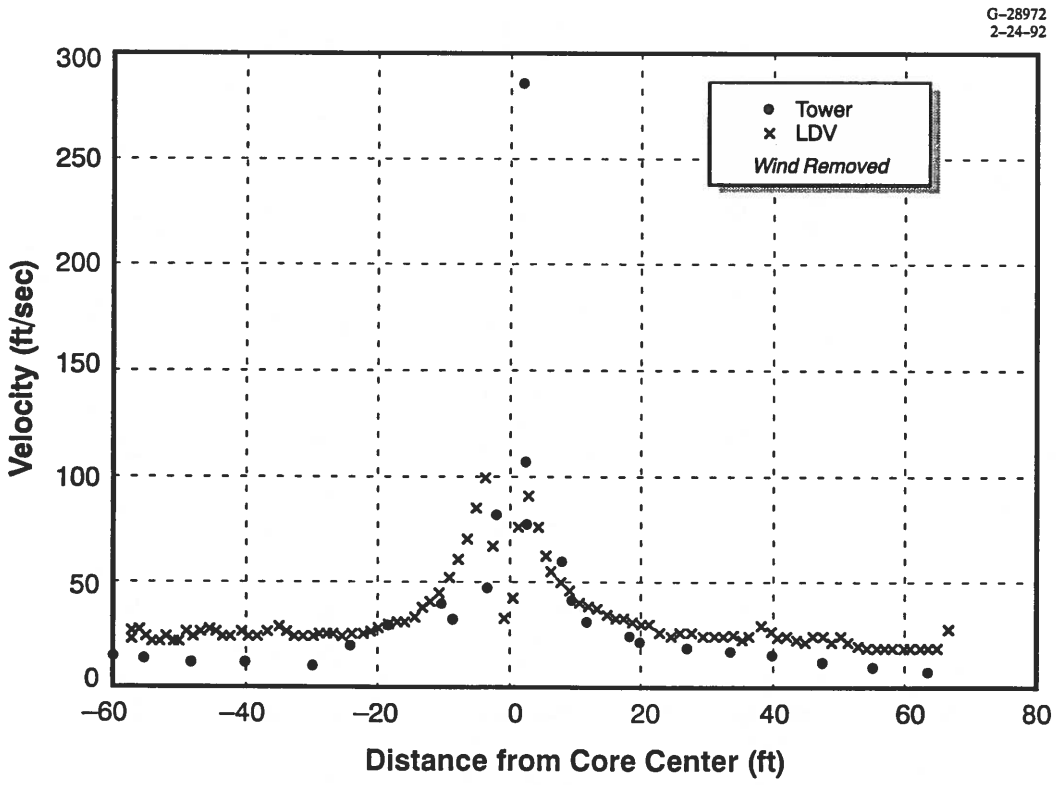

Figure 3.4-2 Corrected LDV and Tower Profiles for Run 10

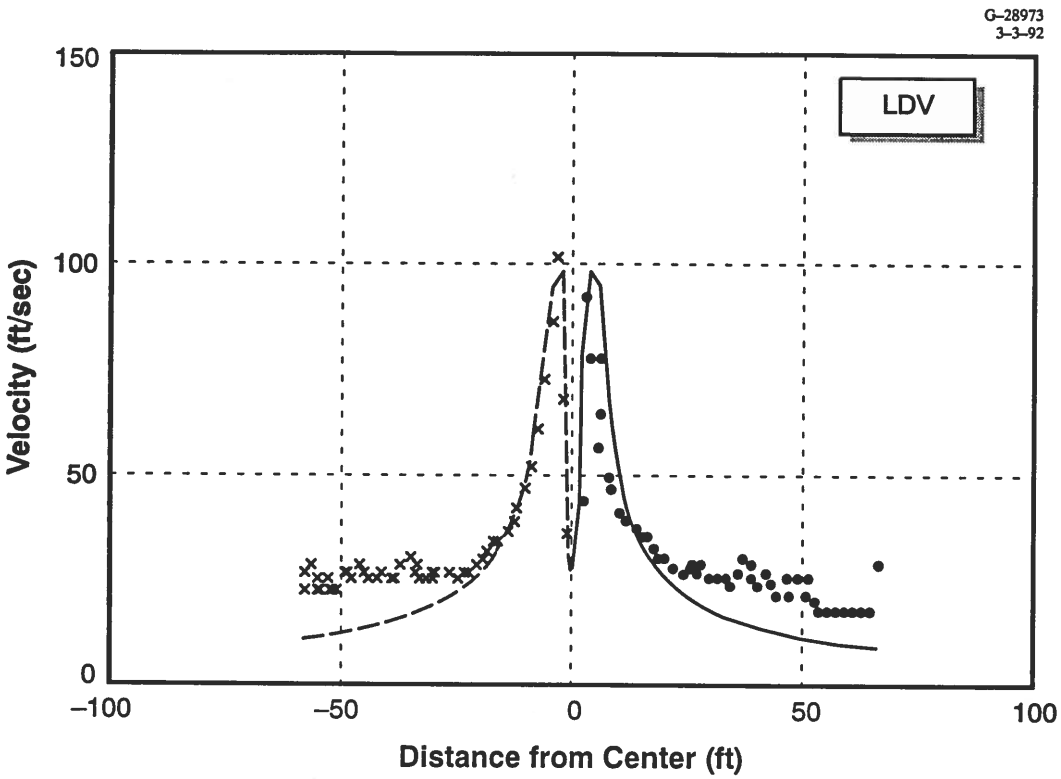

Figure 3.4-3 Corrected LDV Data Fit to Lamb Model

Hence there seem to be discrepancies between the LDV and tower data. However, comparison to results of the LDV analytic simulation show that the observed LDV profile results are predictable, and suggest that vortex models can be used in conjunction with LDV data and *a priori* information to improve estimation of certain vortex parameters, as discussed in the next sections.

3.4.2 Model-Based Predictions for Run 10

The simulation described in Chapter 2 was exercised to explain LDV performance observed in Idaho Falls Boeing 757 Run 10. Input parameters given in Table 3.4-2 were used to define the truth model for the evaluation, and are a combination of *a priori* information and parameters obtained from the tower data. The "true" velocity profile was generated according to a Lamb model, and the LDV operation was simulated in terms of scan rate and integration time, etc., as described in Chapter 2. The resulting simulated LDV velocity estimates are plotted along with the "true" velocity profile in Fig. 3.4-4. The true and LDV profiles match down to a distance of about 4 ft from the vortex center, where a maximum velocity return is recorded. At closer distances, the SNR of the simulated returns is not high enough for identification of velocity, resulting in inaccurate velocity estimates.

Table 3.4-2 LDV Simulation Parameters

PARAMETER	VALUE
Vortex Range	325 ft
LDV Focal Range	325 ft
Scan/Vortex Angle	90 deg
Core radius	1 ft
Core Velocity	290 ft/sec
Wind Magnitude	0 ft/sec*

*Wind is removed from test data

Figure 3.4-4 indicates that the LDV measurements taken directly cannot give good reconstructions of the true velocity profile when the vortex core is small or vortex core velocities are higher than the LDV measurement limits. However, the figure indicates that the LDV data does give an accurate representation of those parts of the velocity profile away from the vortex core. This suggests that parametric models of the vortex, such as Lamb or Rankine, might be fit to the LDV data and used to extrapolate those parts of the velocity profile the LDV cannot measure. Figure 3.4-5 illustrates fitting of a Lamb model to the LDV data (with the *a priori* constraint that core radius equal 1 ft — this is an important piece of information for the extrapolation), and the corresponding tower data. The peak velocity of 290 ft/sec that is missed by the LDV measurements is captured by the extrapolated velocity profile. Note, however, that this result does depend on knowledge of the core radius — a whole family of velocity profiles with arbitrary radii will fit the tails of the LDV profile well.

Average circulation (vortex strength Γ) estimates depend primarily on the vortex velocity profile at radii beyond the core radius. Since the LDV estimates that portion of the profile well, in general, accurate circulation estimates can be obtained from the LDV data. This can be done by numerical integration of the LDV return profile, or more simply by fitting a parametric model (such as Rankine) to the tails of the velocity profile and deriving average circulation estimates from that parametric model.

The LDV data in Fig. 3.4-5 show a dependence of velocity on distance from the core that falls off more slowly than the theoretically predicted 1/distance relation. VNTSC staff have suggested (Ref. 6) that nonorthogonality between the LDV scan direction and the

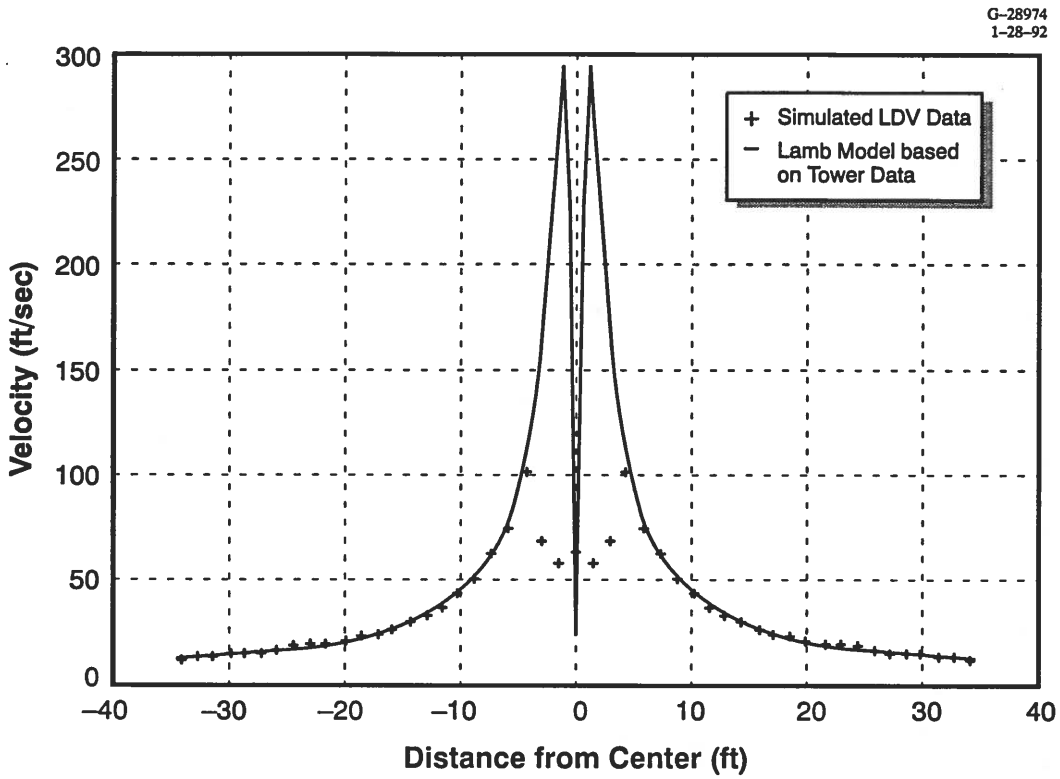

Figure 3.4-4 Analytic Performance Prediction Using Run 10 Parameters

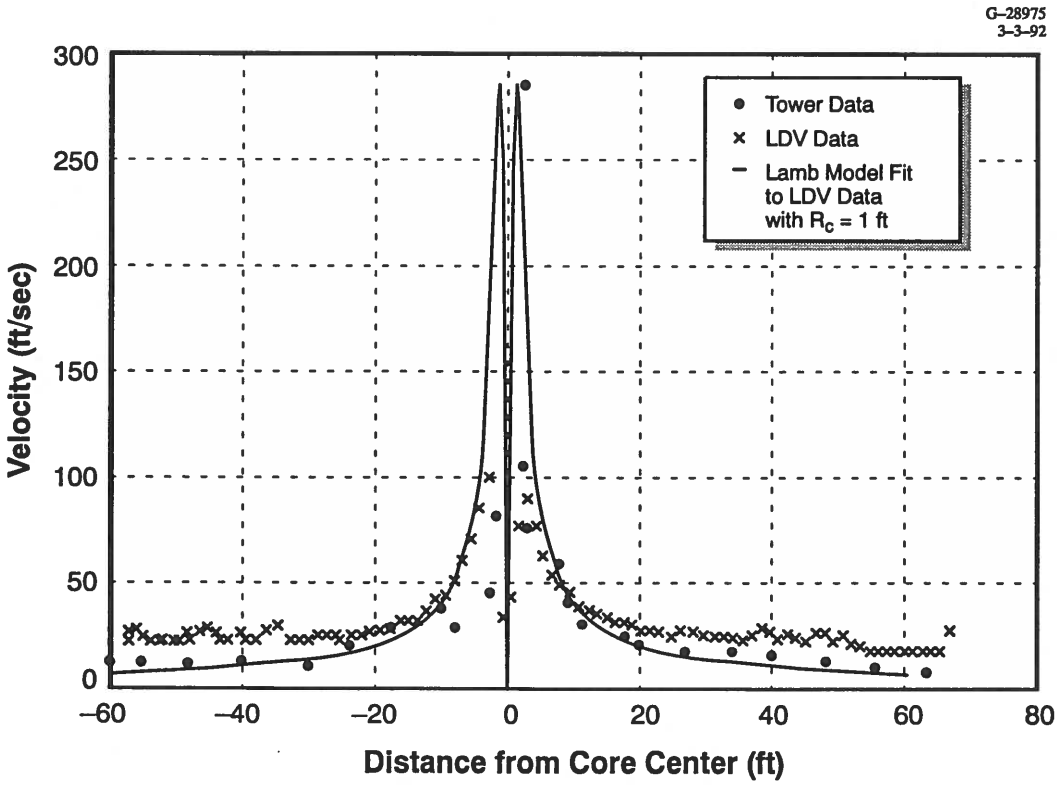

Figure 3.4-5 Parametric Extrapolation of LDV Velocity Profile

vortex axis can contribute to this effect, and Chapter 2 discusses how the nonorthogonality can cause an additional LDV velocity error. An angle 30 deg off-orthogonal, for example, can cause the LDV velocities associated with a given distance from the core to be approximately 13% in error; a 40 deg angle causes a 23% error (error is roughly proportional to the cosine of the cutting angle — see Section 2.3.3). Accounting for this nonorthogonality would improve the fit between the LDV data and the parametric model in Fig. 3.4-5.

The above discussions suggests a technique for more detailed reconstruction of velocity profiles using model-based extrapolation of LDV data. However, the extrapolation depends on the use of prior information through the specification of the parametric model (e.g., Lamb), and through the use of a priori constraints (e.g., core radius of 1 ft). VNTSC staff have also suggested model-based profile estimation and are investigating the use of data from multiple LDV scans as a way of deriving *a priori* information about the radius of the vortex core. As the results of Chapter 2 and this analysis suggest, however, small vortex core radii are not expected to be identifiable from LDV velocity profiles alone.

4. SUMMARY AND CONCLUSIONS

This report describes a quantitative assessment of the LDV (Laser Doppler Velocimeter) wake vortex detection system. The objective of the assessment is to evaluate the capabilities and limitations of the LDV for determining vortex parameters, such as average circulation, peak velocity, and core radius. The assessment was performed with a combination of LDV system simulation and LDV/tower field test data analysis.

The results showed overall that *there are some fundamental limitations on how well the LDV can recover certain vortex parameters, such as core radius and peak velocity. Data analysis results show that actual LDV performance is consistent with the fundamental limitations predicted by the LDV simulation*. The results do show that *there are some improvements that can be made to LDV processing* within these limits, such as improved wind and circulation estimation through the use of parametric model-based data analysis.

Some detailed conclusions on LDV capabilities are:

- Quantization is not a major source of error in vortex velocity measurements
- Return signal power (and SNR) is proportional to distance from the core center, and falls off rapidly inside the core
- Generally, the LDV cannot directly measure peak vortex velocities, due to spatial averaging error, SAW filter limitations, and poor SNR in the peak velocity regions
- SAW filter velocity limiting (100 ft/sec maximum sensing velocity) and poor SNR near the core can cause under-estimation of core strength (up to 15%) and peak velocity (up to 40%) for high peak velocity profiles, such as Idaho Falls Boeing 757 Run 10
- Significant errors in vortex parameter estimation can also be caused when the LDV focal point is not at the vortex center, or when the LDV line-of-sight is not perpendicular to the vortex axis (e.g., errors in estimated vortex strength are directly proportional to off-focus error in percent of range, and to the cosine of the line-of-sight cutting angle)
- If better estimates of peak velocity are required, LDV data should be augmented with additional sensors such as tower anemameters.
- Electronic, environmental, calibration, or other operator errors appear to have small effects on performance in comparison to the effects of fundamental LDV mechanics and system geometry.

Improvements that could be made for more accurate and automated LDV processing include:

- More robust estimation of maximum velocity from SAW spectra, using techniques such as spectral matching or improved automated feature extraction techniques
- Use of parametric modeling of vortex velocity measurements and least squares fitting for improved vortex parameter recovery
- Direct estimation of constant horizontal wind components from velocity profile data and their separation from vortex velocity estimates, using parametric least squares techniques
- Replacement of the current constant step range scanning procedure with one where range increments are proportional to the focal volume, to minimize off-focus errors
- Investigation of the use of multiple scan or multi-sensor (e.g., MAVSS) data to obtain sufficient observability to identify line-of-sight cutting angles or off-focus errors.

REFERENCES

1. Burnham, D.C. Feasibility of measuring aircraft wake vortices at 1500-foot altitude using CW or pulsed laser doppler velocimeters, DOT Project Memorandum DOT-TSC-FA527-PM-85-30, October 1985.

2. Hallock, J.N. and Eberle, W.R., Eds., Aircraft wake vortices: A state-of-the-art review of the United States R&D program, Federal Aviation Administration, Report No. FAA-RD-77-23, February 1977.

3. Burnham, D.C., Hallock, J.N., Tombach, I.H., Broshears, M.R., and Barber, M.R., Ground-based measurements of the wake vortex characteristics of a B-747 aircraft in various configurations, U.S. DOT/FAA, Report No. FAA-RD-78-146, December 1978.

4. Clawson, K.L., NOAA meteorological data summary (level 2 data), Wake Vortex Research Data Package No. NOAA-2, U.S. Dept. of Commerce, December 1990.

5. Clawson, K.L., Idaho Falls hot film data, Letter and Attachments, National Atmospheric and Oceanic Administration, May 1991.

6. Bamdad, C., LDV data analysis project memorandum, Volpe National Transportation Systems Center, October 1991.

TASC

THE ANALYTIC SCIENCES CORPORATION

CORPORATE OFFICE
55 WALKERS BROOK DRIVE, READING MA 01867 (617) 942-2000